1867 Infections in a Children's Hospital Autopsy Population

J Springer, R Craver. Louisiana State University Health Science Center, New Orleans, LA.

Background: Despite advances in antimicrobial therapy, infections/inflammatory lesions may frequently cause or contribute to death in children.

Design: We retrospectively reviewed all autopsies performed at a children's hospital from 1986-2009 and categorized infectious complications as 1)underlying cause of death,2) mechanism of death complicating another underlying cause of death,3) contributing to death 4) agonal or infections immediately before death 5) incidental. Infectious complications were then separated into 3-8 year groups to identify trends over the years.

Results: There were 1369 deaths over 24 years, 608 (44%) underwent autopsy at the hospital, another 122 (8.9%) were coroner's cases not performed at the hospital. There were 691 infectious conditions in 401 children (66%, 1.72 infections/infected patient).There were no differences in the percentage of autopsies with infections over the years, although the number of total infections decreased in the last 8 year period. The number of infections /patient varied over the different time groups. By categories, there were 85 (12.3%), 237(34.3%), 231 (33.4%), 82 (11.9%), and 56(8.1%) infections. The distribution remained similar over the time groups, with the exception of more category 2 and less category 3 infections in 2002-2009 compared to 1994-2001. Leading infectious diseases/complications include bronchopneumonia (188), sepsis (144),acute meningitis (35), pneumonitis (33- including 19 with specific viral agents identified),peritonitis (29), tracheobronchitis (24), necrotizing enterocolitis (19), gastritis (15) disseminated Candida (15), and lymphocytic myocarditis (14). Sepsis was significantly less frequent (p=.0041) in 2002-2009 compared with earlier periods. 159 agents of sepsis in 144 patients included 67 Gram positive cocci, 70 Gram negative rods, 7 other, 15 clinical. Enterococcus was the most common(22). Bacterial meningitis was significantly more frequent in the first time period (p=.0061) compared to the later periods. Strep. pneumoniae was the overall most frequent cause(10).

Conclusions: 66% of pediatric autopsies at a Children's Hospital had an inflammatory lesion, and was stable over the time studied. Most are the mechanism of death or a significant contributing factor, rather than the underlying cause of death. The decrease in meningitis after the 1986-1993 period may be partially attributed to the H. flu vaccine. The decline in deaths with sepsis may be due to increased awareness, education, and standardization of treatment in the institution for recognition and treatment of septic shock.

1868 A Morphometric Study To Establish Subjective Index of Cerebellar Hypoplasia: A Special Emphasis on Cerebellar Hypoplasia in Trisomy 18

Y Tanaka, M Tanaka, R Ijiri, K Kato, K Gomi, Y Itani, H Ishikawa, S Yamashita. Kanagawa Children's Medical Center, Yokohama, Kanagawa, Japan.

Background: Cerebellar hypoplasia (CH) is one of the common abnormalities reported in trisomy 18 (T18) and has been described also in several disorders other than T18. However, CH is a poorly defined condition and no critical morphometric standard for CH has been established.

Design: Nineteen cytogenetically confirmed T18 cases and 63 age-matched control patients were selected from the autopsy files of Kanagawa Children's Medical Center during the last 22 years. In order to evaluate "congenitally small cerebellum", we excluded patients whose ages were more than 6 days. After fixation in buffered formalin for more than two weeks, the cerebrum was cut-off at the level of mid-brain and the brain stem was cut-off at the level of inferior collicles under the standard protocol. The weights of the cerebrum, the brain stem, and the cerebellum were measured precisely. The entire brain weight (EBW) was defined as a sum of the weights of the three parts. Several weight ratios, including the cerebellum weight (CLW) to the EBW, the CLW to the body weight (BW), and the cerebrum weight (CRW) to the BW, were calculated.

Results: All 19 patients with T18 were delivered at over 30 weeks of gestation and were small for gestational age. The BW at autopsy ranged from 575g to 2,538g. The EBW after formalin-fixation ranged from 140.7g to 390.9g. The CLW ranged from 3.90g to 15.48g. The CLW/EBW of all T18 patients was below 4% ranging between 2.59% to 3.96%. Only 3 of the 63 age-matched controls showed the CLW/EBW to be below the standard range or within the range of T18 patients (Figure 1). Diagnoses of the 3 patients were thanatophoric dysplasia (2 patients) and Bowen-Conradi Hutterite syndrome (1 patient), both of which are considered to have CH.

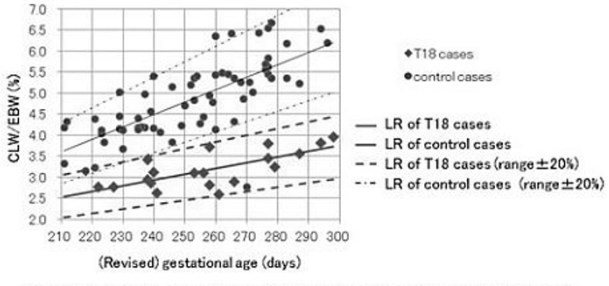

Figure 1 Graph showing standard ranges of CLW/EBW and values of CLW/EBW in T18 patients.
T18: trisomy 18 CLW: cerebellar weight EBW: entire brain weight LR: linear regression.

The CLW/BW was apparently lower in T18 cases than control patients, and the CRW/BW was slightly higher in T18 cases than in control patients.

Conclusions: Although standard for CH is difficult to define, the CLW/EBW obtained from the T18 patients seems to show a distinct tendency. The graph, shown in this abstract, is useful and may serve as a guideline to define CH, with linear regression +20% of T18 cases and/or linear regression -20% of control cases being the borderline for CH.

1869 Expression of Disialoganglioside GD2 in Neuroblastomas of Patients Treated with Immunotherapy

T Terzic, P Teira, S Cournoyer, M Peuchmaur, H Sartelet. Centre Hospitalier Universitaire Sainte-Justine, Montreal, QC, Canada; Hopital Universitaire Robert-Debre, Paris, France.

Background: Neuroblastoma, a malignant neoplasm of the sympathetic nervous system, is one of the most aggressive pediatric cancers with a tendency for widespread dissemination, relapse and a poor long term survival, despite intensive multimodal treatments. Recent use of immunotherapy (a chimeric human-murine monoclonal antibody ch14.18 directed against a tumor-associated antigen GD2, a disialoganglioside) to treat minimal residual disease has shown improvement in event-free and overall survival of high-risk neuroblastomas. However, some patients are resistant to immunotherapy. Therefore, the aim of the study was to analyze GD2 expression in neuroblastomas and see if the resistance to immunotherapy could be explained by the poor expression of GD2.

Design: We realized an immunohistochemical study on 140 cases of neuroblastomas included in TMAs and on 17 frozen specimens of neuroblastomas with an anti-GD2 antibody which has the same epitope as the one used in immunotherapy (monoclonal mouse antibody, 14G2A clone). The intensity of staining was graded as follows: "0", "1+", "2+", 3+" and "4+" when 0%, 1-25%, 26-50%, 51-75% and 76-100% of tumor cells respectively showed positive expression. The immunohistochemical results were interpreted without knowledge of the clinical characteristics. Among our patients, 12 have had immunotherapy and 3 of them showed resistance to it.

Results: Immunohistochemical expression of GD2 was found in 96.5% (135/140) of cases, among which 23 had between 1 and 25% of positive tumoral cells. There was a strong correlation between results in frozen and in paraffin sections. Immunostaining intensity was comparable in tumours and in metastasis (1.76 (mean intensity of GD2) vs 1.69) and also when patients were matched up for age (< or > than one year old, 1.82 vs 1.81) and MYCN amplification (2.00 vs 1.63). However, the mean intensity of GD2 expression was significantly higher (2.66 vs 1.33, p-value 0.02) in patients who responded versus those who were resistant to immunotherapy.

Conclusions: The observations of immunohistochemical expression of GD2 in our study show that most neuroblastomas express GD2, but most importantly that there is a significant difference in tumoral expression of GD2 between patients who respond and those who are resistant to immunotherapy. Thus, immunostaining with GD2 could become an important tool in deciding which patients should receive immunotherapy and so avoid overtreatment, but larger studies should be completed beforehand.

Pulmonary

1870 Combining Inhibitor of DNA – Binding Proteins and Angigenic Markers Expression Predict Long Term Survival of Patients with Non-Small Cell Lung Cancer

L Antonangelo, TS Tuma, FS Vargas, ER Parra, RM Terra, M Acencio, VL Capelozzi. University of Sao Paulo Medical School, São Paulo, Brazil.

Background: Inhibitor of DNA binding (Id) proteins is an emerging promise as biologic marker on oncogenic transformation, cancer progression and tumor angiogenesis, the last, by the regulation of vascular endothelial growth factor (VEGF) expression.

Design: We evaluated Ids (1, 2 and 3), VEGF expression and microvessel density (CD34+) in tumor and stromal cells and their impact on survival of 85 patients with surgically excised lung squamous cell carcinoma and adenocarcinoma. Immunohistochemistry and morphometry were used for the quantitation and Kaplan-Meyer survival curves and Cox regression for the statistical analyses.

Results: It was found that high Id-1 and VEGF expression and high microvessel density were associated with worse prognosis (Log Rank Test, $p<0.001$). The Cox model controlled for histological type, age, lymph node stage, Ids, VEGF and microvessel density demonstrated that age, lymph node stage, Id1 and Id3 expression and vascular density were significantly associated with overall survival. A point at the median for Id1, Id3 and vascular density divided patients into 2 groups of different prognosis. Those with higher expression of Id1, Id3 and vascular density had a higher risk of death than those with lower Id-1, Id-3 and microvessel density.

Conclusions: Inhibitor of DNA binding (Id) proteins and vascular density are strongly related to prognosis, suggesting that treatment strategies aimed for preventing high Ids synthesis, or local responses to angiogenesis may have impact on NSLC survival.

1871 Histologic Spectrum and Clinical Significance of Granulomatous Inflammation in Pulmonary Aspergillosis: A Study of 13 Cases with Comparison to Mycetomas and Invasive Aspergillosis

JF Back, S Mukhopadhyay. State University of New York Upstate Medical University, Syracuse, NY.

Background: The significance of granulomatous inflammation in pulmonary aspergillosis is not well understood. Prior studies have suggested that granulomatous inflammation is the histologic correlate of a tuberculosis-like progressive cavitary disease known as chronic necrotizing aspergillosis. The aim of this study was to describe the histologic spectrum of granulomatous inflammation in pulmonary aspergillosis and determine its clinical significance.

Design: Biopsied or resected cases of pulmonary aspergillosis over an 11-year period (1990-2011) were reviewed. Cases that showed granulomatous inflammation were compared with mycetomas and invasive aspergillosis. Clinical, radiologic and

microbiologic data were reviewed, and histologic slides re-examined with a focus on the characteristics of the inflammatory response.
Results: Granulomatous inflammation was identified in 13 patients (9 men, 4 women) ranging in age from 3 to 76 years, 7 of whom were immunocompromised (3 corticosteroids, 2 acute leukemia, 1 HIV, 1 immunoglobulin deficiency). Only 3 had a tuberculosis-like clinical picture consistent with chronic necrotizing aspergillosis. Granulomas were discovered incidentally in 3 cases. Radiographs showed lung nodules in all 9 cases in which radiologic data was available (4 bilateral, 5 unilateral). All cases showed necrotizing granulomas, with caseous necrosis in 8 and suppurative necrosis in 5. Fungal hyphae consistent with *Aspergillus* were identified within the necrosis in all cases. A radial arrangement of fungi, distinct from the matted arrangement of mycetomas, was noted in 8 cases. No granulomatous inflammation was seen in mycetomas (3) or invasive aspergillosis (3). Cultures were positive for *Aspergillus* in 4 patients. Seven patients received antifungal therapy. Of 7 patients with follow-up data (3-156 months, median 48), 3 improved, 3 showed no evidence of progression, and 1 died of progressive disease.
Conclusions: *Aspergillus* is occasionally found within necrotizing granulomas with caseous or suppurative necrosis within which organisms are often arrayed in a distinctive radial arrangement. Clinically, such lesions present as unilateral or bilateral lung nodules, and are often found in patients with immune deficiency, supporting the notion that they represent a form of semi-invasive aspergillosis. However, only a minority are associated with clinical features of progressive cavitary disease that can be termed chronic necrotizing aspergillosis.

1872 Pulmonary Interstitial Emphysema in Adults: A Potential Diagnostic Pitfall

SM Barcia, KD Jones. University of California San Francisco, San Francisco, CA.
Background: Pulmonary interstitial emphysema (PIE) is well described in premature infants with respiratory distress syndrome and is observed in adults, usually in association with ventilator use. In this condition, air gains access to the lung interstitium via rupture of small alveoli and bronchioles, then dissects through interstitial connective tissue along lymphatic routes. Chronically, angular cystic spaces form, lined by foreign body giant cells and fibrosis. The fibroinflammatory reaction around cyst-like spaces may mimic fibroblast foci and honeycombing, infectious granulomas, or lymphangiectasia, resulting in erroneous diagnoses or unnecessary additional workup. In this study, we investigated the frequency of PIE in explanted lungs and correlate the findings with clinicopathologic diagnoses, ventilator status and duration of disease.
Design: We identified 53 patients who underwent lung transplant at our institution between February 2010 and June 2011. Each case was reviewed by a specialist in pulmonary pathology for the presence of PIE. The electronic medical record was reviewed to identify clinical diagnoses, ventilator status, duration of disease and history of prior biopsy.
Results: 19 of 53 (36%) cases were identified with PIE. Interstitial air reaction was observed in several different diseases. No association was seen between PIE and ventilator status, history of prior surgical biopsy or duration of disease. Histologic features of PIE included elongated or angulated spaces, most commonly around bronchovascular bundles. The cyst-like spaces were lined by scant to prominent foreign body giant cells with macrophages, and surrounded by variable fibrosis and eosinophils. Histochemical (trichrome, Elastic Van Gieson) and immunohistochemical stains (D2-40, CD68, keratin) aided in characterization of the lesions.

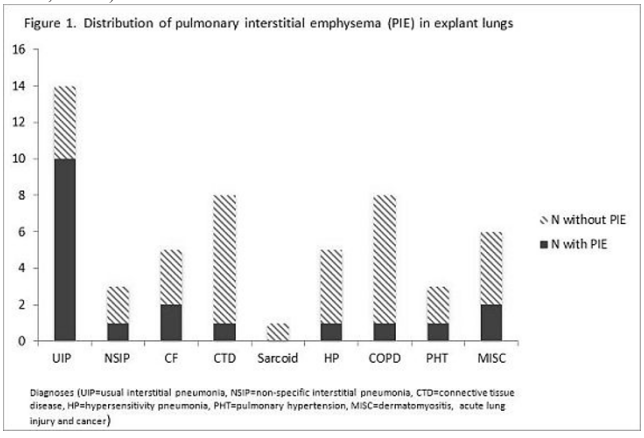

Conclusions: PIE was seen in 36% of adult explanted lung specimens, most commonly in patients with UIP. PIE was not limited to patients who were previously ventilated. These results may indicate that PIE is secondary to physiologic changes from the disease rather than an outside source, as is described in premature infants. Recognition of this unusual reaction is important, as the fibroinflammatory reaction may mimic other interstitial and infectious diseases.

1873 Multi-Institutional Review of Spontaneous Pneumothorax (SP) over an 11 Year Period

D Belchis, C Gocke, K Shekitka. Johns Hopkins University, Baltimore, MD; St. Agnes Hospital, Baltimore, MD.
Background: SP is a well-recognized complication of a variety of systemic and local disorders. In each of these conditions SP affects only a subset of the patients, raising the question of whether or not there are biologic differences in the affected subsets. This multi-institutional study attempted to identify unique clinicopathologic features in a large cohort with SP.
Design: The pathology files of 3 institutions over an 11 year period were searched for cases of SP. Charts and radiographic reports were reviewed. Slides were evaluated for a variety of histologic features.
Results: A total of 110 cases were retrieved: 26 women, 83 men and 1 unknown. The average ages by institution were 59, 46, and 37. 66 cases had identifiable disorders: 40 COPD, 12 cancer, 5 UIP (2 of which also had cancer), 1 pneumoconiosis, 3 infection (2 HIV with pneumocystis, 1 TB), 2 sarcoid, 1 SLE, 1 thrombotic vasculopathy, and 1 LCH. 1 was a presumed case of IPPFE, 1 Marfan's syndrome. 7 patients had a family history of lung disease: 2 with family history of pneumothorax, 2 with family history of lung cancer, and 1 each with family histories of emphysema, COPD and not further classified. A subset of patients had cystic lung disease not otherwise classified and 1 patient had unusual cellular areas suggestive of LAM but negative for HMB-45. 69 were smokers, 14 were non-smokers and 27 unknown. 44 cases had no obvious underlying etiology. In this group, 35 were men, 10 women. The average age was 30 (men) and 39 (women). Morphologic findings were similar to those identified by others including eosinophilic pleuritis, pleural fibrosis, blebs, small airways disease, intraalveolar macrophages and chronic inflammation. In addition, 3 unique clinicopathologic subsets were identified including a novel entity we recently described, pneumothorax-associated fibroblastic lesion (PAFL). Another subset of patients had extensive intraalveolar infiltrate creating a DIP-like appearance. A third subset had cellular alveolar septae.
Conclusions: Approximately 59% of SP have underlying associated disorders. Some of these disorders are not typically associated with SP. The mean age differed across institutions, possibly representing variations in clinical approach to SP or patient response. Several distinct morphologic lesions were identified: PAFL, a subset with cellular septae, and a third with numerous intraalveolar macrophages (DIP-like appearance).

1874 Pulmonary Adenocarcinomas with Signet Ring Cell (SRC) Features: A Clinicopathologic and Molecular Study

JM Boland, JS Jang, JA Wampfler, X Wang, MR Erickson-Johnson, AM Oliveira, P Yang, J Jen, ES Yi. Mayo Clinic, Rochester, MN.
Background: Pulmonary adenocarcinomas (ADCA) with SRC features (SRC+) have been associated with poor outcome and *ALK* rearrangement (*ALK*+). However, their clinicopathologic characteristics and molecular profile are not well known. Herein, we systematically reviewed pulmonary ADCAs for SRCs and evaluated clinical and molecular features of SRC+ cases.
Design: Surgically treated lung ADCAs (n=764) in 3 cohorts representing distinct patient groups were reviewed by 2 pulmonary pathologists: never smoker cohort (n=300), a 2006-7 patient cohort with 5-year follow-up (n=223), and a cohort generated from a pathology search enriched for lepidic growth (n=557). SRC+ tumors had ≥10% SRCs agreed by both pathologists and were TTF1+, cytoplasmic mucin+, and CDX2-. ALK immunohistochemistry (IHC) was performed on all SRC+ cases and *ALK* status was confirmed by FISH for cases with any IHC positivity. DNA was extracted from SRC+ cases, and samples were run on MassArray based Lung Cancer Mutations Screening Panel (LuCaMSP), which tests for 179 individual mutations in 10 genes including *EGFR, KRAS, BRAF, ERBB2, JAK2, AKT1, AKT2, KIT, MET* and *PIK3CA;* positive results were confirmed by gene sequencing.
Results: Fifty-two of 764 cases (7%) were SRC+, which were more likely to occur in men and have higher stage. The 300 never smokers included 226 women (75%); 27 cases (9%) were SRC+, which were more likely to be *ALK*+ than SRC- cases (33% vs 5%, p<0.0001). LuCaMSP analysis on 25 SRC+ cases in this cohort showed the following mutations in *ALK*- cases: 7 *EGFR*, 3 *KRAS*, and 4 *MET* (1 case had both *ALK* and *MET* R970C). SRC+ never smokers were more likely to have lung cancer progression and death: median progression-free survival 2.2 vs. 5.0 years (p=0.0001), median overall survival 3.5 vs. 7.6 (p=0.0038). The 223 patients treated in 2006-7 had 123 women (55%), and 19 (9%) were SRC+. The 557 lepidic enriched cases occurred in 314 women (56%), and 27 (5%) were SRC+. Analysis of the later 2 cohorts yielded the following results: no significant difference in smoking status (never- vs. ever-smokers); confirmation that SRC+ cases are more likely to be *ALK*+; crude 5-year survival rates were 8%-16% inferior in SRC+ cases compared to the SRC- cases, although not reaching statistical threshold; LuCaMSP analysis is ongoing, and 3 of 4 examined cases have *KRAS* mutations.
Conclusions: SRC+ ADCA of lung are associated with male gender and higher stage. Shorter survival was observed in SRC+ cases for all 3 cohorts but was only statistically significant in the never-smoker cohort. SRC+ cases in all cohorts were more likely to be *ALK*+.

1875 Biomarker Profile of Pulmonary Vasculature in Subjects with Portopulmonary Hypertension

N Boroumand, A Duarte, RT Meena, PJ Boor, AK Haque. University of Texas Medical Branch, Galveston, TX; Methodist Hospital, Houston, TX.
Background: Pulmonary arterial hypertension (PAH) consists of a heterogenous group of conditions characterized by vasoconstriction, vascular remodeling of the small pulmonary arteries and progressive right ventricular failure. PAH associated with portal hypertension or portopulmonary hypertension *(*PPH) occurs in 4 to 10 % of subjects with liver disease and portal hypertension. The histopathology of the pulmonary vasculature reveals medial hypertrophy, intimal hyperplasia and plexogenic arteriopathy that is similar to idiopathic and congenital heart disease associated PAH. However, the mechanisms leading to PPH are unclear. Several proposed mechanisms include an excess of endothelin and altered estrogen metabolism. The aim of this study was to determine the quantity and location of endothelin (ET), estrogen (ER), and vascular endothelial growth factor (VEGF) receptors in pulmonary vasculature of subjects with PPH.

Design: We reviewed our hospital autopsy data base from 1994 to 2009 and selected subjects with cirrhosis, right ventricular hypertrophy and histopathology associated with PAH. Paraffin embedded lung tissue was sectioned, treated with antigen retrieval, and immunostained for estrogen (ER- α and ER- β), endothelin (ET-A, ET-B) and VEGF. Two pulmonary pathologists independently reviewed the slides and assessed immunostain intensity.
Results: Fifteen subjects with portopulmonary hypertension were identified. Mean age was 48.7 ± 8.8 yrs; 5/15 (33 %) were female. All subjects demonstrated right ventricular enlargement and histology with medial hypertrophy, intimal hyperplasia and plexogenic arteriopathy. Immunohistochemistry revealed ER- α positivity in 0% of the subjects (0/15) in both endothelial and smooth muscle components, whereas ET-B was positive in 100% of the subjects (15/15) in both endothelial and smooth muscle components. ER- β and ET-A were positive approximately in third of the subjects in endothelial cells. VEGF was positive in all subjects in endothelial cells.
Conclusions: In portopulmonary hypertension, endothelin B receptor was present in endothelial and smooth muscle cells of the pulmonary vasculature in all the subjects. While Endothelin A and Estrogen receptors were either absent or very limited. Endothelin1 is a potent vasoconstrictor, and mediator of cells involved in vascular remodelling, while the effects of estrogens on pulmonary vasculature are beneficial, but complex and not fully understood.

1876 p40 (ΔNp63) and Keratin 34ßE12 Provide Greater Diagnostic Accuracy Than p63 in the Evaluation of Small Cell Lung Carcinoma in Small Biopsy Samples

KJ Butnor, JL Burchette. University of Vermont/Fletcher Allen Health Care, Burlington, VT; Duke University Medical Center, Durham, NC.
Background: The use of p63 has been advocated for separating small cell lung carcinoma (SCLC) from poorly differentiated non-small cell lung carcinoma (NSCLC). However, p63 is not entirely specific in this distinction, with several studies demonstrating that a proportion of SCLCs stain for this marker. p40 (ΔNp63) is purported to be a highly specific marker for squamous cell carcinoma (SQCC). To our knowledge, the staining characteristics of SCLC for p40 (ΔNp63) have not been previous studied to any significant extent. The purpose of this study is to compare the immunohistochemical expression of p40 (ΔNp63), p63, and keratin 34βE12 in SCLC.
Design: Formalin-fixed paraffin-embedded sections from a total of 34 previously confirmed SCLCs (27 bronchoscopic biopsy samples and 7 large resection/autopsy specimens) were immunostained for p40 (ΔNp63), p63, and keratin 34βE12. Staining was defined as positive when ≥ 10% tumor cell nuclei exhibited immunoreactivity.
Results: All 34 SCLCs tested were negative for p40 (ΔNp63) and keratin 34βE12. With respect to p63, 12/27 (44.4%) bronchoscopic biopsy samples were positive, while none of the large specimens exhibited immunoreactivity. Positive and negative control tissues stained appropriately. The rate of p63 staining in bronchoscopic biopsy samples of SCLC differed significantly from that of p40 (ΔNp63) and keratin 34βE12 ($P = 0.005$).
Conclusions: In the first study to specifically examine p40 staining in SCLC, p40 is consistently negative in SCLC. In contrast, p63 immunoexpression is not uncommon in small biopsy samples of SCLC and may be mistakenly interpreted as supportive of squamous differentiation, resulting in misclassification of SCLC as SQCC. To provide greater diagnostic accuracy, p40 (ΔNp63) or keratin 34βE12 should be used instead of p63 in the distinction of SCLC from NSCLC in small biopsy samples.

1877 Comparative Study of FISH and Immunohistochemistry Assays for the Detection of ALK-Positive Non-Small-Cell Lung Cancers: Report of a Series of 878 Cases

F Cabillic, D Chiforeanu, F Dugay, R Corre, H Lena, M Le Calve, N Rioux-Leclercq, M-A Belaud-Rotureau. CHU Pontchaillou, Rennes, France; Faculty of Medicine, Rennes, France.
Background: Crizotinib is indicated for the treatment of anaplastic lymphoma kinase (ALK)-rearranged non-small cell lung cancer (NSCLC). These tumors can be identified by the FDA-approved-ALK companion diagnostic fluorescent *in situ* hybridization (FISH) assay. However, the place of immunohistochemistry (IHC) testing still debates. We studied the performances of these 2 techniques in a series of 878 NSCLC.
Design: The cohort consisted of 608 male and 270 female patients with a NSCLC: 709 adenocarcinomas (ADC), 115 squamous cell carcinomas (SSC), 24 large cell carcinomas (LCC), 2 adenosquamous cell carcinomas (ADSC), 1 large cell neuroendocrine carcinoma and 27 unclassifiable cases (UC). Formol-fixed paraffin-embedded tissue sections were prospectively analyzed between June 2011 and April 2012 by FISH (Abbott-Vysis ALK Break Apart FISH Probe) and IHC (Anti-ALK antibody (ab17127)5A4 clone, Abcam and Roche-Ventana BenchMark XT system).
Results: FISH analyses were non contributive in 209/878 (23%). Among them, 201 were IHC-negative (neg) and 8 IHC-positive (pos). IHC analyses were non contributive in 11/878 (1%) of the cases which were all FISH-neg. A total of 658 cases were successfully analyzed both by FISH and IHC: 17 were FISH-pos/IHC-pos, 8 FISH-pos/IHC-neg, 7 FISH-neg/IHC-pos and 626 FISH-neg/IHC-neg. The overall concordance between the 2 techniques was 98%. An ALK-positivity was detected by FISH and/or IHC in 40/878 (4.6%) of the cases (37 ADC, 1SSC, 1ASC and 1 UC). Among them, 8/40 (20%) couldn't be classified as ALK-positive NSCLC because IHC-pos (3 low and 5 strong immunostaining) / FISH-non contributive results; 5/40 (13%) with a IHC-pos (low immunostaining) / FISH-neg results were classified as ALK-neg NSCLC and 8/40 (20%) FISH-pos / IHC-neg cases were classified as ALK-pos NSCLC. Interestingly, 2 cases showed a strong immunoreactivity by IHC but a FISH-neg result confirmed with several different FISH probes. Finally, only 17/40 cases (43%) were FISH and IHC-pos.
Conclusions: Our data highlight some discrepancies between ALK testing by FISH and IHC inciting to routinely perform these 2 assays in front to enhance the detection rate of the ALK-positive NSCLC.

1878 Hypersensitivity Pneumonia: Where Do Granulomas and Giant Cells Live?

MC Castonguay, JH Ryu, ES Yi, HD Tazelaar. Dalhousie University, Halifax, NS, Canada; Mayo Clinic, Rochester, MN; Mayo Clinic, Scottsdale, AZ.
Background: Characteristic histologic findings in hypersensitivity pneumonia (HP) include chronic bronchiolitis, interstitial pneumonia, non-necrotizing granulomas, and isolated multinucleated giant cells (MNGCs). Although the location of granulomas and MNGCs is said to be of importance in the differential diagnosis ("they should be interstitial in HP"), their distribution has not yet been systematically evaluated. This study was undertaken to determine whether they could also be found in airspaces.
Design: Retrospective study spanning 16 years (1997–2012), evaluating 40 patients with a clinicopathologic diagnosis of HP who underwent lung wedge biopsy at our institution; 2 patients also underwent lung transplantation. The medical records were reviewed for demographic, clinical, and imaging features. Glass slides prepared from wedge biopsy and explant specimens were reviewed by three pathologists to assess multiple histologic features of HP, including the location of granulomas and isolated MNGCs.
Results: Patient ages were from 16 to 79 years (mean, 59), with 24 (60%) women. Historical exposures to potentially responsible antigens were identified in 27 patients, 8 of whom had confirmatory serologies. Classic features of HP were present in the majority of patients (see Table). Granulomas were seen in the airspaces of 28 patients (and strictly so in 6); similarly, isolated MNGCs were present in the airspaces of 25 patients (and solely so in 7); both granulomas and MNGCs were confined to airspaces in 3 patients (each with antigen exposure). Pleural granulomas were seen in 3 cases, and pleural MNGCs in 1 additional case (3 with antigen exposure).

Histologic Features in 40 Patients with HP

Histologic Feature		Present (%)	Absent (%)
Chronic Bronchiolitis		92.5	7.5
Interstitial Pneumonia	Centrilobular Accentuation	75	25
	Diffuse	20	80
Granulomas	Interstitium	65	35
	Airspace	70	30
	Pleural	7.5	92.5
Isolated MNGCs	Interstitium	60	40
	Airspace	62.5	37.5
	Pleura	2.5	97.5
Organizing Pneumonia		85	15
Fibrosis	Centrilobular	57.5	42.5
	Diffuse	7.5	92.5
	Peripheral with Honeycombing	15	85

Conclusions: Granulomas and MNGCs can be found in both the airspaces and interstitium in HP, and can be restricted to airspaces. Surprisingly, pleural granulomas were identified in 3 patients; this finding is at odds with textbooks and the literature and has significant implications for the pathology diagnosis of HP.

1879 Glucose Transporter-1 Protein Expression in Thymic Epithelial Neoplasms: A Marker for Poor Prognosis

SY Chang, SM Jenkins, KK Edwards, M-C Aubry, ES Yi, SD Cassivi, YI Garces, AC Roden. Mayo Clinic, Rochester, MN.
Background: Glucose transporter-1 (GLUT-1) is involved in cellular glucose uptake and has been shown to be increased in malignant epithelial and mesothelial cells. In fact, we and others have demonstrated that GLUT-1 expression is higher in thymic carcinomas (TCa) than in thymomas. Evidence also suggests that GLUT-1 expression in carcinoma cells may be associated with resistance to radiation and chemotherapy and increased recurrence and metastasis. We studied the prognostic value of GLUT-1 expression in thymic epithelial neoplasms (TEN).
Design: Specimens from patients treated for TEN were included. Three pathologists independently classified all cases according to WHO. Type AB, B1 and B2 thymomas were excluded due to the high number of lymphocytes. Sections were stained for GLUT-1. The percentage of GLUT-1+ cells was expressed as 100*(number of + epithelial cells) / total number of epithelial cells (mean of 5 HPF counted). Cases with >5% GLUT-1+ cells were considered positive since most cases showed a few scattered GLUT-1+ epithelial cells. Logistic and Cox proportional hazards regression models were used for statistical analysis.
Results: 49 patients (20 women, 29 men; median age, 63 years, range, 18-85) were included. Pathologists agreed upon type A (n=16) and B3 (n=14) thymoma, or TCa (n=19). The median follow-up (n=44) time was 3.6 years (range, 12 days–20.5 years). GLUT-1 positivity was associated with modified Masaoka stage (p=0.01), increased risk of metastasis/recurrence (n=10, HR=8.72, p=0.01) and death (n=24, HR=2.72, p=0.03). GLUT-1 expression was also associated with WHO type (p=0.005) and was more commonly positive in TCa vs. type B3 and type A thymomas (% GLUT-1 positive cases, 78.9 vs 50.0 vs 18.7, respectively). In high-grade TCa GLUT-1 was expressed by a higher percentage of tumor cells (median, 80%) compared to low/intermediate grade TCa (median, 41%) (difference statistically not significant). When controlled for Masaoka stage and WHO, GLUT-1 expression was not an independent prognostic marker, however.
Conclusions: Our results show that increased GLUT-1 expression is associated with poorer prognosis, higher tumor stage and morphology when evaluated in type A and B3 thymoma and TCa. Although multivariate analysis does not show GLUT-1 as an independent prognostic marker in TEN, GLUT-1 expression may be useful in evaluating patient prognosis when combined with cell-kinetic parameters or other prognostic marker. Larger studies are necessary to evaluate GLUT-1 as prognostic factor in TCa.

1880 Hydrophilic Polymer Embolus (HPE) Vasculopathy of the Lung

JM Choi, RI Mehta, AP Burke, RI Mehta. University of Maryland Medical Center, Baltimore, MD; State University of New York Upstate Medical University, Syracuse, NY.

Background: Hydrophilic polymers are commonly applied as coating on endovascular device surfaces and have the potential to strip off within the bloodstream during use in patients, causing hydrophilic polymer emboli (HPE). Recent reports document cardiovascular complications with associated morbidity and mortality in rare patients. The focus of this study was to evaluate the histologic features and tissue responses to HPE involving the lungs.

Design: Ten cases of pulmonary HPE were retrospectively reviewed (2010-2012). Hematoxylin and eosin, Masson trichrome, and elastic-stained sections of formalin-fixed, paraffin-embedded tissue were evaluated. The study incorporated 7 autopsy cases; 2 lung explants (including 1 retransplanted explant); and 1 wedge biopsy. The mean patient age was 56 years (age range: 22 to 73 years); 7 patients were male.

Results: Histologic appearances of actively biodegrading HPE were extremely variable. In all cases, lamellated granular basophilic material, consistent with polymer, was identified within small-to-medium sized vessels in peripheral lung. Seven of these cases showed localized involvement, while the remaining three showed diffuse dissemination with involvement of multiple lobes. Affected vessels ranged from 13 to 1280 μm in diameter (average: ~150 μm). The total number of HPE ranged from 1 to 430 per case (average: ~80 microemboli). Tissue responses included vascular occlusion (n=10); intravascular fibrocollagenous change (n=7); microthrombus formation (n=5); hemorrhage (n=4); recanalization (n=2); infarction (n=2), and diffuse alveolar damage (n=1). Inflammatory changes included intra- and peri-vascular mononuclear (n=10), neutrophil (n=6), and foreign body giant cell (n=5) reaction; granulomatous change (n=3); microabscess formation (n=2), and vasculitis (n=2). None of the cases were correctly diagnosed at the time of prospective review.

Conclusions: Hydrophilic polymer emboli are characterized by variable histologic appearances and cause significant pathologic changes when deposited in pulmonary vessels. This vasculopathy represents a newly recognized disease associated with modern interventional therapies. A heightened clinical awareness of this iatrogenic complication may lead to more accurate and timely diagnosis in affected patients.

1881 Pulmonary Cystic Lung Disease in Birt-Hogg-Dube Syndrome: Can Histology Discriminate from Bullous Emphysema?

A Fabre, R Borie, MP Debray, B Crestani, C Danel. St Vincent's University Hospital, Dublin, Ireland; Hopital Bichat-Claude Bernard, APHP, HUPNVS, Paris, France.

Background: Birt-Hogg-Dubé syndrome (BHDS) is an autosomal dominantly inherited genodermatosis, which predisposes to fibrofolliculomas, renal neoplasms and lung cysts that can lead to spontaneous pneumothorax.

Design: We report a study of 5 cases (1 man, 4 women) with genetically confirmed BHDS who presented with pneumothorax, where surgical resection of pulmonary tissue confirmed cystic lung disease, including 2 cases who had recurrent pneumothorax (interval 1-2 years). We compared these series to a cohort of 6 control cases (primary spontaneous pneumothorax, BHDS negative) matched for sex, age and bulla topography. We reviewed smoking status, and HRCT findings.

Results: This retrospective study of histological surgical material included 1 man (mean age at surgery= 32) and 4 women (mean age at surgery =42 [37-50]) with BHDS. When histological surgical material was available (n=7 including two recurrent cases), 4/5 had a history of recurrent pneumothorax and 5/7 involved the right side. Ex-smoking was noted in 3 BHDS case. Histological analysis showed that compared to controls, BHDS- cysts were either subpleural but in all cases peribronchiolar ("punch-out aspect") and lacked inflammation or fibrosis. There were lined by flat or hyperplastic TTF-1+ pneumocytes. There was no relationship to the terminal bronchiole or pulmonary artery. In BHDS cases, pleura was thickened but lacked apical cap-like fibroelastotic scars, as seen in 3/6 controls. In all cases there was reactive eosinophilic pleuritis from the pneumothorax. One BHDS case with recurrent pneumothorax had fibroblastic hemosiderin laden nodules in the cyst wall and evidence of peri-cystic hemorrhage. Granulomas were not seen. BHDS cases did not show any evidence of respiratory bronchiolitis but this was seen in 4/6 control cases (5/6 current smokers, one ex-smoker, mean pack-years: 14.8) and for all controls, CT showed bullous emphysema. In all BHD, CT showed true cystic lung disease with thin walled oval-shaped cysts in subpleural areas cases where the diagnosis was suggested.

Conclusions: While the features of BHD are histologically non specific, their "punch-out" appearance close to the broncho-vascular bundles, in the context of scannographic cystic lung disease and non/ex-smoking, may suggest the diagnosis of BHD.

1882 Detection of Soluble Mesothelin in Serum and Pleural Effusion of Malignant Pleural Mesothelioma: A Contribution to Cytology

F Fedeli, PA Canessa, P Ferro, E Battolla, P Dessanti, A Vigani, L Chiaffi, MC Franceschini, V Fontana, B Bacigalupo, MP Pistillo, S Roncella. ASL5, La Spezia, Italy; ASL5, Sarzana (SP), Italy; IRCCS A.O.U., San Martino-IST, Genova, Italy; AIL, La Spezia, Italy.

Background: Soluble mesothelin (SM) is an FDA approved biomarker for diagnosing and monitoring MPM. It has been reported that the sensitivity of cytology (Cyt) for the diagnosis of MPM pleural effusions (PE) is about 30%. In this study we assessed the contribution that SM detection in serum and PE can give to improve the diagnosis and the routine screening of MPM in addition to Cyt.

Design: PE was obtained by thoracentesis and Cyt was evaluated on fixed smears stained by Papanicolaou's method in a total of 102 patients. Cyt, PE-SM and serum-SM levels were simultaneously evaluated for each patient. We studied 43 patients with MPM (26 epithelioid (Ept), 9 sarcomatoid (Src), 4 biphasic (Bph), 2 desmoplastic (Dsm), 2 papillary (Ppl)), 36 patients with pleural benign lesions (BNG) and 23 patients with non-MPM pleural metastasis (MTS). SM levels were detected by the MesoMark ELISA kit.

Results: By the Youden's index we found that the SM cut-off level for diagnosis of MPM was 1.08 nM in serum and 12.70 nM in PE. Serum-SM levels were > cut off in 20/43 (Se=46.5%) MPM (11 Ept, 4 Src, 4 Bph, 1 Ppl), in 3/36 (8.3%) BNG and in 6/23 (26.1%) MTS, (Sp=84.7). In contrast, PE-SM levels were > cut off in 30/43 (Se=69.8%) MPM (19 Ept, 5 Src, 2 Ppl, 4 Bph), in 3/36 (8.3%) BNG and in 4/23 (17.4%) MTS, (Sp=88.1%). Cyt allowed the diagnosis in 11/43 (Se=25.6%) cases of MPM (6 Ept, 3 Src, 1 Bph, 1 Ppl) and in 11/23 (47.8%) MTS while it was negative in 36/36 (100%) BNG. Comparison between serum-SM and Cyt demonstrated discrepancy for diagnosis in 41/102 (40.2%) cases. The serum-SM pos/Cyt neg cases were: 16/43 (37.2%) MPM (8 Ept, 4 Src, 3 Bph, 1 Ppl), 3/36 (8.3%) BNG and 5/23 (21.7%) MTS. In contrast, the serum-SM neg/Cyt pos cases were: 7/43 (16.3%) MPM (3 Ept, 3 Src, 1 Ppl,), 0/36 (0.0%) BNG and 10/23 (43.5%) MTS. Comparison between PE-SM and Cyt demonstrated discrepancy for diagnosis in 43/102 (42.2%) cases. The PE-SM pos/Cyt neg cases were: 23/43 (53.5%) MPM (15 Ept, 4 Src, 3 Bph, 1 Ppl), 3/36 (8.3%) BNG and 3/23 (13.0%) MTS. The PE-SM neg/Cyt pos cases were: 4/43 (9.3%) MPM (2 Ept, 2 Src), 0/36 (0.0%) BNG and 10/23 (43.5%) MTS.

Conclusions: SM detection may be an adjunct to Cyt for the routine screening of PE in MPM but it cannot replace it. Our data also suggest that detection of SM in PE can contribute to improve the diagnosis of Cyt in MPM more than detection of SM in serum.

1883 D2-40 as a Marker To Differentiate Malignant Mesothelioma from Non-Small Cell Carcinoma

J Felipe Lima, MC Aubry, AC Roden. Mayo Clinic, Rochester, MN.

Background: The distinction of malignant mesothelioma from other malignancies is important to guide therapy. However, the morphologic differentiation of malignant mesotheliomas from other tumors can be challenging despite several proposed panels of immunostains. D2-40 is an antibody directed against human podoplanin, a transmembrane mucoprotein that is expressed in lymphatic endothelial cells. D2-40 has been proposed as a useful marker for mesothelial differentiation. However, evidence suggests that D2-40 might also be expressed in some sarcomas and sarcomatoid carcinomas. Herein we studied the expression of D2-40 in pleural malignant mesotheliomas and compared its expression pattern to lung and other metastatic non-small cell carcinomas and sarcomatoid carcinoma.

Design: 85 cases of pleural malignant mesothelioma, non-small cell carcinoma of the lung, sarcomatoid carcinoma, and metastatic adenocarcinomas were selected based on pathology reports (1995 to 2012). Sections were stained with D2-40 antibody and were reviewed by two pathologists. Staining intensity (score 0-3+) and distribution (negative, focal, diffuse) were assessed. Membranous staining with or without cytoplasmic staining was considered positive.

Results: Diagnoses, staining intensity and distribution of all cases are summarized in Table 1.

Summary of D2-40 staining intensity and distribution (n=85)

Diagnosis (n)	Intensity (n)			Distribution (n)		Negative (n)
	3+	2+	1+	Diffuse	Focal	
Mesothelioma						
Epithelioid (23)	16	2	0	15	3	5
Biphasic (9)	3	2	0	5	0	4
Sarcomatoid (8)	6	0	0	3	3	2
Adenocarcinoma						
Lung (19)	1	0	0	0	1	18
Metastatic (13)	0	0	0	0	0	13
Squamous cell carcinoma (12)	7	0	0	0	7	5
Sarcomatoid carcinoma (1)	0	0	0	0	0	1

14 (of 40) malignant mesothelioma had strong (3+) and diffuse staining, 11 of which were of epithelioid type. No other malignant tumor tested revealed that staining pattern. Although some of the squamous cell carcinomas had strong (3+) staining for D2-40, staining was focal and predominantly in the periphery of the tumor cell nests.

Conclusions: Our results confirm that D2-40 is a useful marker to facilitate the distinction of malignant mesothelioma of the pleura from carcinomas. D2-40 is expressed in the majority of malignant mesotheliomas, independent of the morphologic subtype. Furthermore, strong and diffuse D2-40 expression by the tumor cells is only seen in malignant mesotheliomas. Squamous cell carcinomas can be strongly positive for D2-40 but staining is only focal. Larger studies are necessary to establish the value of D2-40 to distinguish malignant mesothelioma from sarcomatoid carcinomas and sarcomas.

1884 Overexpression of the Tumor Stomal Marker Periostin Is Correlated with p53 Levels in Non-Small Cell Lung Cancer (NSCLC) Detected by Immunohistochemistry Using Lung Cancer Tissue Microarray (TMAs)

TJ Gniadek, C Choi, Y Tian, H Zhang, E Gabrielson, F Askin, QK Li. Johns Hopkins University School of Medicine, Baltimore, MD.

Background: Periostin is a recently identified stromal marker. Its overexpression has been related to aggressive tumor behavior, advanced tumor stage, and increased metastatic potential in several types of cancer, including breast and prostate cancer. Recent studies have also suggested that periostin may be involved in NSCLC and that elevated levels of p53 and cyclin D1 may play a role in periostin expression. In this study, we evaluate the expression of periostin in different subtypes of NSCLC and correlate its expression with p53 and cyclinD1 levels.

Design: Using pathology archives from our academic center, two lung cancer tissue microarrays (TMAs) were constructed using surgical material, which include 81 cases of adenocarcinoma (ADC) and tumor-matched normal lung tissues as well as 91 cases of squamous cell carcinoma (SQCC). The anti-human periostin mab was used at 1:1000 dilution. Anti-p53 and cyclinD1 were used per Johns Hopkins histology standard

protocols. The staining patterns were scored semi-quantitatively as: 0 negative, 1 weak and focal, and 2 strong and diffuse. The association between Periostin and p53/cyclinD1 expression was analyzed using Goodman and Kruskai's gamma methods.
Results: The overall expression of periostin was high in 52% of ADC and 51% of SQCC. The expression of p53 was detected in both ADC and SQCC. There was a statistically significant association between periostin overexpression and elevated p53 levels in SQCC, but not in ADC (p-value: 0.0026 vs 0.13, respectively). The expression of cyclinD1 was not associated with periostin expression in either SQCC or ADC TMAs (p-values: 0.59 and 0.67).
Conclusions: Within this data set, the correlation between overexpression of periostin by tumor stromal fibroblasts and elevated p53 levels differed between SQCC and ADC of the lung. Our data suggest that overexpression of periostin may involved in p53 signaling pathway in certain subtype of cancer. While research continues into the mechanism and prognostic significance of periostin expression, these data may help refine periostin as a prognostic marker and lead to a better understanding of the tumor biology that leads to increased expression.

1885 Radiologic-Pathologic Correlation before Signout Significantly Reduces Overdiagnosis of Pulmonary Adenocarcinoma In Situ and Minimally Invasive Adenocarcinoma in Surgically Resected Lung Nodules

S Harari, J Ko, H Pass, D Naidich, J Suh. NYU Langone Medical Center, New York, NY.
Background: The 2011 IASLC/ATS/ERS multidisciplinary classification of lung adenocarcinoma defined the entities of adenocarcinoma in situ (AIS) and minimally invasive adenocarcinoma (MIA) as early-stage tumors that should have 100% and near 100% 5-year disease-specific survivals, respectively. However, it can be challenging to distinguish between areas of lepidic (in situ) growth and invasion even on permanent slides. Our aim is to investigate whether radiologic-pathologic correlation is good clinical practice for diagnosis of AIS and MIA.
Design: The radiologic and pathologic characteristics of 103 surgically resected lung adenocarcinomas at one institution (2006-10) were reviewed independently. Each tumor was re-classified using the 2011 terminology while blinded to imaging studies. All cases of possible AIS and MIA with radiologic-pathologic discrepancies underwent additional review. Next, all cases of surgically resected AIS and MIA at the same institution (2011-12) that were diagnosed following correlation with radiologic findings were collected prospectively and reviewed for discrepancies. The numbers of cases that required a change in diagnosis from AIS and MIA between the two sets were compared.
Results: 11 possible cases of AIS and 19 possible cases of MIA were identified on retrospective review, of which 4 AIS and 13 MIA were analyzed for discrepancies. 3 cases of AIS were changed to acinar predominant adenocarcinoma (APA), 3 cases of MIA were changed to lepidic predominant adenocarcinoma (LPA) and 3 cases of MIA were changed to APA. Overall, 21/30 (70%) cases were confirmed: 8/11 (73%) AIS and 13/19 (68%) MIA. In contrast, 6 cases of AIS and 6 cases of MIA were identified prospectively, of which 1 AIS and 2 MIA were analyzed for discrepancies. All 12 cases (100%) were confirmed. The difference in the numbers of cases requiring a change in diagnosis to more invasive adenocarcinomas (LPA or APA) between the two study groups was statistically significant (p-value = 0.0413).
Conclusions: Review of the CT appearance of lung nodules before signout reduces overdiagnosis of AIS and MIA in surgical resections by nearly one-third. Although it requires additional time and effort to access imaging studies and reports, radiologic-pathologic correlation should be performed when considering a final pathologic diagnosis of either tumor.

1886 Proteomic Approach Revealed Galectin-4 as a Lymph Node Metastasis Predictor in Lung Adenocarcinoma

T Hayashi, T Saito, K Takamochi, K Mitani, S Oh, K Suzuki, T Yao. Juntendo University, School of Medicine, Tokyo, Japan.
Background: Lung cancer remains the most common cause of cancer related death. Despite advances in treatment modalities, powerful prognostic and metastasis predictive markers remains unclear. The purpose of this study was to develop lymph node (LN) metastasis predictive markers in lung adenocarcinomas using a protemic approach.
Design: We examined the proteomic profile of 10 lung adenocarcinomas (5 cases with LN metastasis and 5 cases without LN metastasis) using two-dimensional difference gel electrophoresis. The predictive performance of candidates was further validated by immunohistochemistry on surgically resected specimens of 709 lung adenocarcinomas (stage I to IV). Positive staining was defined as >10% positive carcinoma cells.
Results: We identified 6 spots whose intensity was different between lung adenocarcinoma with and without LN metastasis. Subsequent mass spectrometric protein identification showed that two of six spots derived from galectin-4, a carbohydrate-binding protein belonging to the galectin family. Immunohistochemically, LN metastasis occurred 28.1 % and 15.8 % for patients with galectin-4-positvie and galectin-4-negative adenocarcinomas, respectively (P=0.0003). Notably, when we classified all adenocarcinomas by IASLC/ATS/ERS classification of lung adenocarcinoma, this trend became more obvious in acinar type predominant (LN metastasis rate: 46.9% in galectin-4-positive cases and 15.6% in galectin-4-negative cases. P<0.0001).
Conclusions: We proposed galectin-4 as a biomarker for LN metastasis predictor in lung adenocarcinomas, especially for acinar type predominant, which is the most common subtype of lung adenocarcinoma. Furthermore, this result may provide an optimum therapeutic implication after surgical treatment for lung cancer patients.

1887 Analysis of Napsin A Expression in Mucinous Lung Tumors on Histological and Cytological Specimens

JJ Heymann, RS Hoda, T Scognamiglio. Weill Cornell Medical College, New York, NY.
Background: Napsin A is a sensitive and specific marker for lung adenocarcinoma (ADCA) and can be used to distinguish primary from metastatic lung tumors. Mucinous lung tumors may be difficult to distinguish morphologically and immunohistochemically (IHC) from metastatic mucinous tumors. Napsin A expression has not been extensively studied in mucinous lung tumors. In this study, Napsin A expression was evaluated in lung and non-pulmonary mucinous tumors to determine its utility in differentiating primary from metastatic mucinous tumors.
Design: IHC for Napsin A was performed on formalin-fixed, paraffin-embedded surgical specimens or fine needle aspiration biopsy-derived, paraffin-embedded cell block (CB) specimens. Intensity and percentage of positive cells was scored by 2 pathologists as 0 (negative), 1+ (weak), 2+ (moderate), and 3+ (strong). Positive expression (+) was defined as granular, cytoplasmic staining in >10% of cells.
Results: Thirty-four primary mucinous lung tumors were identified from 2005 to 2012, of which 18 (53%) were Napsin A+. Of these, 3 (17%), 10 (56%), and 5 (28%) demonstrated 3+, 2+, and 1+ staining, respectively. Thirty-three non pulmonary mucinous tumors (10 breast, 11 colon, 5 ovary, 5 pancreas, 2 appendix) were evaluated, of which 16 (48%) were Napsin A+. Of these, 1 (6%), 14 (88%), and 1 (6%) demonstrated 3+, 2+, and 1+ staining, respectively. Zero of 10 breast and 1 of 5 ovarian tumors were Napsin A+. The 1 positive specimen showed focal, 2+ staining. Fifteen of 18 gastrointestinal primary tumors (pancreas, colon, and appendix) were Napsin A+. Concordant CB material was available for 11 surgical lung tumor specimens. Napsin A positivity was concordant between surgical and CB specimens in 6 cases (55%, 2 positive and 4 negative). In 3 of the 5 discordant cases, Napsin A expression was detected on the surgical but not the cytology specimen. The CB material in these cases were paucicellular. In 2 of the 5 discordant cases, Napsin A was negative on the surgical specimen and showed diffuse, 1+ staining on the CB.
Conclusions: Napsin A has decreased sensitivity (53% in this study) as an IHC marker of mucinous lung ADCA compared to non-mucinous lung ADCA. Because it may also be expressed by mucinous tumors originating in other sites, it is unlikely to be reliable as a sole IHC marker of lung origin for mucinous tumors (52% specificity in this study), although it may be useful in distinguishing mucinous lung ADCA from mucinous tumors of breast or ovarian origin. Interpretation of Napsin A staining may be problematic in mucinous tumor specimens of low cellularity such as CBs.

1888 Diagnostic Utility of p16 FISH in Distinguishing between Biphasic Mesothelioma and Epithelioid Mesothelioma

K Hiroshima, D Wu, K Nabeshima, T Yusa, D Ozaki, Y Nakatani, T Nishikawa. Tokyo Women's Medical University Yachiyo Medical Center, Yachiyo, Chiba, Japan; Fukuoka University, Fukuoka, Japan; Chiba Rosai Hospital, Ichihara, Chiba, Japan; Chiba University, Chiba, Japan; Tokyo Women's Medical University, Tokyo, Japan.
Background: Some of biphasic mesotheliomas may be difficult to distinguish from epithelioid mesothelioma with atypical fibrous stroma. Prognosis of patients with biphasic mesothelioma is reported to be worse than that of epithelioid mesothelioma, but better than that of sarcomatoid mesothelioma. The aim of this study was to analyze the p16 deletion in epitheliod and sarcomatoid component of biphasic mesothelioma and define the diagnostic criteria of biphasic mesothelioma.
Design: We analyzed 48 cases of pleural mesothelioma. Tumors were grouped into three categories: epithelioid, sarcomatoid and biphasic mesothelioma. Fluorescence in situ hybridization (FISH) of p16 was performed on formalin-fixed, paraffin-embedded sections using dual color locus-specific p16 probe. Both epithelioid and sarcomatoid component was analyzed separately in eight cases of biphasic mesothelioma and two cases of sarcomatoid mesothelioma with minor component of epitheliod subtype. FISH analysis was also performed in three cases of epithelioid mesothelioma with atypical cellular fibrous stroma.
Results: The percentages of homozygous deletion are 55.6% (10/18), 100% (22/22), and 87.5% (7/8) in epithelioid, sarcomatoid, and biphasic mesothelioma, respectively. Both epitheliod and sarcomatoid component harbor homozygous deletion of p16 in seven of biphasic mesotheliomas and two of sarcomatoid mesotheliomas with minor component of epithelioid subtype. In one of biphasic mesotheliomas, both component lacks homozygous deletion of p16. Fibrous stroma in three epitheliod mesotheliomas does not harbor homozygous deletion of p16. The median survival for patients are 22 months for epithelioid mesothelioma, 12 months for biphasic mesothelioma, and 5 months for sarcomatoid mesothelioma (p = 0.0015). p16 homozygous deletion is associated with shorter survival.
Conclusions: p16 is deleted in all of sarcomatoid mesotheliomas. Frequency of p16 deletion in biphasic mesothelioma is higher than that in epithelioid mesothelioma contrary to the description in 2012 IMIG guidelines for pathological diagnosis of mesothelioma. Deletion of p16 should be confirmed in fibrous component of mesothelioma when the distinction between biphasic mesothelioma and epithelioid mesothelioma with atypical fibrous stroma is difficult.

1889 Co-Expression of Estrogen Receptor-a36 and Extra-Nuclear Estrogen Receptor-a66 Is Associated with Advanced Pathological and Clinical Stages in Non-Small Cell Lung Cancer

J Huang, AC Mackinnon, A Leuvano, N Rao. Medical College of Wisconsin, Milwaukee, WI.
Background: Previous evidence has suggested that over-expression of estrogen receptors is strongly associated with tumor proliferation and progression, not only in breast cancer but also in lung cancer, particularly in non-small cell lung cancer (NSCLC). It is also well known that estrogen receptor beta (ERβ) is strongly over-expressed,

although nuclear associated ER-alpha (ER-α66) is negative or weakly expressed in most NSCLC. ER-α36, a novel spliced form of ER-α66, is highly expressed in breast cancer. Recent studies, by others and us, have demonstrated that ER-α36 is strongly associated with HER2 and EGFR, and triggers non-genomic signaling pathways in breast cancer. Whether ER-α36 expression is associated with pathological and clinical stage in NSCLC has not been studied.

Design: Expression of ER-α36, Nuclear ER-α, Extra-nuclear ER-α, ER-β, PR, HER2 and EGFR was evaluated by immunohistochemistry (IHC) in 71 NSCLC (adenocarcinoma) patients. The association, between ER-α36 expression and clinicopathological characteristics, clinical stage and other biomarkers, was also evaluated. Statistical significance was measured using Fisher's exact test.

Results: ER-α36, extra-nuclear ER-α, ER-β were expressed in all 71 patients. Strong expression of ER-α36, extra-nuclear ER-α, ER-β (Allred score ≥ 6) was observed in 46 (65%), 42 (59%) and 40(56%) patients, respectively. EGFR was expressed in 44 (62%) patients. Nuclear ER-α, PR and HER2 were negative in all patients. ER-α36 and extra-nuclear ER-α were co-expressed in 40(56%) patients. Interestingly, the patients with co-expression of ER-α36 and extra-nuclear ER-α were strongly associated with both clinical stage III – IV (P<0.001),and pathological stage T3 – T4 (p<0.05); Co-expression of ER-α36 and extra-nuclear ER-α was also strongly associated with EGFR (P<0.001), and negatively associated with ER-β (P<0.05).

Conclusions: We have demonstrated that ER-α36 is highly expressed in NSCLC and is co-expressed with extra-nuclear ER-α. Co-expression of ER-α36 and extra-nuclear ER-α appears to associate with advanced clinical and pathological stages in NSCLC. ER-α36/extra-nuclear ER-α expression also associates with EGFR, and suggesting that ER-α36 may play a critical role in activating non-genomic signaling pathways in lung cancer.

1890 Pulmonary Large Cell Carcinoma Is Clinicopathologically and Molecularly Similar to Solid Subtype Adenocarcinoma

DH Hwang, AS Perry, LM Sholl. Brigham and Women's Hospital, Boston, MA; Banner MD Anderson Cancer Center, Gilbert, AZ.

Background: Accurate histologic subtyping of non small cell lung carcinoma is critical to clinical management. According to the World Health Organization (WHO), large cell carcinoma (LCC) encompasses tumors that are not readily diagnosed as adenocarcinoma (ACA) or squamous cell carcinoma on morphologic grounds; however, the diagnosis of LCC can lead to confusion when it comes to triaging for molecular analysis. We have noted a high degree of morphologic similarity between solid-predominant ACA and many tumors diagnosed as LCC. This study compares the clinicopathologic and molecular features of solid ACA and LCC.

Design: Cases diagnosed as LCC or solid ACA on pulmonary resection specimens (excluding biopsies) were retrieved from the pathology department archives from 2000-2012. Diagnoses were confirmed following review of H&E, mucicarmine, and TTF-1 and P63 immunohistochemistry (IHC) stains. Tumors with solid growth and lack of squamous or neuroendocrine differentiation were included. Distinction between solid ACA and LCC was made according to WHO criteria (≥ 5 intracellular mucin droplets in at least 2 HPF for solid ACA). Targeted genotyping was performed for *KRAS* codons 12-13 and *EGFR* L858R and exon 19 deletions, and FISH and/or IHC (clone D5F3) for ALK rearrangement. Patient outcomes were derived from the electronic medical record following approval from the hospital institutional review board.

Results: 29 solid ACA and 30 LCC were included. There was no difference in the ratio of female patients (56 v 52%), median age (60 v 66), stage at diagnosis (64 v 69% were stage I) and percent smokers (96 v 97%) between solid ACA and LCC cohorts, respectively. Other than the presence or absence of mucin droplets, the dominant pathology in both groups was similar, with solid nests of polygonal cells with moderate cytoplasm, frequent clear cell change, vesicular chromatin, and prominent nucleoli. KRAS was mutated in 32% of solid ACA versus 41% of LCC (p = 0.5); 55% of KRAS mutations were G12C. No EGFR mutations were identified. One ALK rearrangement was detected in the solid ACA group. Risk of progression at 5 years was 21% for solid ACA v 27% for LCC (p=0.76).

Conclusions: LCC (without neuroendocrine features) appears to be morphologically, molecularly, and clinically indistinguishable from solid-subtype ACA. These tumors occur in smokers and have a preponderance of smoking-associated KRAS mutations. We propose that these tumors be reclassified as mucin-poor solid adenocarcinomas.

1891 Diagnostic Value of Immunohistochemistry for the Detection of the BRAFV600E Mutation in Primary Lung Adenocarcinoma Caucasian Patients

M Ilie, E Long-Mira, V Hofman, B Dadone, C-H Marquette, J Mouroux, J-M Vignaud, H Begueret, J-P Merlio, D Capper, A von Deimling, J-F Emile, P Hofman. Pasteur Hospital, Nice, France; Central Hospital, Nancy, France; Haut-Lévêque Hospital, Pessac, France; Institute for Pathology, University of Heidelberg, Heidelberg, Germany; Ambroise Paré Hospital, Boulogne, France.

Background: Non-small cell lung carcinoma (NSCLC) patients with a BRAFV600E mutation benefit from targeted therapy. The usefulness of immunohistochemistry (IHC) as an alternative approach for detection of BRAFV600E in NSCLC patients has not been evaluated until now. This study compared the specificity and sensitivity of IHC with other methods for detection of BRAFV600E in primary lung adenocarcinoma.

Design: BRAF mutations were analyzed by DNA sequencing of a Caucasian subpopulation of selected 450/1509 (30%) EGFR, KRAS, PI3KA, Her2 and EML4-ALK wild-type (wt) primary lung adenocarcinomas. Detection of the BRAFV600E mutation was performed by IHC using the VE1 clone antibody and compared to results of other molecular methodologies.

Results: 40/450 (9%) of tumors harbored a BRAF mutation, which corresponded to either a BRAFV600E or a non BRAFV600E mutation in 21/450 (5%) and 19/450 (4%) cases, respectively. IHC VE1 assay was positive in 19/21 (90%) BRAFV600E mutated tumors and negative in all BRAFnonV600E mutated tumors.

Conclusions: IHC using the VE1 clone is a specific and sensitive method for the detection of BRAFV600E and may be an alternative to molecular biology for detection of mutations in NSCLC.

1892 Full-Field Optical Coherence Tomography (FFOCT): A Potential Alternative to Frozen Section Analysis

M Jain, N Narula, B Salamoon, N Altorki, S Mukherjee. Weill Medical College of Cornell University, New York, NY.

Background: Full-field optical coherence tomography (FFOCT) a real-time imaging technique generates high-resolution 3D tomographic images from fresh (unprocessed) tissues. Lack of tissue processing and associated artifacts, along with the ability to generate large-field images quickly, warrants its exploration as an alternative to frozen section analysis. We assessed the potential of FFOCT in distinguishing lung tumor from adjacent normal tissue in lobectomy specimens.

Design: Fresh sections from tumor and adjacent normal lung (n=13 lobectomy specimens) were imaged with a commercial FFOCT device. A blinded analysis was conducted by the attending lung pathologist at WCMC. Sample stacks from tumor and adjacent normal lung were shown to familiarize with FFOCT images. Then "test" stacks (normal=10 and tumor=16) were presented in a blinded manner, and the pathologist commented on the presence or absence of tumor. These observations were confirmed on the corresponding H&E slides.

Results: Normal components of lung such as alveoli, pleura and blood vessels were readily identified with FFOCT. Presence of tumor was correctly identified in 15/16 stacks. In 1 case, adenocarcinoma with lepidic-predominant pattern was diagnosed as "equivocal". In tumor-free lung, absence of tumor was reported with confidence in 5/10 stacks and was considered "equivocal" in the rest. This false positive diagnosis was mainly encountered in areas with collapse lung architecture.

Figure 1

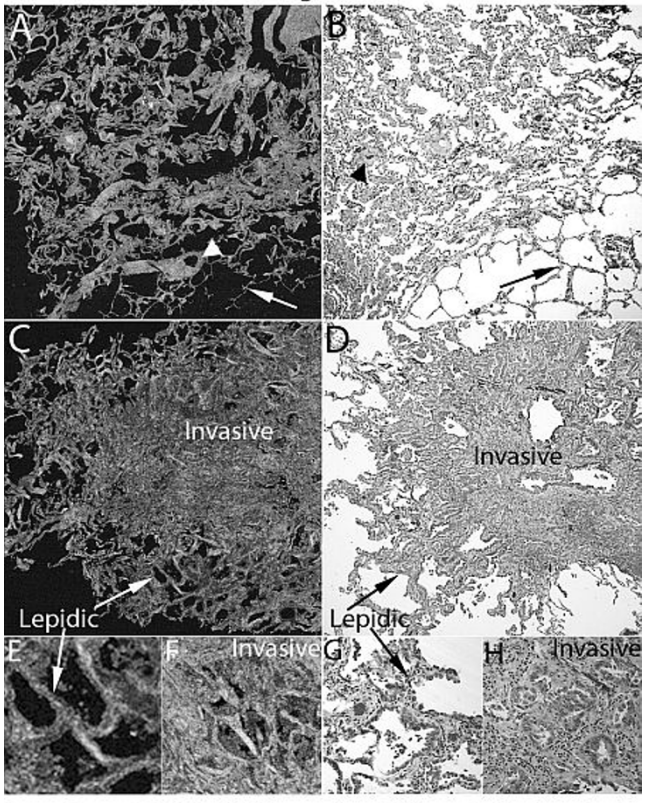

Figure 1. Comparative FFOCT and H&E images of lung. A-B, Non-neoplastic lung tissue showing alveoli (arrows) and blood vessel (arrowheads). C-D, Invasive adenocarcinoma with lepidic and invasive patterns. E-H, Zoomed images from panels C and D showing lepidic and invasive patterns. (FFOCT field of view: A, C = 3.5mm2. H&E total magnifications: B, D = 40X. Insets: FFOCT: E,F = 2x zoom. H&E: G, H = 200X).

Conclusions: Our study provides preliminary evidence for the utility of FFOCT in identifying lung tumors, opening up the potential for using it in limited lung resections during intraoperative consultations. The high false positive rates found in this study could be reduced by: (1) increased experience and sample size; (2) carrying out morphometric analysis and color-coding areas of interest (.cellular vs. extracellular); (3) using fast-staining nuclear dyes to distinguish cellular areas from collapsed areas; (4) exploring multimodal imaging approaches (e.g., combining with fluorescence etc.).

1893 Multiphoton Microscopy: A Potential "Optical Biopsy" Tool for Real-Time Evaluation of Lung Tumors without the Need for Exogenous Contrast Agents

M Jain, N Narula, A Aggarwal, N Altorki, S Mukherjee. Weill Medical College of Cornell University, New York, NY.

Background: Multiphoton microscopy (MPM), an optical imaging technique that generates subcellular-resolution images from unprocessed and unstained tissue. While miniaturization of MPM for in vivo use is in progress, here we assess its diagnostic potential in fresh *ex vivo* human lung tissue, utilizing a bench-top system.

Design: Fresh sections from tumor and adjacent non-neoplastic lung {n = 20 lobectomy specimens} were imaged with MPM and then compared with corresponding hematoxylin and eosin (H&E) slides.

Results: Alveoli, bronchi, blood vessels, pleura, smokers' macrophages and lymphocytes were readily identified with MPM in non-neoplastic tissue. Atypical adenomatous hyperplasia / adenocarcinoma in situ (a preinvasive lesion) was identified in tissue adjacent to the tumor in one case. Out of 20 tumor sections imaged, 2 were non-diagnostic due to extensive necrosis and elastosis, confirmed later on H&E and Verhoeff's stain, respectively. Of the remaining 18 cases, all adenocarcinoma (16/16), were correctly diagnosed on MPM, along with their histological patterns. Of the 2 cases of squamous cell carcinoma, 1 was correctly diagnosed, whereas the second was misdiagnosed as adenocarcinoma due to pseudo-gland formation. Increase in collagen was noticed in invasive adenocarcinomas, particularly with acinar and solid patterns.

Figure 1

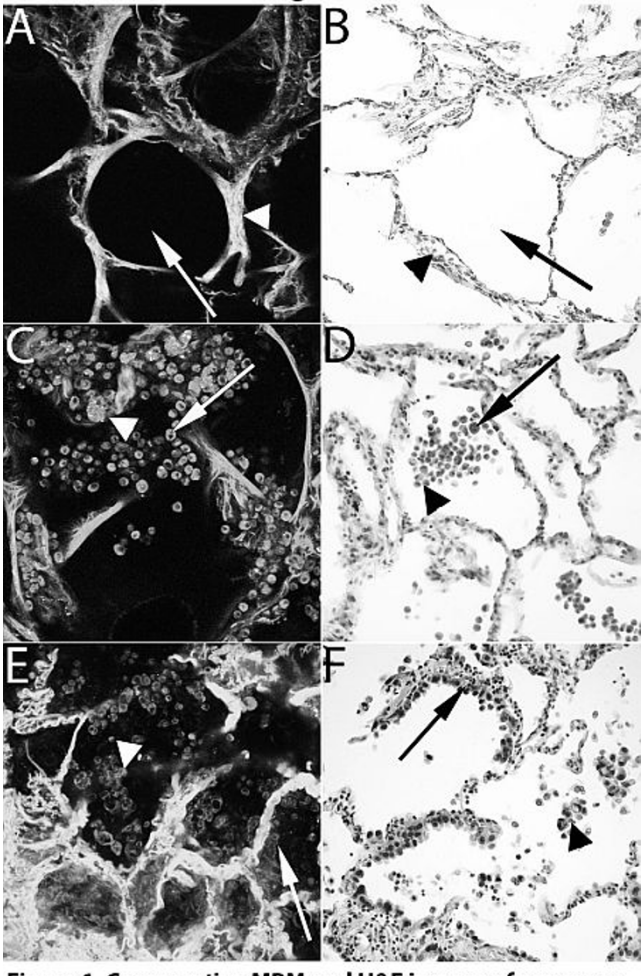

Figure 1. Comparative MPM and H&E images of non-neoplastic lung and adenocarcinoma. A-B, Alveoli (arrows) with septal wall (arrowheads). C-D, Alveoli with carbon-laden and non carbon-laden macrophages (arrows; blue and arrowheads; green, respectively). E-F, Adenocarcinoma with lepidic predominant pattern (arrows) and few clusters of free-floating tumor cells (arrowheads).(MPM total magnifications: A, C,E = 300X. H&E total magnifications: B, D,F = 200X).

Figure 2

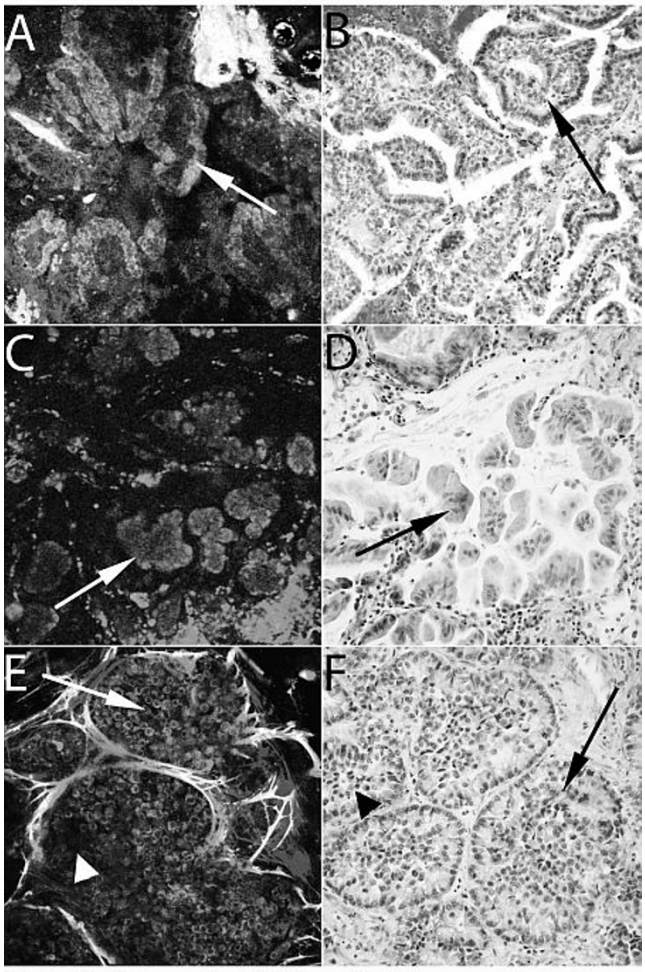

Figure 2. Comparative MPM and H&E images of invasive adenocarcinoma of lung showing various histological patterns. A-B, Papillary pattern (papillae with fibrovascular core; arrows). C-D, Micropapillary pattern with small papillae (arrows) lacking true fibrovascular cores. E-F, Solid (arrows) and acinar patterns (arrowheads). (MPM total magnifications: A, C, E = 300X. H&E total magnifications: B, D, F = 200X).

Conclusions: Our study demonstrates the utility of MPM for differentiating neoplastic from non-neoplastic lung tissue and identifying the histological subtype of tumor. We foresee future real-time applications using miniaturized instruments for directing lung biopsies, assessing their adequacy for subsequent histopathological analysis and intraoperatively for evaluating surgical margins in limited lung resections.

1894 Correlation of EGFR Immunohistochemistry and Molecular Analysis in Lung Adenocarcinoma

E Jeffrey, G Tesha, C Cynthia. Emory University, Atlanta, GA.

Background: Lung adenocarcinomas with epidermal growth factor receptor (EGFR) mutations portend increased survival and response to targeted therapy. 90% of mutations that respond to gefitnib and erlotinib are delE746-A750 in exon 19 (del 19) and L858R in exon 21 (L858R). Accepted method of analysis is PCR amplification and sequencing of exons 18 through 21, performed by reference laboratories. Monoclonal antibodies are available against the two common mutations; studies show that immunohistochemistry (IHC) correlates with mutational analysis on cytology specimens. The aims of our study are: 1) to augment the number of cases evaluated in the literature; 2) to validate stains for our laboratory; and 3) to evaluate use of IHC as screening for mutational analysis referral.

Design: Of 444 specimens with EGFR mutational analysis from 2010-2012, we identified 54 mutated cases with paraffin blocks for staining. 58 known wild-types were selected as negatives. Two rabbit monoclonal Abs with specificities for 15 bp, E746-A750 deletion in exon 19, and exon 21 L858R (Cell Signaling Technology, Inc., Danvers, MA) were used at 1:50 dilution with high pH antigen retrieval. IHC slides were blindly reviewed and staining was scored: 0 (none); 1+ (faint membrane/cytoplasm); 2+ (moderate membrane); 3+ (intense/crisp membrane). Cutoff for positivity was >10% of tumor cells staining 1+ or any amount of 2+ or 3+.

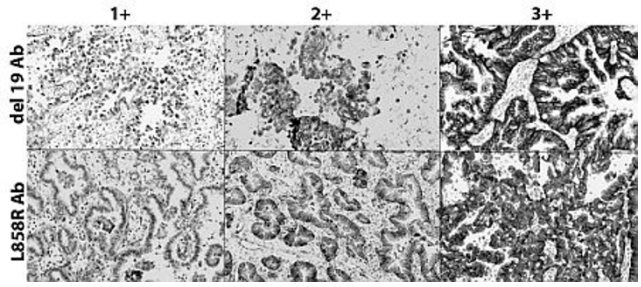

Results: Fifty-four known EGFR mutations by molecular analysis included: twenty-four (del 19); twenty-one (L858R); nine (various mutations including insertion 20 and T790M). By IHC, four false negatives were identified in the del 19 group; zero in the L858R group and three in the various mutation group. Results of 58 known wild type (no mutations by molecular analysis) included: one false positive (del 19); two false positives (L858R).

IHC and Molecular Correlation

	PCR - EGFR Mutated (54)	PCR- EGFR WT (58)
+IHC # (%)	47 (87)	3 (5)
-IHC # (%)	7 (13)	55 (95)

Sensitivity = 0.87; Specificity = 0.95; Positive Predictive Value = 0.94; Negative Predictive Value = 0.89

Conclusions: The two antibodies del 19 and L858R reliably ascertain EGFR mutational status. IHC is comparatively inexpensive, quick and easy to perform, and could serve as a first line test in patients with pulmonary adenocarcinoma.

1895 Complex Glands (Cribriform and Fused Glands) Are Patterns of High Grade Adenocarcinoma in the Lung

P Joubert, N Rekhtman, AL Moreira. Memorial Sloan-Kettering Cancer Center, New York, NY.

Background: The recently proposed IASLC/ATS/ERS classification of pulmonary adenocarcinoma has a prognostic value by classifying the heterogeneous adenocarcinomas according to the predominant component of the tumor. The classification recognizes 5 patterns of adenocarcinoma: lepidic, acinar, papillary, solid, and micropapillary. Furthermore, an independent grading system for lung adenocarcinomas was recently proposed which is based on a combination of the two most predominant amounts of these 5 patterns. However, the occurrence of other patterns that do not fit into these defined morphologies poses a challenge for applying this classification and grading systems.

Design: 283 resected pulmonary adenocarcinomas were reviewed and classified according to above systems. The amounts of the standard 5 patterns as well as non-standard patterns, including cribriform, ragged/fused glands were recorded for each case. The association of non-standard patterns with the predominant type of adenocarcinoma, tumor grade, and disease free survival (DFS) were evaluated.

Results: Ragged/fused glands and cribriform pattern were seen in 28%, 18.7% of cases, respectively. The amount of cribriform and ragged/fused glands ranged from 10 to 100% of the entire tumor. Ragged/fused glands and cribriform patterns were associated with solid growth pattern ($p<0.001$ Fisher exact test) and high tumor grade ($P<0.0001$ Fisher exact test). Disease-free survival for tumors containing complex glandular patterns was similar to high grade tumors (log rank $p= 0.8523$), and significantly worse than low-grade tumors.

Conclusions: It is important to recognize the presence of these variant patterns of adenocarcinoma, which should be considered as patterns of high grade adenocarcinoma and not be interpreted as acinar adenocarcinoma which is prognostically a pattern of intermediate grade.

1896 Napsin A Expression in Neuroendocrine Tumors of the Lung

P Joubert, H Wang, MS Roh, MC Pietanza, I Sarkaria, WD Travis, N Rekhtman. Memorial Sloan-Kettering Cancer Center, New York, NY; College of Medicine, Dong-A University, Busan, Korea.

Background: Napsin A is an aspartic proteinase involved in surfactant protein maturation, which is normally produced by type 2 pneumocytes. Recently, Napsin A has emerged as a useful supplement to TTF-1 as a marker of lung adenocarcinomas. A comparative study of Napsin A and TTF-1 expression in a large series of lung neuroendocrine tumors has not been performed.

Design: A total of 297 lung neuroendocrine tumors, including typical carcinoids (TC) n=89, atypical carcinoids (AC) n=89, small cell lung carcinomas (SCLC) n=37, and large cell neuroendocrine carcinomas (LCNEC) n=82, were evaluated for Napsin A (rabbit antibody, Ventana) and TTF-1 (8G7G3/1; DAKO) expression by immunohistochemistry on tissue microarray (TMA) sections, containing three representative cores per case. The percentage of positive tumor cells and intensity of staining (1+, 2+, 3+) were recorded.

Results: The staining results are summarized in the table below. Napsin A immunoreactivity was found in none of TCs, ACs, and SCLCs, whereas 8/82 (10%) of LCNECs showed a strong and diffuse labeling. TTF-1 reactivity was seen in 22% TCs, 40% ACs, 70% SCLCs and 46% LCNECs. When positive, TTF-1 labeling was typically strong and diffuse in SCLCs and LCNECs, while usually weak and focal in carcinoid tumors.

	Napsin A			TTF-1		
	Number of positive cases (%)	Percentage of positive cells (mean±SD)	Intensity of staining (mean±SD)	Number of positive cases (%)	Percentage of positive cells (mean±SD)	Intensity of staining (mean±SD)
TC	0/88 (0)	-	-	20/89 (22)	27±30	1.2±0.41
AC	0/89 (0)	-	-	33/83 (40)	29±26	1.13±0.34
SCLC	0/37 (0)	-	-	26/37 (70)	71±32	1.90±0.68
LCNEC	8/82 (10)	79±23	2.25±0.66	39/84 (46)	69±29	2.04±0.53

SD: standard deviation

Conclusions: To our knowledge, this is the first report of Napsin A expression in a subset of LCNECs. Conversely, all other lung neuroendocrine tumors are consistently Napsin A-negative, which contrasts with the well-known expression of TTF-1 in all types of lung neuroendocrine tumors. Based on these data, we conclude that unlike TTF-1, Napsin A cannot be used as a marker of a lung origin for carcinoid tumors. Furthermore, Napsin A cannot be used to reliably differentiate lung adenocarcinomas from LCNECs, although Napsin A reactivity raises the possibility that a subset of LCNECs has a histogenetic relationship to adenocarcinomas.

1897 MECT1-MAML2 Fusion Transcript Expression in Lung Mucoepidermoid Carcinoma

N Kalhor, J Fujimoto, J Rodriguez, LA Byers, MS Kies, WL Hofstetter, AK El-Naggar, D Bell. University of Texas MD Anderson Cancer Center, Houston, TX.

Background: Mucopeidermoid carcinoma (MEC) of tracheobronchial tree is a rare primary lung malignancy. Over the last two decades, an association between salivary gland MEC and *MECT1-MAML2* gene fusion has become well established. This translocation appears to confer a low grade histology and favorable prognosis in MEC. However, its frequency and clinicopathological significance in tracheobronchial MECs is not well established due to their low incidence.

Design: Thirteen cases of tracheobronchial mucoepidermoid carcinoma were retrospectively analyzed for *MECT1-MAML2* fusion transcript by a nested-PCR assay using formalin-fixed, paraffin-embedded specimens. All patients underwent surgical resection of the tumor except for one patient with a high grade MEC who had multifocal involvement of the tracheobronchial tree. Clinical data of the patients were obtained from their clinical records. Histologically, cases included in this study consisted of 10 low grade and 3 high grade MECs.

Results: Eight of eleven (73%) cases with successfully amplified DNA were positive for *MECT1-MAML2* fusion transcripts. All the fusion-positive tumors were low grade. It is interesting to note that 7/11 cases were misdiagnosed on biopsy material. The most common diagnoses mistaken for MEC in biopsy material were adenocarcinoma and squamous cell carcinoma.

Conclusions: We demonstrate that low grade tracheobronchial MECs are frequently (88%) associated with *MECT1-MAML2* fusion transcript. The presence of MAML2 rearrangement can be used as supportive evidence in diagnosis of tracheobronchial MECs.

1898 Expression of microRNA miR-205 in Pulmonary Squamous Cell Carcinoma and Adenocarcinoma

K Kalra, L Xue, EE Chang, R Pillai, MB Amin, DJ Luthringer. Cedars-Sinai Medical Center, LA, CA; BioGenex Laboratories, Fremont, CA.

Background: Lung cancer represents a heterogeneous group of tumors comprised of mostly squamous cell carcinomas (SCC) and adenocarcinomas (AD). These tumors can be challenging to classify due to heterogeneity, sampling, and lack of differentiation. Targeted molecular therapies for lung cancer treatment require accurate classification for optimal response. MicroRNAs (miRNAs) are endogenous, non-coding RNAs with critical functions on gene regulation. microRNA expression profiles have great potential in tumor diagnosis and prognosis since they play essential roles in tissue differentiation during normal development and oncogenesis. miR-205 has been shown to regulate E-cadherin and possibly target PTEN, and thus have role in tumor supressor function. The purpose of this study is to explore the utility of miR-205 expression in distinguishing SCC and AD.

Design: Samples of 10 formalin-fixed paraffin-embedded lung cancers (5 AD; 5 SCC) were classified using H&E staining and confirmed by IHC using anti-TTF1 (BioGenex, BGX397A) and anti-p63 (BioGenex, AM418) antibodies. 5 normal lung samples served as controls. FAM-labeled miR-205 (BioGenex, HM205) and One-step ISH Detection Kit (BioGenex, DF400) were used in this study. Slides were heated in Nucleic Acid Retrieval Solution I (NAR-I, BioGenex) for 10 min at 92C, subjected to hybridization buffer for 30 min, incubated with 40 nM of microRNA probe for 60 min at 50 C followed by stringency washes. The signal was amplified with anti-fluorescein antibody and poly-HRP labeled secondary antibody, which can develop brown color with DAB chromogen. Scramble probes served as negative control. The staining results were independently reviewed by pathologists to render diagnostic impression.

Results: Using miRNA *in situ* hybridization system, we found that miR-205 was up-regulated in 4/5 (80%) of lung SCC and 2/5 (40%) of AD. Scramble (negative controls) probes were non-reactive.

Conclusions: This result suggests miR-205 may have the potential to differentiate SCC from AD. Additional studies are in progress to determine the utility of miR-205 expression in differentiating sub-types of lung cancer. Importantly, microRNAs may be utilized as a diagnostic tool in lung cancer classification.

1899 Expression of IMP3 and Deletion of p16 Are Diagnostic and Prognostic Biomarkers in Mesothelial Proliferations

M Karanian, N Le Stang, F Galateau Salle. CHU Caen Cote De Nacre, Caen, France.

Background: IMP3 is an oncofetal protein known as sensitive and specific marker of malignancies. Few studies were available about IMP3 expression in mesothelial proliferations. P16 deletion is one of the most common molecular abnormalities in malignant mesothelioma. First aim was to confirm the utility of IMP3 to distinguish benign from malignant mesothelial proliferations, alone or in association with p16 deletion. Second aim was to study IMP3 expression in a spectrum of mesothelial pathology.

Design: IMP3 expression was studied by immunochemistry (dako) and p16 deletion was studied by Fluorescence in situ hybridization (vysis) in 35 epithelioïd mesothelioma (EM), 26 mesothelioma in situ (MIS), 37 atypical mesothelial proliferations (AMP) and 20 reactive mesothelial proliferations (RPM). Expression of IMP3 was considered positive when more than 10% tumor cells showed cytoplasmic staining. Intensity staining was graded as very weak, weak to moderate, moderate to strong and strong. P16 was deleted when more than 50% tumor cells showed 1 allelic probe and 2 centromeric probes. Fischer exact test and log rank test were used.

Results: IMP3 expression was significantly more frequent in EM (24, 65%) and in MIS than in AMP (11, 29%) and RMP (0%) (p=0,0015). IMP3 staining was significantly stronger in EM (21, 60%) and MIS (16, 62%) than in AMP (6, 16%) (p>0,0001). P16 deletion was more frequent in EM (18, 51%) and MIS (12, 46%) than in AMP (6, 17%) and RPM (0%). IMP3 expression was mostly observed in cases with p16 deletion (29, 81%) than in cases without deletion (23,29%) (p=0,001). Survival was significantly decreased in IMP3 positive cases (14 versus 55 months, p<0,001), in cases with a strong IMP3 staining (11 versus 55 months, p>0,001) and finally in cases with a deletion of p16 (14 versus 40 months, p<0,0001). IMP3 was more sensitive (67%) than p16 deletion (50%), both were very specific (100%) for mesothelioma. Using 2 tests concomitantly increase the sensitivity (75%). IMP3 staining was heterogeneous in 31 (59%) that can be a limit in small biopsies.

Conclusions: To our knowledge, this is the first time that IMP3 appears as a prognostic marker in mesothelioma. For the diagnosis of mesothelioma versus reactive mesothelial proliferation, IMP3 expression is more sensitive than p16 deletion and highly specific.

1900 Pathway Interplay: Activation of EGFR, ERK, and AKT in Early-Stage Lung Adenocarcinomas

AE Kovach, V Morales-Oyarvide, DE Shvetz, S Tammireddy, V Klepeis, EJ Mark, D Dias Santagata, AJ Iafrate, M Mino-Kenudson. Massachusetts General Hospital (MGH), Boston, MA; MGH, Boston, MA.

Background: Lung adenocarcinomas have several driver mutations including *EGFR* and *KRAS* mutations that share downstream signaling for tumor initiation and maintenance. The activation/phosphorylation of signaling pathways relative to driver mutations has not been well studied in clinical samples. We investigated the phosphorylation states of EGFR, ERK (a target of KRAS in the MAPK pathway), and AKT (PI3K pathway) in molecularly defined early-stage lung adenocarcinomas and evaluated their interaction with each other, with driver mutations, and with clinicopathologic characteristics.

Design: The cohort consisted of 155 resected Stage 0-2 lung adenocarcinomas previously analyzed for *EGFR*, *KRAS*, and other driver mutations by a multiplex PCR-based assay. Tumors were stained on tissue microarrays with antibodies against phospho (p)-EGFR, p-ERK, and p-AKT. Average composite scores were assigned using H-scores (0-300). Cut-offs for positivity were based on mean scores and expression in normal epithelium. Clinicopathologic parameters included smoking status, tumor size, predominant histological pattern, and recurrence-free survival (RFS).

Results: p-EGFR expression was associated with p-AKT expression (p<0.001) but not with p-ERK expression. p-ERK expression was associated with *KRAS* mutations (p<0.0001) but not with *EGFR* or other mutations. Neither p-EGFR nor p-AKT expression was associated with any mutation including *EGFR*. Similarly, p-ERK expression was more prevalent in tumors from smokers (p=0.020) and those with in situ carcinoma or minimal invasion (p=0.023). Interestingly, the 3-year RFS was significantly better in subjects with p-EGFR expression than those without (p=0.037), and p-ERK expression was associated with improved 3-year RFS across the entire cohort (82.6% vs. 65.4%, p=0.025) and in cases with extensive invasion (75.4%vs. 65.4%, p=0.086). Other clinicopathologic correlations were not found.

Conclusions: These results confirm that *KRAS* mutations correlate with activation of the downstream target ERK, especially in early stage tumors and that ERK inhibition may be in turn an effective therapeutic strategy for *KRAS* mutants. Factors in addition to *EGFR* mutations may activate EGFR, which is more likely to activate PI3K-AKT than MAPK/ERK, at least on the protein level. Whether p-EGFR and/or p-ERK expression predict improved survival after resection of early stage lung adenocarcinomas needs to be evaluated in larger studies.

1901 The Pathology of Pulmonary Vein Radiofrequency Ablation

AE Kovach, GZ Cheng, CL Channick, R Channick, HA Gaissert, A Muniappan, RL Kradin. Massachusetts General Hospital (MGH), Boston, MA; MGH, Boston, MA.

Background: Radiofrequency ablation of pulmonary veins is a common therapeutic intervention for atrial fibrillation. Pulmonary vein stenosis and venoocclusive disease are recognized complications of this procedure. A recent case at our hospital showed associated inflammatory pseudotumor formation. The spectrum of pathologies addressing post-ablation complications has not been previously reviewed.

Design: Two surgical resections from MGH were reviewed by light microscopy, one of pseudotumor formation with associated pulmonary vein stenosis. A literature search was performed for the following terms: "histology," "pathology," and "histopathology" each with "pulmonary vein radiofrequency ablation atrial fibrillation." Pathologic features of the MGH cases were compared with those in existing reports.

Results: Published descriptions were identified from 22 subjects, including 1 from MGH. The earliest lesions (2-6 days post-ablation) demonstrated hyperemic pulmonary vein branches (23%), some obliterated by thrombi (14%), and vacuolar changes in associated nerve fibers (14%). At 21-22 days post-ablation, well-delineated ablation sites were present and consistent with direct thermal injury, with fragmented collagen, granulation tissue, necrotic foci, and thinned adjacent myocardium. More established lesions (4-37 months) had transmural fibrosis of the intervened pulmonary vein (53%), pulmonary venoocclusive change of collateral veins associated with marked ventilation-perfusion mismatches (14%), thrombosis and pulmonary parenchymal infarction (9%), interstitial and mediastinal fibrosis (9%), venous tortuosity (5%), and hypertensive arteriopathy (5%). In an additional recent case at MGH, a left hilar soft tissue mass was identified in association with superior pulmonary vein stenosis in a patient 4 years post-ablation. On resection, this proved to be an inflammatory pseudotumor composed of myofibroblasts in an organizing pneumonia-type pattern with adjacent osseous metaplasia. Pulmonary venoocclusive change was also a prominent feature.

Conclusions: Literature on the histopathology of post-radiofrequency ablation complications is limited. The severity of vascular pathology appears to increase with the post-ablation interval. Although pulmonary vascular changes are the most common finding in more established lesions, fibroinflammatory changes including mediastinal fibrosis and pulmonary pseudotumor formation, likely later complications of thermal injury, should be considered in the differential diagnosis of these cases.

1902 Intrapulmonary Mesothelioma Simulating Interstitial Lung Disease: A Distinctive Variant of Mesothelioma. Report of 5 Cases and Review of the Literature

BT Larsen, JRH Klein, H Hornychova, R Nuti, S Thirumala, KO Leslie, TV Colby, HD Tazelaar. Mayo Clinic, Rochester, MN; University of Manitoba, Winnipeg, MB, Canada; Charles University Prague, Hradec Kralove, Czech Republic; Texas Tech University Health Science Center, Lubbock, TX; AmeriPath, Lubbock, TX; Mayo Clinic, Scottsdale, AZ.

Background: Mesothelioma is an uncommon thoracic malignancy that typically encases lungs and mediastinal structures in a thick rind, while relatively sparing lung parenchyma. We describe an unusual presentation of mesothelioma characterized by diffuse intrapulmonary growth, without significant pleural involvement, clinically simulating interstitial lung disease.

Design: We identified 5 patients (median age 56 yrs, all men) with intrapulmonary mesothelioma in our pathology consultation practices from 2010-2012. Clinical history, imaging, and pathology materials were reviewed.

Results: Clinical symptoms included chronic shortness of breath with or without cough (4 cases) and acute shortness of breath with bilateral pneumothorax (1). Chest imaging showed diffuse ground glass opacities in all cases, as well as reticular abnormalities (2), small pleural effusions (2), and scattered small nodular densities (1). Pleural plaques, thickening, or masses were not seen. A presumptive clinicoradiologic diagnosis of interstitial lung disease was made in all cases, and wedge biopsies were performed. Histologic evaluation revealed plump epithelioid or bland spindled cells with various growth patterns, including areas of alveolar filling by tumor cells mimicking desquamative interstitial pneumonia (DIP), nodular hyalinized fibrosis mimicking pneumoconiosis, lepidic growth mimicking reactive pneumocytes or adenocarcinoma in situ, and tubulopapillary and micropapillary patterns mimicking invasive adenocarcinoma. Initial diagnoses by referring pathologists included DIP (1), hypersensitivity pneumonitis (1), reactive changes (1), and mesothelioma (2). Consultative review revealed focal microscopic pleural involvement in 4 cases. Additional immunohistochemistry showed at least 3 positive mesothelial markers and at least 3 negative adenocarcinoma markers in all cases, consistent with mesothelioma. Median survival with and without chemotherapy was 28 months (3) and 3.5 weeks (2), respectively.

Conclusions: "Diffuse parenchymal pulmonary mesothelioma" is a rare and distinctive presentation that clinically mimics interstitial lung disease. Recognition of this occurrence is essential to avoid misdiagnosis.

1903 Neurotrophic Tyrosine Kinase Receptor Type 1 and 2 (NTRKA and NTRKB) Expression in Non Small Cell Lung Cancers (NSCLC)

K Laziuk, A Tarasen, CE Sheehan, JS Ross. Albany Medical College, Albany, NY.

Background: The *NTRKA* and *NTRKB* genes encode for tyrosine kinase receptors that regulate the MAPK pathway and play roles in neuronal development and differentiation. *NTRKA* and *NTRKB* mutations have been reported in NSCLC, but their prognostic significance is not currently known.

Design: Formalin-fixed, paraffin-embedded sections from 138 NSCLC, including 42 squamous cell carcinomas (SCC), 63 adenocarcinomas (AC), and 33 bronchoalveolar carcinomas (BAC), were immunostained by a manual method with NTRKA and NTRKB rabbit monoclonal antibodies (Cell Signaling Technology, Danvers, MA). The staining pattern was semiquantitatively assessed based on staining intensity and distribution and the results were correlated with morphologic and prognostic variables.

Results: Immunoreactivity for NTRKA and NTRKB was predominately cytoplasmic. NTRKA overexpression was noted in 36/138 (26%) tumors and correlated with tumor type [50% SCC vs 21% AC vs 6% BAC, p<0.0001] and high grade [32% high vs 4% low, p=0.003], and male gender (34% male vs 16% female, p=0.016). NTRKB overexpression was noted in 27/138 (20%) tumors and correlated with tumor type [52% SCC vs 8% AC vs 0% BAC, p<0.0001] and high grade [27% high vs 0% low, p=0.002], and male gender (29% male vs 7% female, p=0.001), while showing a trend

toward correlation with tumor size [28% >= 3.0 cm vs 15% < 3.0cm, p=0.076). There was significant co-expression of the two proteins (p<0.0001). On multivariate analysis, advanced stage (p=0.002) independently predict shortened survival.

Conclusions: Increased expression of NTRKA and NTRKB protein in NSCLC is associated with tumor subtype and grade in NSCLC. Given the recent evidence that NSCLC harboring a gene fusion based activation of *NTRKA* could be sensitive to tyrosine kinase inhibitors, further study of NTRK expression in NSCLC appears warranted.

1904 Correlation of Cytomorphology and Molecular Findings in *EGFR, KRAS,* and *ALK*-Positive Lung Carcinomas

Z Li, S Dacic, L Pantanowitz, W Khalbuss, M Nikiforova, SE Monaco. University of Pittsburgh Medical Center, Pittsburgh, PA.

Background: There is increasing emphasis on the subclassification of non-small cell lung carcinomas (NSCLC) and the molecular features in order to guide treatment. Histological studies have suggested some morphological features that predominate in mutation positive tumors. Our aim was to look at cytology cases that were positive for *EGFR*, *KRAS, or ALK* and to determine if these positive cases had distinct cytomorphology.

Design: FNA cases of NSCLC that had mutation studies for *EGFR* or *KRAS* or FISH studies for *ALK* were identified from our archives between 2007-2012. The slides were evaluated for cytological features, and correlated with histological follow-up and molecular data.

Results: 62 (39%) out of 160 cases were positive for mutation, including 39 (31%) positive for KRAS and 20 (14%) for *EGFR* (12 *EGFR* 19, 7 *EGFR* 21, 1 *EGFR* 20), and 4 (3%) for *ALK*. One case (0.6%) was positive for *EGFR* 19 and *ALK*. The majority of the cases were primary lung FNAs (60%), and 50 (79%) were available for review. Table 1 summarizes the findings. More of the *ALK* and *KRAS* cases had a diagnosis of NSCLC, favor adenocarcinoma (ADC) or NSCLC NOS than EGFR cases (25% and 51%, vs. 5%). Eosinophilic granular cytoplasm was seen in more *ALK* and *KRAS* cases than *EGFR* cases (100% and 32% vs. 6%). The mean nuclear grade was higher in KRAS and ALK cases than in EGFR cases (2.2 and 2.3 vs. 1.9). Necrosis was also more common in *ALK* and *KRAS* cases (67% and 65% vs. 13%). Sixteen cases with histological follow-up showed ADC in 14 cases (88%) and NSCLC NOS in 2 cases (12%).

Table 1. Summary of mutation-positive cases.

Type of Case			ALK1+	KRAS+	EGFR+	Total
Cytology Diagnosis	Adeno # (%)		3 (75)	19 (49)	19 (95)	41 (65)
	NSCLC, favor Adeno # (%)		1 (25)	11 (28)	1 (5)	13 (21)
	NSCLC, NOS # (%)		0 (0)	9 (23)	0 (0)	9 (14)
Cytology findings	Nuclear grade	1	0/3	3/31	5/16	8/50
		2	2/3	19/31	8/16	29/50
		3	1/3	9/31	3/16	13/50
	Cytoplasm	Eosinophilic, granular	3/3	10/31	1/16	14/50
		vacuolated, glassy	0/3	21/31	15/16	36/50
	background	clean	1/3	11/31	14/16	26/50
		necrotic	2/3	20/31	2/16	24/50

*Note: 1 case was positive for both EGFR exon 19 mutation and ALK rearrangement. Legend: ADC, adenocarcinoma; NSCLC, non-small cell lung carcinoma NOS

Conclusions: These data show a similar proportion of cytology cases positive for *EGFR*, *KRAS*, or *ALK* as reported in the literature. The cytological features of *ALK* and *KRAS*-positive tumors in our series included more nuclear pleomorphism, necrosis and less vacuolated cytoplasm, than in *EGFR*-positive tumors, which may explain the less definitive subclassification in the *ALK and KRAS*-positive tumors.

1905 Increased Claudin 4 Expression Is Associated with Aggressiveness of Pulmonary Neuroendocrine Tumors

J Li, S Lu, S Mangray, B Aswad, R Monahan, L Noble, M Resnick, E Yakirevich. Alpert Medical School of Brown University, Providence, RI.

Background: Claudins are members of a large family of tight junction proteins, which regulate cellular adhesion, polarity, and glandular differentiation. Dysregulation of claudin protein expression has been described in a number of malignancies, including lung carcinomas; however, expression of claudins in pulmonary neuroendocrine tumors (PNT) has not been addressed. Our goal was to investigate the protein expression patterns of claudins 1,3,4,7and 8 in PNTs.

Design: Sixty seven cases of PNTs were retrieved from the archives of Rhode Island Hospital including 38 typical carcinoids (TC), 11 atypical carcinoids (AC), 9 small cell carcinomas (SCC), 4 large cell neuroendocrine carcinomas (LCNEC), and 5 combined small cell/large cell neuroendocrine carcinomas (CSLNEC). Paraffin embedded tissue microarrays were analyzed for IHC expression of claudins 1,3,4,7, and 8. The immunoreactivity was assessed based on a combined score of the extent and intensity on a scale of 0-3+.

Results: In the normal lung tissue bronchial epithelial cells exhibited membranous claudin staining for all of the claudins studied. Alveolar cells demonstrated diffuse membranous immunoreactivity for claudins 7 and 8, focal staining for claudins 3 and 4, and were negative for claudin 1. In PNTs all claudins exhibited membranous staining pattern. A relatively low frequency of moderate to strong claudin expression (2-3+) varying from 2.6 to 36.3% was observed for claudins 1,3, and 7 in TC, AC, and SCC. Claudin 8 was weakly expressed in TC and AC, and was negative in all SCC cases. In contrast to other claudins, claudin 4 exhibited significantly higher expression in the more aggressive tumor subtypes as opposed to TC (p<0.001). Moderate to strong (2-3+) claudin 4 expression was detected in 2.6% of TC, 18.2 % of AC, 55.6% of SCC, 75% of LCNEC, and 80% of CSLNEC. Interestingly, while the majority of LCNEC were positive for claudin 4, none were positive for claudins 1,3, and 7 and only one case was positive for claudin 8.

Expression of Claudin Proteins in PNTs

	TC (n=38)	AC (n=11)	SCC (n=9)	LCNEC (n=4)	CSLNEC (n=5)
Claudin 1	5.3 %	27.3 %	11.1 %	0.0 %	0.0 %
Claudin 3	10.5 %	18.2 %	22.2 %	0.0 %	20.0 %
Claudin 4 *	2.6 %	18.2 %	55.6 %	75.0 %	80.0 %
Claudin 7	21.6 %	36.3 %	33.3 %	0.0 %	20.0 %
Claudin 8	16.2 %	27.3 %	0.0 %	25.0 %	60.0 %

* P<0.001

Conclusions: This study is the first to comprehensively examine the expression of claudins 1,3,4,7 and 8 in PNTs. Claudins are differentially expressed and overexpression of claudin 4 in SCC, LCNEC, and CSLNEC suggests that this protein may be involved in progression to more aggressive tumor subtypes.

1906 *EGFR* Exon 20 Mutations: Molecular Spectrum, Incidence and Clinicopathologic Characteristics

Y-C Liu, K Nafa, JE Chaft, N Rekhtman, B Reva, MF Zakowski, MG Kris, M Ladanyi, ME Arcila. Memorial Sloan-Kettering Cancer Center, New York, NY.

Background: The central role that EGFR tyrosine kinase inhibitors such as erlotinib have assumed in lung adenocarcinoma treatment has created the need for a more comprehensive understanding of various *EGFR* mutations. In contrast to the more common mutations in exons 19 and 21 of *EGFR*, primary mutations in exon 20 occur at a lower frequency and are not as well characterized. We report the molecular spectrum, clinicopathologic characteristics and incidence of these mutations in a large cohort of lung adenocarcinomas.

Design: A cohort of 3000 lung adenocarcinoma specimens, collected between 2009 and 2012 were subjected to a stepwise genotyping algorithm. Cases were first tested for common mutations in *EGFR* (exons 19 and 21) and *KRAS* (exon 2) and, if negative, further analyzed for *EGFR* exon 20 mutations. All samples underwent extended genotyping for other driver mutations in *EGFR, KRAS, BRAF, NRAS, PIK3CA, MEK1, and AKT* by mass spectrometry genotyping; a subset was evaluated for *ALK* rearrangements by FISH.

Results: A total 70 *EGFR* exon 20 mutated cases were identified, accounting for 11% of all *EGFR* mutations (70/624) for an overall incidence of 2.3% (95%CI 1.8 to 2.8%). In-frame insertions composed the vast majority of the mutations (89%, 62/70), varying widely in size (range 3 to 12 bps) and position and resulting in 19 unique variants. These *EGFR* exon 20 mutations were mutually exclusive with other recurrent genetic alterations except for *PIK3CA*. Molecular modeling predicted potentially different effects on erlotinib binding for the different types of *EGFR* exon 20 insertions. Insertions were more common in never-smokers (p<0.0001). There was no association with sex, race, or stage. Point mutations were comparatively rare (n=8, 1% of all *EGFR* mutants), and included S768I (5), R776 (2), and D770N (1); 25% (2/8) occurred in conjunction with other minor *EGFR* mutations. Morphologically, exon 20 mutated tumors were similar to those with common *EGFR* mutations.

Conclusions: *EGFR* exon 20 insertions represent the third most common type of *EGFR* mutation. Their structural heterogeneity predicts potential differential response to EGFR inhibitors.

1907 Intratumoral Blood Vessels and Basement Membranes Show Laminin ß1 Overexpression in Pulmonary Squamous Cell Carcinoma and Adenocarcinoma: A Potential Target for Nanomedicine Drugs

AE Lo, AM Marchevsky, MN de Peralta-Venturina. Cedars-Sinai Medical Center, Los Angeles, CA.

Background: Laminins (LAM) are trimeric proteins that play important roles in cell adhesion to basement membranes, tumor differentiation and migration, tumor aggressivenes and angiogenesis. Vascular LAM-411 with β1 chain predicts prognosis in gliomas and other neoplasms. Cells that overexpress LAM receptor can be targeted with radioactive nanomedicine drugs in vivo for imaging and tumor suppression growth. LAM β chain expression has not been previously evaluated in normal and neoplastic lung.

Design: Twenty lung adenocarcinoma (ADC) and 20 lung squamous cell carcinomas (SCC) resection specimens were studied with immunohistochemistry (IHC) using monoclonal Laminin β1 antibody (LB1) (clone 3G133) from Abcam (Cambridge, MA) at 1:100 dilution and Laminin β2 (LB2) (clone C4) from Santa Cruz Biotechnology (Santa Cruz, CA) at 1:3K dilution. IHC was performed on 4-mm tissue sections using the Ventana Benchmark Ultra (Tuscon, AZ) using on board high pH antigen retrieval and Ventana ultraview DAB Detection Kit. Laminin β2 was also treated with Ventana Protease1 for 8 minutes. The slides were subsequently counterstained with Mayer's hematoxylin. The extent and degree of immunoreactivity in normal blood vessels (BV) and in tumoral BV and basement membrane (BM) were assessed by 2 observers and semiquantitated using a scale of 0:none, 1+:focal/weak, 2+: continuous/strong).

Results: Normal pulmonary BV larger than capillaries showed diffuse and patchy 2+ immunoreactivity for LB2 and only patchy 1+ LB1 immunoreactivity. Intraalveolar capillaries were mostly negative in all cases for both LB1 and LB2. Intratumoral BV in 95% of SCC and 55% of ADC showed 2+ LB1 immunoreactivity. In contrast, the intratumoral BV of both SCC and ADC showed LB2 immunoreactivity in only 35% of cases. Both SCC and ADC expressed 2+ LB2 BM immunoreactivity in 70% of cases. BM immunoreactivity for LB1 was seen in 55% of SCC and 10% of ADC.

Conclusions: Our results show no apparent difference in LB2 immunoreactivity between tumoral and normal pulmonary BV. In contrast, the results show an apparent upregulation of LB1 in lung carcinomas with continous strong immunoreactivity for this antigen in the neovessels of most pulmonary SCC and 55% of ADC. LB1 immunoreactivity was also detected with lower frequencies in the BM of both tumor types. These preliminary findings suggest that LB1 may offer a target for in-vivo imaging and/or suppression of tumor growth in these pulmonary neoplasms.

1908 Expression of Laminin ß1 and ß2 Chains in Malignant Mesothelioma

AE Lo, MN de Peralta-Venturina, AM Marchevsky. Cedars-Sinai Medical Center, Los Angeles, CA.

Background: Laminins (LAM) are αβγ basement membrane and extracellular matrix glycoproteins that play an important role in cell adhesion, tumor migration and metastases. LAM 411 (formerly LAM 8) β chains overexpression has been described in gliomas and other tumors but not in malignant mesothelioma (MM). LAM receptors can be blocked using antisense oligonucleotides delivered by nanobioconjugate drug, resulting in *in-vivo* tumor growth inhibition and there is great interest at identifying the overexpression of LAM β chains in MM and other neoplasms in an effort to develop novel LAM targeted therapeutic modalities.

Design: Twenty pleural malignant MM decortication specimens and 18 lobectomies for adenocarcinoma were studied with immunohistochemistry (IHC) using monoclonal LAM β1 antibody (clone 3G133) from Abcam (Cambridge, MA) at 1:100 dilution and LAM β2 (clone C4) from Santa Cruz Biotechnology (Santa Cruz, CA) at 1:3K dilution. Staining was evaluated in tumor cells and tumoral blood vessels (BV) in the 20 MM. Normal mesothelial cells and pleural BV were evaluated in the 18 lobectomy specimens. Extent of immunoreactivity was semi-quantitated as 0+ :<5%, 1+: 5%-25% and 2+: 26%-100%. The intensity of stainings were semi-quantitated by 2 observers from 0+: none, 1+: weak/discontinous and 2+: strong/diffuse. The proportions of staining between MM and normal pleura were compared, by compartment, using the Fishers exact test.

Results: LAM β1 and β2 are significantly overexpressed in the tumor cells of MM, with β1 staining also significant in the tumoral blood vessels compared with normal vessels.

LAM β1 and β2 Expression Distribution

	STAINING DISTRIBUTION (n)					
	Negative		1+		2+	
LAM Chain	β1	β2	β1	β2	β1	β2
Tumor Cells (n=20)	6	5	4	1*	10*	14*
Mesothelial Cells (n=18)	15	13	2	3	1	2
Tumor BV (n=20)	1	2	3	1*	16*	17
Normal BV (n=18)	3	0	5	0	10	18

BV= blood vessels, * p<0.05

LAM β1 and β2 Expression Intensity

	STAINING INTENSITY (n)					
	Negative		1+		2+	
LAM Chains	β1	β2	β1	β2	β1	β2
Tumor Cells (n=20)	6*	5*	5	3	9*	12*
Mesothelial Cells (n=18)	15	13	2	4	1	1
Tumoral BV (n=20)	1	2*	3*	0	16*	18
Normal BV (n=18)	3	0	9	3	6	15

BV= blood vessels, * p<0.05

Conclusions: The overexpression of LAM β1 and β2 in tumor cells of MM and differential staining for tumoral blood vessels by β1 identify a potential therapeutic target in these neoplasms. Future studies with LAM targeted therapeutic modalities are needed to determine whether this novel approach could help improve on the currently dismal prognosis of patients with these neoplasms.

1909 p53 Immunostaining Should Be Used in Conjunction with p16 in Differentiating Metastatic Cervical Squamous Cell Carcinoma Involving the Lung from Primary Lung Squamous Cell Carcinoma

D Maeda, T Inoue, S Morita, M Fukayama. Graduate School of Medicine, University of Tokyo, Tokyo, Japan.

Background: Histological distinction between primary lung squamous cell carcinoma (PLSCC) from metastatic uterine cervical squamous cell carcinoma involving the lung (MCSCCL) is often difficult. In this study, we evaluated the utility of p16 and p53 immunohistochemistry in distinguishing MCSCCL from PLSCC.

Design: A total of 40 cases of female lung SCC (29 cases with no past history of other primaries including cervical cancer [definite PLSCC] and 11 with a past history of cervical cancer [possible MCSCCL]), and 31 cases of primary invasive uterine cervical SCC (PCSCC) were retrieved from the archive of the Department of Pathology of the University of Tokyo Hospital. Immunohistochemistry for p16 and p53 were performed. First, we compared the immunophenotypes of definite PLSCCs and PCSCCs. Next, we applied the panel to the "possible MCSCCL" group to examine its utility.

Results: Diffuse (≥90%) p16 immunoreactivity positivity was observed in 29/31 (94%) of PCSCCs and 7/29 (24%) of definite PLSCCs. Diffuse p53 positivity (≥90%) was observed specifically in definite PLSCCs (48%; 14/29 cases). None of the PCSCCs showed diffuse overexpression of p53.

p16 and p53 expression in primary lung SCC and primary cervical SCC

	p16		p53	
	PLSCC (n=29)	PCSCC (n=31)	PLSCC (n=29)	PCSCC (n=31)
<4%	13 (45%)	0 (0%)	11 (38%)	22 (71%)
5-14%	1 (3%)	0 (0%)	2 (7%)	8 (26%)
15-49%	3 (10%)	0 (0%)	1 (3%)	1 (3%)
50-89%	5 (17%)	2 (6%)	1 (3%)	0 (0%)
≥90%	7 (24%)	29 (94%)	14 (48%)	0 (0%)

PLSCC; primary lung squamous cell carcinoma, PCSCC; primary cervical squamous cell carcinoma

The p16 (diffusely postive) / p53 (negative or focally positive) phenotype was observed in 94% of PCSCCs, whereas only 7% of definite PLSCCs revealed such phenotype. Of the 11 cases of possible MCSCCLs, 9 showed the p16 (diffusely positive) / p53 (negative or focally positive) phenotype and two showed the p16 (negative or focally positive) / p53 (negative or focally positive) phenotype.

Conclusions: Because a significant proportion (24%) of PLSCCs showed diffuse p16 immunoreactivity, we conclude that p16 should not be used as a sole marker to distinguish PLSCC from MCSCCL. Immunohistochemistry for p53 should be applied in adjunction because diffuse p53 positivity occurs specifically in PLSCC. By applying the p16 / p53 panel, we were able to assume that 2 cases of the lung SCC with a past history of cervical cancer were most likely PLSCCs.

1910 Elastic-Collagen Profile in Emphysematous Airspaces from Different Chronic Fibrosing Lung Disorders

LJ Marcal, L Antonangelo, ER Parra, FS Vargas, WR Teodoro, ECT Nascimento, VL Capelozzi. University of Sao Paulo Medical School, São Paulo, Brazil.

Background: Parenchyma elastic and collagen components of chronic fibrosing lung disorders has been exhaustively investigated, but little attention has been aimed at the emphysematous airspaces present in bullous disease, smoking-related interstitial disease and usual interstitial pneumonia. The aim of this study was to evaluate whether elastic deposition accompanies collagen deposition in the repairing process of emphysematous airspaces in chronic fibrosing lung injuries.

Design: The elastic and collagen fibers distribution were evaluated in emphysematous airspaces of bullous type I and II disease, smoking-related interstitial fibrosis and of usual interstitial pneumonia (UIP). Lung specimens obtained by surgical lung biopsy or by bullectomy divided the patients into four groups: 1) type I bullous disease (SPT-I; n=7); 2) type II bullous disease (SPT-II; n=12); 3) smoking-related interstitial pneumonia (SRIP; n=5) and 4) usual interstitial pneumonia/idiopathic pulmonary fibrosis (UIP/IPF; n=5). Collagen and elastic fibers were identified respectively by Picrosirius-polarization and Weigert's resorcin-fucsin staining and quantified by image analysis.The results were expressed in percentual area.

Descriptive Results

Staining	Disease	Mean	Std. Deviation	Std. Error	Minimum	Maximum
Picro-sirius	STP-I	40.71	15.87	6.00	18.56	61.67
Picro-sirius	STP-II	40.58	15.95	4.60	15.67	63.35
Picro-sirius	SRIP	30.18	9.23	4.13	25.31	46.64
Picro-sirius	UIP/IPF	40.99	13.99	6.26	24.76	60.07
Resorcina	STP-I	19.97	10.63	4.02	3.71	33.76
Resorcina	STP-II	18.42	6.17	1.78	10.19	26.70
Resorcina	SRIP	11.86	9.72	4.35	1.87	25.62
Resorcina	UIP/IPF	18.49	9.95	4.45	12.43	35.77

Results: The proportion of collagen fibers was two times higher when compared with the elastic component in the four groups. In addition, a lower percentage of elastic and collagen fibers were observed in SRIP when compared with UIP/IPF, SPT-I and SPT-II. Table 1.

Conclusions: A smaller amount of elastic and collagen fibers accompanies the remodeling of the emphysematous airspaces in smoking-related interstitial pneumonia when compared to the other fibrosing diseases, suggesting a different remodeling spectrum in chronic fibrosing lung diseases.

1911 Epithelial-Mesenchymal Transition (EMT) in Active Fibroblastic Foci in IPF/UIP

O Matsubara, K Miyai, Y Ishikawa, Y Nakatani, EJ Mark. National Defense Medical College, Tokorozawa, Saitama, Japan; Cancer Institute, Koto-ku, Tokyo, Japan; Chiba University, Chiba, Japan; Massachusetts General Hospital and Harvard Medical School, Boston, MA.

Background: Idiopathic pulmonary fibrosis (IPF) is a progressive lung disease with bad prognosis characterized by interstitial fibrosis with irreversible distortion of pulmonary architecture. The histopathology of IPF includes myofibroblasts within active fibroblastic foci (AFF). Previous studies suggest that lung myofibroblasts are derived from epithelial cells through epithelial-mesenchymal transition (EMT). EMT participates in repair and scar formation following epithelial injury in vitro. AFF are distinct findings and a marker of IPF/usual interstitial pneumonia (UIP). They would seem to be sites where fibrotic responses are initiated. We examined the cellular and molecular mechanisms of EMT responsible for the formation of AFF and their role in tissue remodeling.

Design: We investigated the molecular profile of AFF in 16 video-assisted thoracoscopic surgery (VATS) lung biopsies of IPF/UIP and a variety of control lung samples, focusing on the immunohistochemical expression of the molecules involved in EMT and cellular proliferation, namely E-cadherin, beta-catenin, vimentin, alpha-smooth muscle actin, tissue growth factor (TGF)-beta, connective tissue growth factor, and Ki-67. We used a standard indirect avidin-biotin horseradish peroxidase method with various antigen retrievals.

Results: In IPF/UIP these molecules are abnormally expressed in hyperplastic alveolar cells and mesenchymal cells localised to AFF. The spindle cells expressed alpha-smooth muscle actin and vimentin. The hyperplastic alveolar cells lost in part or in entirety epithelial markers (E-cadherin and beta-catenin) and expressed TGF-beta and connective tissue growth factor. Alveolar cells in controls expressed E-cadherin and beta-catenin. Ki-67 positive alveolar cells and spindle cells were increased compared to the controls.

Conclusions: EMT with abnormal proliferation of cells and re-epithelialisation is at the leading edge of AFF formation. Abnormal proliferation of myofibroblasts also has a role in the remodeling process. TGF-beta presumably stimulates myofibroblast proliferation within AFF.

1912 Expression of PD-1 in Non-Small Cell Carcinoma of the Lung

AP Matynia, ML Wallander, S Tripp, WL Akerley, MB Cohen. University of Utah, Salt Lake City, UT; ARUP Institute for Clinical and Experimental Pathology, Salt Lake City, UT.

Background: Despite advances in treatment, lung cancer remains a leading cause of cancer related mortality in the United States. Advances in cancer immunotherapy, which attempts to stimulate the host immune system to reject tumors, have the potential to improve outcomes. Blockade of immune checkpoints, including the programmed cell death protein 1 (PD-1) pathway, is a new target for cancer immunotherapy. Interaction of the PD-1 receptor on peripheral T-lymphocytes with its ligands (PD-L1 and PD-L2), which are expressed in peripheral tissues and some cancers, inhibits T-cell function and subsequently leads to immune system evasion. Preliminary trials of anti-PD1 and anti-PD-L1 antibodies showed promising results in patients with non-small cell carcinoma of the lung (NSCLC). An objective response was observed in 18% and 10% of heavily pretreated NSCLC patients, following anti-PD1 and anti-PD-L1 antibody therapy, respectively. Patients with squamous cell carcinoma (SCC) had slightly better response rates. It is essential to identify suitable immunotherapy biomarkers in order to identify patients likely to respond to such therapies.

Design: We examined 45 cases of adenocarcinoma (AC) (excision and biopsy specimens) and 19 cases of SCC (excision specimens) with available formalin-fixed, paraffin-embedded tissue blocks. All cases were stained for PD-1 (polyclonal, R&D Systems) using standard immunohistochemical techniques. Staining in the carcinoma cells and infiltrating lymphocytes were scored separately. Carcinoma cells were scored as: 0 (negative) to 3+ (strongly positive); and PD-1 positive lymphocytes as: 0 (absent), 1 (rare), and 2 (easily identifiable).

Results: All ACs were negative for PD-1 staining in the tumor cells. The number of infiltrating PD-1 positive lymphocytes varied from absent in 15 cases, rare in 19 cases, to easily identifiable in 12 cases. Only one case of SCC (~[/underline]5%) showed 1+ staining for PD-1 in the tumor cells and also had easily identifiable PD-1 positive infiltrating lymphocytes. Of the remaining SCCs, infiltrating PD-1 positive lymphocytes were absent in 7 cases, rare in 3 cases, and easily identifiable in 8 cases.

Conclusions: In NSCLC, PD-1 expression on tumor cells is rare, 5% in SCC. PD-1 positive infiltrating lymphocytes are present in 67% and 63% of AC and SCC of the lung, respectively. PD-L1 and PD-L2 expression needs to be evaluated and correlated with PD-1 expression, and is being evaluated.

1913 Combined Use of p16 FISH and Bap1 Immunohistochemistry Optimizes Diagnosis of Malignant Pleural Mesothelioma

SM McGregor, A Minor, C Fitzpatrick, AN Husain, E Hyjek, W Vigneswaran, T Krausz. University of Chicago Medicine, Chicago, IL.

Background: Malignant pleural mesothelioma (MPM) is a challenging diagnosis that must frequently be made on small biopsies, making useful molecular markers highly desirable. Homozygous deletion of 9q21 (including the *CDKN2A* locus, which encodes p16) and loss of Bap1 expression by deletion or mutation are common in MPM. Combined analysis of these genes may improve diagnostic accuracy.

Design: We analyzed 22 primary MPM cases (9 epithelioid, 10 biphasic, 3 sarcomatoid) for p16 and Bap1 using immunohistochemistry (IHC) and fluorescence in-situ hybridization (FISH). Seven reactive mesothelial hyperplasia cases served as controls. Nuclear and cytoplasmic p16 staining was scored as negative (<1%), sporadic (<5%), focal (<25%) or diffuse (>25%). Bap1 nuclear staining was scored as positive or negative. Fibroblasts and lymphocytes served as internal positive controls. FISH was scored according to the raw number of signals per cell using the beta inverse statistic to determine cut-off values.

Results: Bap1 staining was diffusely positive in all controls and was either diffusely positive or negative in mesothelioma cases. Importantly, p16 staining was not diffuse in controls, ranging from negative (1/7) to focal (3/7). FISH detected no deletions in any controls. Results for mesothelioma cases are depicted in Table 1.

Table 1: IHC and FISH for p16 and Bap1 in Primary Mesothelioma Cases

	Epithelioid	Biphasic	Sarcomatoid	Sensitivity	Specificity	Positive Predictive Value	Negative Predictive Value
p16 Negative IHC	4/9	10/10	3/3	77%	86%	94%	45%
p16 Homozygous Deletion	2/9	8/10	3/3	59%	100%	100%	56%
Bap1 Negative IHC	8/9	6/10	0/3	64%	100%	100%	47%
Bap1 Homozygous Deletion	3/9	5/10	0/3	36%	100%	100%	67%
Combined Bap1 Negative IHC and/or p16 Homozygous Deletion	8/9	10/10	3/3	96%	100%	100%	88%

Conclusions: The sporadic nature of p16 staining is concerning for false positives (negative staining) in the setting of limited material, whereas Bap1 IHC staining is diffuse, making it appropriate for use on small biopsies. In contrast to p16 IHC, the use of FISH to detect p16 deletions is highly specific and has a high PPV. When combined, Bap1 IHC and p16 FISH serve as a highly sensitive and specific panel in the diagnosis of MPM that is also cost effective. These results should be interpreted as an adjunct to morphology and must be validated in a larger case series before being applied for routine clinical use.

1914 *ALK* Gene Rearrangement Testing in Non-Small Cell Lung Carcinoma by ThinPrep-FISH

EC Minca, BP Portier, Z Wang, J Brainard, C Farver, Y Feng, PC Ma, V Arrossi, N Pennel, RR Tubbs. Cleveland Clinic Foundation, Cleveland, OH.

Background: Anaplastic lymphoma kinase (*ALK*) gene rearrangements in advanced non-small cell lung carcinomas (NSCLC) are an indication for targeted therapy with ALK-specific inhibitors, including crizotinib. *ALK* rearrangement status is commonly assessed by fluorescence *in-situ* hybridization (FISH) on formalin-fixed paraffin-embedded (FFPE) samples using the IVD-class FISH system approved by the US FDA as a companion diagnostic tool for crizotinib-based treatment eligibility. Cytologic preparations may represent alternative valuable material in cases of FFPE-FISH failure or unavailability. Here we assessed the feasibility of FISH on ThinPrep samples for detecting *ALK* rearrangements in a NSCLC case series at our institution.

Design: The study included 40 matched ThinPrep and FFPE samples from patients with advanced NSCLC clinically referred for ALK testing. FISH was performed using the AMV *ALK* Break Apart FISH Probe Kit (Abbott Molecular, USA). IHC for ALK was performed on FFPE samples with the D5F3 rabbit monoclonal antibody (Cell Signaling Technology) and ultrasensitive OptiView DAB IHC Detection Kit with amplification (Ventana Medical Systems). Statistical analysis was performed using the GraphPad Prism software (GraphPad Software).

Results: ThinPrep-FISH for *ALK* rearrangements was informative in 39/40 cases: 34 negative (mean 4.8%, median 4%, range 0-12% positive cells), 5 positive (mean 44.4%, median 20%, range 16-88% positive cells). IHC for ALK was informative in 35/40 cases: 30 negative, 5 positive, 100% concordance with ThinPrep-FISH on matched samples. FFPE-FISH was informative in 19/40 cases: 13 negative, 6 positive. 2 discordant positive cases approximated the FFPE-FISH cut-off of 15% positive cells (15% and 18%) and were negative by IHC, in agreement with the ThinPrep-FISH result. Overall, ThinPrep-FISH provided significantly more informative results that FFPE-FISH (97.5% vs 47.5%, $p<0.001$), 100% concordance with ultrasensitive IHC and 88.8% agreement with FFPE-FISH on a limited number of cases.

Conclusions: ThinPrep-FISH can reliably detect *ALK* gene rearrangements in cytologic preparations from patients with NSCLC. The high concordance between ThinPrep-FISH with IHC and FFPE-FISH warrants the routine use of ThinPrep-FISH for clinical *ALK* molecular testing in NSCLC cases with unavailable or limited FFPE material.

1915 Acute Exacerbation of Non-Specific Interstitial Pneumonia Compared to That of Usual Interstitial Pneumonia

A Miyamoto, A Sharma, M Nishino, M Mino-Kenudson, EJ Mark. Toranomon Hospital, Tokyo, Japan; Massachusetts General Hospital, Boston, MA.

Background: Usual interstitial pneumonia (UIP) and nonspecific interstitial pneumonia (NSIP) are related forms of interstitial lung disease. Acute exacerbation (AE) is a recognized complication of UIP but is much less appreciated in NSIP.

Design: To compare the features of acute exacerbation in UIP with those of NSIP, we performed a detailed retrospective analysis of 42 patients from a single institution who had an initial pathologic diagnosis of UIP or NSIP. All patients were discussed at a multidisciplinary conference (MDC) involving pathologists, a pulmonologist, and a radiologist.

Results: Of the 42 patients initially diagnosed as UIP or NSIP, 15 were determined to have a disease other than UIP or NSIP at the MDC, leaving 27 cases for further analysis. The MDC classified the remaining cases as having stable UIP (n=4), acute exacerbation of UIP (AE-UIP, n=6), stable NSIP (n=6), and acute exacerbation of NSIP (AE-NSIP, n=7). Four patients with UIP were transplanted and classified as indeterminate for AE because the timing of symptoms was unclear. Characteristic histologic features of AE were more numerous in patients who were classified as having AE-NSIP compared to AE-UIP.

Conclusions: Patients with AE-NSIP have qualitatively similar but quantitatively greater pathology as patients with AE-UIP. This finding suggests similarities in the pathogenesis of NSIP and UIP and supports our hypothesis that the more severely scarred lungs in UIP has less reserve than those of NSIP and may be more prone to acute clinical deterioration after a lesser degree of acute lung injury.

1916 Targeted Cancer Genome Sequencing in Thymic Epithelial Tumors

AL Moreira, M Robert, W Helen, H James, RJ Gregory, L Marc, BF Michael. Memorial Sloan-Kettering Cancer Center, New York, NY.

Background: There have been very few studies dedicated to the understanding of the biology of thymomas and thymic carcinomas (TCA). An improved understanding of the molecular characteristics of thymoma and TCA may lead to a better comprehension of tumorigenesis, and more importantly lead to new therapeutic targets, thus opening new treatment options for these patients.

Design: Paired tissue (tumor and normal, paraffin-embedded) from 13 thymic carcinomas and 6 WHO type B3 thymomas were evaluated by exon capture of 275 cancer related genes (Agilent SureSelect Target Enrichment system), followed by next-generation sequencing (Illumina HiSeq). This approach identifies all sequence variants, small insertions and deletions, and copy number alterations involving the target genes.

Results: Mutations were identified in 11 of 13 (85%) TCA with a median of 1 mutation per tumor (range 0-26). All TCA were classified as squamous cell carcinoma; one with 26 mutations was a CD5 positive poorly-differentiated carcinoma. The most mutated genes were TP53 (n=3), SMAD4 (n=2) and CYLD (n=2); and chromatin remodeling genes KDM6A (n=3), SETD2 (n=2), MLL3 (N=2), and MLL2 (n=2). TP53 and KDM6A were seen as a single mutation in one tumor each. The most frequently amplified genes were APC and SOX2 (each n=5), MDM4, AKT3, IGFR1, and FBXW7 (each n=4). In this small sample, the 3 TCA with TP53 mutation appeared to exhibit more aggressive

behavior: all 3 patients presented as Masaoka stage 4 and received neoadjuvant therapy. Two patients with TP53-mutated TCA died of disease (mean survival 2.2 years). In contrast 2 other stage 4 patients without TP53 mutations are alive with disease and 2 others died of unrelated causes. All other TCA patients were Masaoka stage 1 to 3 at diagnosis and are alive. Among the B3 thymomas, mutations were identified in 4 of 6 tumors. Mutations in BCOR (BCL6 co-repressor) were seen in 3 thymomas and MLL3 (involved in histone methylation) in one tumor. The most frequently amplified genes were DDR2, AKT3, CDC73 (each n=4), PIK3R1, ABL2, IKBKE, and FH (each n=3).
Conclusions: Exon capture sequencing of cancer genes in thymic epithelial tumors revealed a low frequency of mutation and gene amplifications. However, there is a different pattern of molecular alterations between TCA and B3 thymomas. TCA have more mutations in TP53 gene whereas B3 thymomas may have a higher frequency of mutations in the BCOR gene.

1917 Correlation between Morphologic Phenotype and Genotype of Lung Adenocarcinoma Based on a New IASLC/ATS/ERS Classification with Nuclear Grading

N Motoi, S Sato, Y Saito, H Ninomiya, K Takeuchi, Y Ishikawa. Cancer Institute, Japanese Foundation for Cancer Research (JFCR), Tokyo, Japan.

Background: Recent advantages of molecular study reveal several subsets of lung adenocarcinoma (AdCa) with specific genetic alterations of receptor tyrosine kinase (RTK), including EGFR, ALK, RET and ROS, which are dramatically response to targeted inhibitors for rearranged RTK. The goal of this study is to evaluate the correlation between genetic alteration and histologic phenotype of lung AdCa.
Design: 319 surgically resected lung AdCa were examined genetic alterations of EGFR by Cycleave or direct sequencing, ALK by FISH and immunohistochemistry and KRAS by PCR-RFLP and direct sequencing methods. Resected materials were reviewed detail histologic findings, using HE-stained slides of whole tumor. Histologic predominant subtype of AdCa, based on a new IASLC/ATS/ERS classification, and nuclear grading were evaluated. Correlation between genetic alteration and histologic phenotypes was examined.
Results: Genetic alterations of this study were 150 EGFR, 44 ALK, 9 KRAS and 116 wild-type. EGFR mutated AdCa had 55.4% lepidic- (lep), 40% papillary- (pap), 2.6% of acinar- (aci) and 2% of solid- (sol) predominant subtypes. ALK AdCa had 20.5% of lep, 36.4% pap, 18.2% aci, 22.7% sol and 2.3% micropapillary predominant subtypes. Kras mutated AdCa were 44.4% pap, 33.3% aci and 22.2% sol. All wild type AdCa were 35.3% of lep, 53.4% pap, 5.2% aci- and 6% sol. Presence of mucinous cells were observed in 4.7, 90.9, 66.7, and 26.7% of EGFR, ALK, KRAS and wild type AdCa, respectively. EGFR and ALK showed lower nuclear grade compared to KRAS. In summary, the most common histologic phenotype of EGFR AdCa was lepidic-predominant, non-mucinous with low nuclear grade; ALK AdCa was papillary, mucinous with low nuclear grade, and KRAS was papillary, mucinous with high nuclear grade.
Conclusions: Our data suggested significant correlation between genotype and histologic phenotype. Although, it should be mentioned that we couldn't exclude any possibility of absence or presence of some specific genomic alteration based on histologic features.

1918 *EGFR, KRAS* and *ALK* Molecular Tests Can Be Performed Using Existing Stained Histologic Slides, Including Small Biopsies: A Proof-of-Concept Study

S Mukhopadhyay, J Tull, S Zhang. State University of New York Upstate Medical University, Syracuse, NY.

Background: Testing pulmonary adenocarcinomas in small biopsies for *EGFR* and *KRAS* mutations and *ALK* gene rearrangements is now standard practice. However, tissue in paraffin blocks is occasionally depleted by histology and/or immunohistochemistry (IHC), leaving no cells for molecular studies. Our aim was to determine whether tumor cells from existing stained histology slides can be used for *EGFR*, *KRAS* and *ALK* testing, especially in small biopsies.
Design: Ten pulmonary adenocarcinomas with known *EGFR* mutations (5), *KRAS* mutations (2) or *ALK* gene rearrangments (3) were re-tested for *EGFR*, *KRAS* and *ALK* using stained histologic slides. For PCR analysis, tumor cells were marked on existing hematoxylin-eosin (H&E) stained slides under a microscope and macro-dissected from the marked areas with a 19 gauge needle. DNA was isolated and tested for *EGFR* (exon 19 deletion and L858R mutation) and *KRAS* mutations. Based upon our preliminary data that FISH for *ALK* on H&E stained slides is uninterpretable due to eosin autofluorescence, FISH for *ALK* was instead performed on existing negative control slides prepared during initial IHC. After ISH with an *ALK* break-apart probe, signals were visualized with a fluorescent microscope. *ALK* FISH was considered positive if ≥15% of tumor cells showed break-apart and/or 5'deletion fluorescent signals.
Results: DNA sufficient for *EGFR* and *KRAS* testing was obtained from H&E-stained slides in all 10 cases, yielding 5 *EGFR* mutations/deletions and 2 *KRAS* mutations identical to the original results using the paraffin block. Satisfactory FISH signals for *ALK* testing were obtained from all 10 IHC negative control slides, 3 showing *ALK* split signals identical to the original results using the paraffin block.

Molecular Findings Using Stained Histology Slides

Case	Specimen	EGFR (H&E)	KRAS (H&E)	ALK (neg ctrl slides)
1	CB, lung	Exon 19 del	wt	n
2	Bone curettings	Exon 19 del	wt	n
3	FNA lymph node	Exon 19 del	wt	n
4	CB, lung	Exon 21 mut	wt	n
5	CB, lung	Exon 21 mut	wt	n
6	CB, lung	wt	G12C mut	n
7	Lobectomy	wt	G12C mut	n
8	CB, lung	wt	wt	Pos
9	CB, liver	wt	wt	Pos
10	Lobectomy	wt	wt	Pos

CB-core biopsy, wt-wild type, n-normal signal

Conclusions: Tumor cells derived from existing H&E-stained slides can be used for PCR-based assays (*EGFR* and *KRAS*), and cells on existing IHC negative control slides (rather than H&E) can be used for *ALK* FISH testing, even in small biopsies. This approach can obviate the need for repeat biopsies in cases in which the paraffin block is depleted by histology and/or IHC.

1919 Genomic Rearrangements in Lung Adenocarcinoma: Lineage Relationship between In Situ and Invasive Components

SJ Murphy, FR Harris, M-C Aubry, J Felipe Lima, SH Johnson, BW Eckloff, CT Seto, M Asiedu, T Peikert, P Yang, G Vasmatzis, DA Wigle. Mayo Clinic, Rochester, MN.

Background: The molecular events in the initiation and progression of invasive lung adenocarcinoma remain poorly characterized. Some are thought to develop through an adenocarcinoma in situ, minimally invasive adenocarcinoma, invasive adenocarcinoma sequence; however, the direct evidence for this remains sparse. The goal of our study was to assess lineage relationships between in situ and invasive components within adenocarcinomas with prominent lepidic growth pattern.
Design: Frozen tissue from 14 lung adenocarcinomas with mixtures of invasive (INV) together with an adjacent in situ component (IS), varying in ratio between 40 to 80%, were selected from our Lung Specimen Registry. Laser capture microdissection of each component was performed for each tumor. Genomic DNA was isolated using a direct *in situ* whole genome amplification methodology, and Next Generation Sequencing performed using an Illumina Mate Pair library protocol. Discordantly mapping Mate Pair sequence reads were determined using binary indexing mapping algorithms and potential genomic rearrangements verified by PCR.
Results: Multiple identical genomic break points unique to a patient tumor were identified within both the IS and INV components in 13 (of 14) cases. The total number of events per case ranged from 4 to 215 and the number of identical events shared between the IS and INV components ranged from 30 to 90%. Chromosomal catastrophe was observed in 2 cases; in one, it was common to both the IS and INV components but in another was only seen in the IS component with just one common event shared with the INV component. Recurrent genomic breakpoints between cases were also observed, with the 2 most common loci involving 8q24.3 and 12q14.1 in 5 and 4 of the 14 cases respectively. PCR validation on selected alterations confirmed that a subset of genomic break points identified with the Mate Pair protocol in both the IS and INV in all cases and not in germ line DNA. A small number of these genomic breakpoints also validated in associated non-neoplastic tissues. However, further evidence predicted these events to be restricted to zonal regions surrounding the tumor tissue.
Conclusions: Our study demonstrates unique chromosomal alterations present in both the IS and INV components of individual lung adenocarcinomas suggesting clonal relatedness and progression. The identification of identical genomic events in restricted regions of the adjacent non-neoplastic lung lends support to a potential mutant stem cell populating the local tumor environment from which the adenocarcinomas emerged.

1920 EML4-ALK Fusion Gene-Positive Lung Cancer: Its Usefulness in Immunohistochemical Screening and Its Histological Variation

K Nagata, M Shimizu, S Ishiguro. Saitama Medical University International Medical Center, Hidaka, Saitama, Japan; PCL Japan, Suginami-ku, Tokyo, Japan.

Background: ALK fusion gene-positive (ALK+) lung cancer was discovered in 2007, and its clinical application of targeted therapy for ALK by crizotinib began in 2012 in Japan. Therefore, in all EGFR/KRAS-negative adenocarcinomas, an examination for ALK rearrangements is recommended. However, ALK-fluorescence in situ hybridization (FISH) testing is time- and cost-consuming, and it is not suitable for a large-scale screening, in contrast to immunohistochemistry (IHC). Regarding the histological types, ALK+ lung cancer has been reported to be associated with a specific histologic type, such as solid, micropapillary, and papillary-predominant patterns and tumor cells with a signet ring or hepatoid cytomorphology.
Design: We prospectively evaluated 259 cases of lung cancer, including primary surgical specimens, metastatic lesions, small biopsy specimens, and cytology cell block specimens, in which all cases were EGFR/KRAS-negative. We investigated the usefulness of ALK+ lung cancer screening by IHC, and evaluated a histologic type of ALK+ lung cancer. The result of IHC was classified into positive, equivocal, and negative. FISH was performed in all cases except for some IHC-negative cases.
Results: Twenty-two cases out of 23 IHC-positive cases were positive for FISH, and 1 out of 3 IHC equivocal cases were positive for FISH (total 8.9%). In the IHC-negative cases, all cases revealed FISH negativity. Of the FISH-positive cases, male-to-female ratio was 5:17, and average age was 56.2 (ranging from 35 to 77 years). As for the histological type, 43% (10/23) showed solid adenocarcinoma; 22% (5/23) acinar adenocarcinoma; 26% (6/23) papillary adenocarcinoma; and 4% (1/23) micropapillary carcinoma. More than half of the cases (12/23) showed intracytoplasmic mucin production including signet-ring appearance.
Conclusions: A good correlation was observed between IHC-positive cases and FISH-positive cases. No specific histologic types were found in ALK+ lung cancer. Our study

indicates that immunohistochemical screening is useful and should be performed in all cases of lung cancer since histologic type alone cannot precisely detect ALK+ lung cancers. Further study is needed to evaluate whether or not FISH should be performed in all IHC-positive cases.

1921 Intraalveolar Fibrin Is Associated with Poor Outcomes in Cryptogenic Organizing Pneumonia

M Nishino, SK Mathai, WJ O'Donnell, RL Kradin. Massachusetts General Hospital, Boston, MA.

Background: Organizing pneumonia (OP) is a histopathologic pattern of response to lung injury that is characterized by intraalveolar filling by fibroblasts aggregated with immature collagen. Fibrin is a marker of acute microvascular injury, and variable amounts of intraalveolar fibrin are seen in OP; however, its relevance to clinical outcomes has not been assessed. We hypothesize that intraalveolar fibrin deposition in lung tissue of patients with idiopathic OP is associated with poor clinical outcomes.

Design: Patients with OP on pathology were identified, and hematoxylin and eosin-stained sections of formalin-fixed lung tissue were subclassified by the amount of intraalveolar fibrin associated with OP (none/low vs. medium/high). Biopsies with hyaline membranes and cases for which clinical data was not available were excluded. Clinical features (survival, rehospitalization, clinical relapse, pulmonary function testing, treatment, chest imaging) were compared between the groups at twelve months after biopsy. A poor clinical outcome was defined as a clinical relapse, hospitalization, or death due to OP.

Results: Eighty-six patients had histopathologic OP on biopsy; 32 patients were exluded due to lack of clinical follow-up, presence of another predominant histopathologic pattern, and presence of hyaline membranes. Of the remaining 54 patients with OP, 26 patients were further excluded due to presence of underlying systemic disease (e.g., autoimmune disease, malignancy) or drug-related pulmonary toxicity, leaving 28 patients with cryptogenic OP. Average age at biopsy was 62, and 11 patients showed significant intraalveolar fibrin (medium/high). Patients with intraalveolar fibrin were more likely to relapse (55% vs. 13%, p=0.03). This difference in groups persisted when patients with suspected aspiration (n=6) were excluded (p=0.02).

Conclusions: The histopathological presence of significant intraalveolar fibrin in lung biopsies of patients with cryptogenic organizing pneumonia appears to augur a less favorable clinical outcome.

1922 Focal Pulmonary Alveolar Proteinosis Is a Common Reaction and Progression Indicator in Idiopathic Pulmonary Fibrosis

S Nunomura, T Tanaka, K Otani, K Tabata, Y Kondoh, K Kataoka, T Johkoh, H Taniguchi, J Fukuoka. Toyama University Hospital, Toyama, Japan; Tosei General Hospital, Seto, Japan; Kinki Central Hospital, Itami, Japan.

Background: We have experienced cases of chronic interstitial pneumonia (IP) showing focal histologic features simulating pulmonary alveolar proteinosis (PAP). The occurrence and the meaning of focal PAP (fPAP) in the cases of chronic IP are unclear.

Design: 146 cases with chronic IP were selected from the consultation archive of Toyama University Hospital. Clinical records and histological specimens were reviewed. Immunohistochemical staining for fPAP; against surfactant protein-A (SP-A) was performed for unstained slides. Idiopathic pulmonary fibrosis (IPF) cases with fPAP were extracted and compared to the IPF cases without fPAP. Histological findings such as honeycomb cyst (HC), fibroblastic focus, and small airway disease were observed, and cases were separated to positive or negative based on the severity in each finding. Several statistical tests were performed depending on the distribution of the data.

Results: Twenty of 146 cases (13.7%) were identified to have fPAP [Figure A, B]. Focal PAP was strongly positive to SP-A [Figure C]. Among those 20 cases, 15 cases were IPF, and the incidence of fPAP in IPF patients was 15/56 (26.8%). In the comparison between IPF with and without fPAP, HC was solely associated with fPAP among histological findings ($P = 0.016$) [Table 1]. Furthermore, lower %FVC and higher serum KL-6 were associated with fPAP ($P = 0.022$, 0.005, respectively).

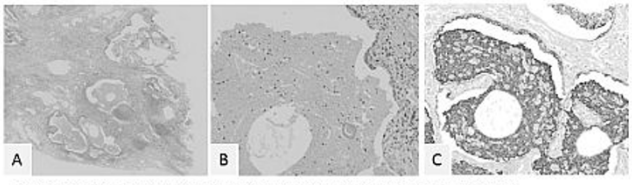

A, B) Note honeycomb cysts contain accumulation of granular materials. (H&E stain, x 0.6 and x 4.0).
C) Anti-SP-A staining highlights focal PAP. (x4.0)

Histological findings of idiopathic pulmonary fibrosis with and without focal pulmonary alveolar proteinosis

	fPAP (n=15)	No fPAP (n=21)	P value
Honeycomb cyst	13 (87%)	10 (47%)	0.016
Fibroblastic foci	12 (80%)	14 (67%)	0.468
Small airway disease	7 (47%)	15 (71%)	0.133
Cellular interstitial pneumonia	6 (40%)	5 (24%)	0.465
Dust deposition	4 (27%)	7 (33%)	0.729
Lymphoid follicle	5 (33%)	5 (24%)	0.709

fPAP, focal pulmonary alveolar proteinosis;

Conclusions: We found that the IPF frequently show fPAP. Focal PAP in IPF associated with decline of %FVC, severity of HC, and serum KL-6, all of which indicates that presence of fPAP may be a histopathological indicator of disease progression.

1923 Pulmonary Metastatic Nodules of Endometrial Stromal Sarcoma; a Histopathologic Review of 10 Cases

JY Park, CO Sung, SY Song, JH Han, SJ Jang, K-R Kim. University of Ulsan College of Medicine, Seoul, Korea; Sungkyunkwan University School of Medicine, Samsung Medical Center, Seoul, Korea.

Background: Lung is the most common metastatic site in cases of endometrial stromal sarcoma (ESS). However, the diagnosis on small biopsy specimen is frequently challenging because of relatively low incidence of the tumor, long disease free interval before metastasis, and rarity of pathologic description regarding pulmonary metastatic lesion of ESS, and it is especially true when the pulmonary lesion is the first manifestation of the disease.

Design: We scrutinized histopathologic findings and immunohistochemical features for CD10, estrogen and progesterone receptors, D2-40, and CD31 in 46 metastatic pulmonary nodules from nine patients with low grade ESS and miliary nodules in one patient on wedge resected specimens to seek any helpful findings for the diagnosis of small biopsy samples and to investigate the route of metastases to the lung.

Results: All lesions formed well circumscribed nodules on bilateral lungs with the size ranging from 100μm to 2.3cm. Prominent interstitial collagen deposit (49%), absence of spiral arteriole-like vasculature (27%), microcystic change due to cystic dilatation of bronchiolar lumens (21%), myxoid degeneration (12%), foam cell change (5%), and smooth muscle differentiation (2%) were noted in the metastatic lesion. CD10 decorated normal alveolar septa as well as the tumor cells, but ER was positive only in the tumor cells of all cases. The tumor showed peribronchiolar distribution with characteristic tight subepithelial growth in 59%, perivascular distribution in 35%, and perilymphatic distribution in 49%. One case with numerous miliary micronodules showed mixed patterns of peribronchial, perivascular, perilymphatic, paraseptal and subpleural distributions.

Conclusions: Frequent secondary change in metastatic ESS might be an obstacle for correct diagnosis on small biopsy samples. Thus, awareness of frequent secondary changes, and the distribution patterns will be helpful for the diagnosis. Considering that abundant normal lymphatic channels are distributed around the bronchovascular trees, and within visceral pleura and interlobular septae, and that frequent peribronchiolar distribution of metastatic lesions in our cases with the presence of lymphatic tumor emboli in some cases, lymphatic metastasis might be an important route of pulmonary metastasis.

1924 Down Regulation of Angiotensin II Receptor Type 1 (AGTR1) Contrast with Up Regulation of Type 2 (AGTR2) in Idiopathic Pulmonary Fibrosis

ER Parra, ADP Ruppert, MP Rangel, VL Capelozzi. University of São Paulo Medical School, São Paulo, Brazil.

Background: Idiopathic pulmonary fibrosis (IPF) is the most common form of idiopathic interstitial pneumonia. IPF represents a progressive and lethal disorder and is of major concern due to its unresolved pathogenesis and limited responsiveness to currently available therapies. IPF is characterized by alveolar injury, fibroblast proliferation and extracellular matrix (ECM) accumulation with severe loss of respiratory function. Angiotensin II (ANGII) signaling, mediated via angiotensin II receptor type 1 (AGTR1) or type 2 (AGTR2), controls tissue remodeling in fibrosis, but the relevance of AGTR2 and AGTR1 remains elusive.

Design: Twenty-seven patients with biopsy-proven IPF disease with pulmonary evaluation by high-resolution computed tomography (HRCT) and pulmonary function tests were studied. Ten normal lung tissues (NLT) were included with controls. AGTR1 and AGTR2 in lung parenchyma were detected by immunohistochemistry and quantified by histomorphometry.

Results: Quantitative analysis revealed a significant increase of AGTR2 expression in epithelial, endothelial and fibroblastic cells from patients with IPF when compared to NLT group. In contrast, AGTR1 expression levels are decreased in these cells from patients with IPF when compared with NTL. Pulmonary function tests no showed correlation with expression of AGTR1 or AGTR2. The median follow-up was 42.70 months. Ten patients were still alive, 17 died from causes related to IPF. Kaplan Meier curve, showed that the 5-year survival rate in patients with <0.05% of AGTR1 levels was 58.20% versus 24.66% in the group with ≥ 0.05% of AGTR1 levels ($p < 0.05$).

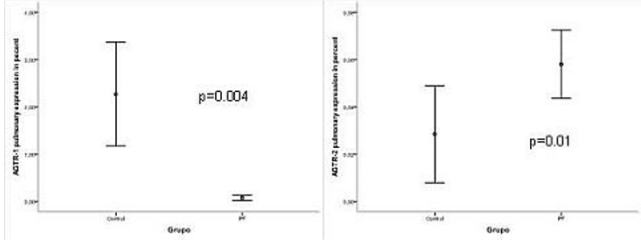

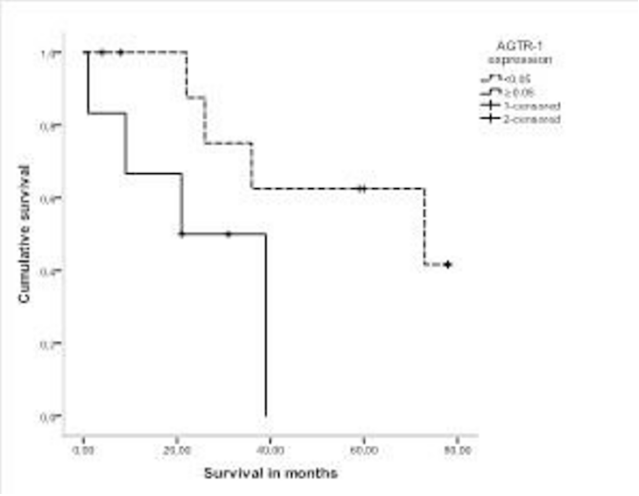

Conclusions: In summary, we demonstrated increased expression of AGTR2 and decreased expression of AGTR1 in lung tissues from patients with IPF suggesting that they may be promising markers of prognosis in these patients.
Financial Support: FAPESP, CNPq.

1925 Expression Profiles of the Regulatory Master *p63* Gene in Pulmonary Adenocarcinoma Recapitulate the Normal and Developmental Lung

G Pelosi, F Perrone, E Tamborini, E De Paoli, A Fabbri, P Scanagatta, R-A Romano, S La Rosa, U Pastorino, M Papotti. Fondazione IRCCS Istituto Nazionale dei Tumori, Milan, Italy; State University of New York at Buffalo, Center for Excellence in Bioinformatics and Life Sciences, Buffalo, NY; Unsubria University at Varese, Varese, Italy; San Luigi Gonzaga Hospital and University of Turin, Turin, Italy.
Background: Little is known about the role of *p63* gene, an important player in the development of squamous epithelia and pulmonary squamous cell carcinoma (SQC), in the growth of lung adenocarcinoma (AD).
Design: One hundred twenty consecutive AD were assessed by immunohistochemistry (IHC) for the presence of transactivating (TA) and non-TA (hence simply p40) isoform assessment, by interphase fluorescence in situ hybridization (FISH) for *p63* gene status, and by quantitative (q)-PCR for mRNA levels of α, β, γ, δ, and ε isoforms, whether TA- or non-TA. Fifteen SQC samples, a few human spontaneous abortion specimens and delta-Np63(p40) gene-knockout (KO) mice were used as controls. AD were classified according to the last IASLC/ATS/ERS classification.
Results: TA isoforms were found by IHC in 20% of AC (range 10-70% tumor cells) regardless of their growth patterns or variants, whereas non-TA (p40) isoforms were seen in only 1-2% tumor cells of up to 5% AC but were consistently accumulated in all SQC samples. By q-PCR, AD showed a prevalence of TA-α over β isoforms, whereas the reverse held true for SQC in which prevailed non-TA-α over β, γ, δ and ε, in that order. In human fetuses, TA and non-TA were early acquired during development but never expressed by alveolar cells, and p40-KO mice normally developed lungs. No relationship was observed between *p63* gene status as assessed by FISH and protein expression or mRNA accumulation, as well as no survival or clinical association was found.
Conclusions: The expression of the diverse p63 gene isoforms in lung AD recapitulates the normal and developmental lung and is highly conserved among different species. Non-TA isoform expression is likely to reflect the growth of bronchial epithelium-derived tumor cells but they are not required for the development of alveolar cells, whether in humans or mice. The consistent combination of p40 positivity in SQC and p40 negativity in AD reflects the different role of *p63* gene in the cell lineage-dependent tumor development and may have diagnostic implications.

1926 Claudin-4: An Effective Immunohistochemical (IHC) Marker Distinguishing Primary and Metastatic Lung Adenocarcinoma from Pleural Epithelioid Malignant Mesothelioma

AS Perry, GS Pinkus, JM Corson. Brigham and Women's Hospital, Harvard Medical School, Boston, MA.
Background: Distinction of metastatic adenocarcinoma from epithelioid malignant mesothelioma (MM) is a well-known diagnostic challenge. Numerous antibodies are useful in this distinction but none with absolute (100%) sensitivity and specificity. Claudin-4, a tight junction protein has recently been reported (Facchetti et al, Virchows Arch. 2007, 451:669-680) as helpful to distinguish lung adenocarcinoma (LAC) and adenocarcinoma of other organs from MM. This study compares the expression of claudin-4 in a large series of LAC (n=83) and pleural epithelioid MM (n=76).
Design: Cases were retrieved from the files of the Brigham and Women's Hospital (Boston, MA) from the period 2005-12 and diagnoses were confirmed. Immunohistochemistry was performed on formalin-fixed paraffin embedded tissue sections following heat-induced epitope retrieval (EDTA/steamer) using a monoclonal antibody to claudin-4 and an immunoperoxidase technique. Appropriate positive (LAC) and negative (isotype control) control slides were processed for all studies. Staining intensity and percentage of cells immunoreactive for claudin-4 was evaluated.
Results: Claudin-4 immunoreactivity was present in all cases (100%) of LAC (primary n=60; metastatic n=23). Most (75-100%) of the neoplastic cells were immunoreactive in 75 cases (90%) of LAC. Claudin-4 reactivity was generally of strong intensity and was expressed in a predominantly membranous pattern. Staining intensity was independent of histologic grade (well differentiated n=7; moderately differentiated n=20; poorly differentiated n=56) and biopsy site (lung n=60; pleura n=23). All 76 cases of mesothelioma were totally negative for membranous reactivity. In this series of cases, the sensitivity and specificity of distinguishing between LAC and MM was 100% for both.

Membranous Claudin-4 Expression

Intensity	LAC (n=60)	Metastatic LAC involving pleura (n=23)	Pleural MM (n=76)
Absent	0 (0%)	0 (0%)	76 (100%)
Weak	0 (0%)	0 (0%)	0 (0%)
Moderate	5 (8%)	6 (26%)	0 (0%)
Strong	55 (92%)	17 (73%)	0 (0%)

Conclusions: This study demonstrates that immunohistochemical expression of Claudin-4 is associated with lung adenocarcinoma, both primary and metastatic, exhibits a strong membranous staining pattern, and is highly effective in distinguishing LAC from pleural epithelioid MM.

1927 Adult Pulmonary Interstitial Emphysema: A Clinically and Pathologically Underdiagnosed Entity with Distinct Clinicopathologic Features

S Pokharel, LM Sholl, SO Vargas. Brigham and Women's Hospital, Harvard Medical School, Boston, MA.
Background: Pulmonary interstitial emphysema (PIE) is identified by the presence of air in the connective tissue of the peribronchovascular sheath, interlobular septa and visceral pleura. It is described in premature infants but is not well characterized in adults.
Design: Pathology reports were searched for the term "interstitial emphysema" in pulmonary wedge resection, lobectomy, and pneumonectomy specimens obtained from January 2005 to September 2012. For patients with documented PIE, clinicopathologic data were recorded and archived slides were reviewed.
Results: During the study period, 5 lung resection reports documented the presence of PIE, including 4 pneumonectomies for lung transplantation and one volume reduction wedge biopsy post-lung transplantation. All reports with a diagnosis of PIE had been reviewed by a pathologist with pediatric expertise, responsible for approximately 13% of an adult lung pathology service caseload. Patients (mean age 59 ± 7 yr) included 4 nonsmokers and 1 former smoker. One had a history of pneumothorax, and 4 had a history of positive-pressure ventilation, 1 of whom had Nissen fundoplication complicated by pneumomediastinum and subsequent rapidly progressive lung disease. In none of the patients was PIE suspected clinically. Slides from 4 patients were available for review. All demonstrated characteristic histologic features of PIE, including cystic air-filled spaces lined with histiocytes/synoviocyte-like cells and giant cells, predominantly along bronchovascular bundles and subpleural areas. Fibrous scar tissue surrounding the cysts showed abundant delicate collagen fibers with occasional myxoid foci, often associated with interspersed eosinophils. The extent of PIE ranged from mild/moderate (n=2) to extensive (n=2); when extensive, PIE was the dominant pathologic finding. Lymphatic channels were at least mildly dilated in all cases. Other pathologic features included cystic bronchiectasis (n=1, with cystic fibrosis) and honeycomb change (n=3).
Conclusions: PIE is found in adult lungs following positive-pressure ventilation, pneumothorax, and thoracic surgery. It is underrecognized clinically. In a subset of severe interstitial lung disease cases, it constitutes a major pathologic feature. Histologically, it shows not only the classically described cystic spaces, but also a peculiar and distinctive pattern of peri-cyst fibrosis. It may be underdiagnosed by pathologists with limited exposure to diseases more commonly appreciated in the pediatric population.

1928 Neoplasms in Lung Explants: A Retrospective Review of 311 Consecutive Orthotopic Lung Transplants

J Poling, PB Illei. Johns Hopkins Medical Institutions, Baltimore, MD.
Background: There are only few case reports of neoplasms in explanted lungs and only one case series describing multiple incidences. Many of the same risk factors for the development of non-neoplastic lung diseases, most notably tobacco exposure, are also risk factors for the development of lung carcinomas. Clinically undetected neoplasms discovered in the explanted lung(s) may necessitate treatment following transplantation that may affect both short- and long-term survival.
Design: We reviewed the surgical pathology reports of 311 consecutive lung explants performed at our institution. Routine workup included serial sectioning (at 0.5-1.0 cm) with careful palpation of the entire lung parenchyma and histologic analysis of multiple sections from all lobes, the bronchial margin and hilar lymph nodes. For patients with tumors we reviewed the clinical records including follow-up treatment and survival data, pre-transplant imaging studies, and tobacco history.
Results: Seven of 311 (2.2%) lung explants had neoplasms. Common reasons for OLT included COPD (31%), UIP/IPF (22.5%), cystic fibrosis (18%), sarcoidosis (5.1%) and scleroderma (4.2%). Tumors were seen in COPD (x2), UIP/IPF (x2), sarcoidosis (x2) and cystic fibrosis. Summary of tumor types and clinical data are shown in table 1. Of the patients with tobacco status documented, 4/4 (100%) had a significant smoking history. On pre-operative imaging several patients abnormal findings, but these were attributed to the underlying non-neoplastic processes.

Table 1.

Reason for OLT	Age/ Sex	Tumor type	Therapy	Follow up
COPD	49 F	SQCA 1.5 cm	None	Day 454 Died of DAD, NED
COPD	57 F	SCLC 0.4 cm & SqCIS @ margin	Cisplatin-Etoposide & RT	Day 458 NED
UIP/IPF	54M	ACA bilateral	None	Day 45 DOD
UIP/IPF	62	Typical carcinoid (0.2 cm)	None	Day 20 NED
Sarcoidosis	61 M	Garnular cell tumor (0.7 cm)	None	Day 693 NED
Sarcoidosis	48 M	MALT lymphoma, bilateral	None	Day 628 NED
Cystic fibrosis	59 F	Catleman Disease	None	Day 927 NED

Conclusions: Although not common, clinically undetected neoplasms are present in explanted lungs. The majority of these neoplasms are early stage and do not require additional therapy. Similar to the general population strong smoking history increases the risk of tumors in OLT. Explanted lungs should be carefully examined grossly and microscopically because of the small size of these tumors. Routine sections should include the bronchial margins and hilar lymph nodes.

1929 Granulomatous and Lymphocytic Interstitial Lung Disease (GLILD) in Common Variable Immunodeficiency (CVID) – Histological and Immunohistochemical Analysis of 12 Cases of a Rare Entity

N Rao, N Chase, JM Routes, AC Mackinnon. Medical College of Wisconsin, Milwaukee, WI.

Background: CVID is a primary immunodeficiency of unknown etiology characterized by low serum IgG, inability to make specific antibodies and variable T cell defects. Up to 20% of patients with CVID can develop clinical evidence of a progressive restrictive diffuse parenchymal lung disease called GLILD. The constellation of pulmonary changes in GLILD have not been described comprehensively in the pathology literature. We present the histological and immunohistochemical features in a series of 12 cases of this rare entity.

Design: Twelve (12) cases of GLILD form the basis of the study. Open lung (11) and transbronchial (1) biopsies were evaluated for interstitial and alveolar inflammation, lymphoid aggregates with or without germinal centers, granulomata, organizing pneumonia and interstitial fibrosis. Immunohistochemical stains were performed on six cases for a panel of antibodies including CD3, CD 20, CD4, CD8, Human Herpes Virus-8 (HHV-8), and CD 68. The proportion of T and B lymphocytes and CD4+ and CD8+ subsets of T cells were calculated by image analysis.

Results: Follicular bronchiolitis (12/12 cases), lymphoid interstitial pneumonia (LIP) (11/12) and granulomatous inflammation (11/12) were consistent features; organizing pneumonia (7/12) and interstitial fibrosis (6/12) were also seen, although architectural remodeling reminiscent of the usual interstitial pneumonia (UIP) pattern was seen only in 1 case. Epithelioid cell granulomata bore some resemblance to sarcoidosis with circumscription and absent necrosis but without the distinct lymphangitic distribution pattern. Quantitative immunohistochemical analysis showed that CD3+ T cells comprised 69.7 – 98.9% of all lymphocytes (mean – 81.7%); and CD4+ cells comprised 58.2 – 94.2% of all T lymphocytes (mean – 71.8%). HHV-8 was negative in all cases and CD68 highlighted numerous histiocytes, including mononuclear epithelioid histiocytes comprising the granulomata.

Conclusions: We have characterized the pathologic features of GLILD, a rare entity occurring in patients with CVID. Consistent histologic features include follicular bronchiolitis, LIP and sarcoid-like granulomata. Organizing pneumonia and interstitial fibrosis can be seen, and the latter may portend poor prognosis. The histologic overlap, and the predominance of CD4 positive cells, point to a T helper cell driven immune process somewhat analogous to sarcoidosis.

1930 Clinical, Pathological and Molecular Predictive Factors for the Development of Brain Metastasis in Patients with Lung Adenocarcinoma

K Raparia, C Villa, M Mehta, P Cagle. Northwestern University, Chicago, IL; Methodist Hospital, Houston, TX.

Background: Metastasis to brain comprises 24-45% of all cancer patients, of which the most common primary site is lung. It is important to predict which lung cancer patients are at higher risk of developing brain metastases, so that prophylactic therapies can be better directed. We hypothesize that lung adenocarcinomas, which metastasize to the brain show distinct morphologic and molecular features and outcomes.

Design: We evaluated clinical and pathological feature of patients with Stage 4 lung adenocarcinoma with known epidermal growth factor receptor (EGFR) mutation, v-Ki-ras2 Kirsten rat sarcoma viral oncogene homolog (KRAS) mutation and anaplastic lymphoma kinase (ALK) gene rearrangement status, diagnosed at our institution between 2008 and 2011. Overall survival (OS) was analyzed using the Kaplan-Meier and Cox proportional hazard methods.

Results: 58 of 126 patients with stage 4 lung cancer (46%) had brain metastases. Of the patients with brain metastases, 37 (64%) were women and had a median age of 62 years (range 32-92 years). 26% patients had solitary, and 74% had multiple lesions in the brain. Majority of these patients (52%) had metastatic deposits at other sites including bone, adrenal, contralateral lung, liver, choroid and peritoneum. Patients with brain metastasis had larger lung nodules (p=0.006) and were slightly older in age (68 vs. 64 years, p=0.044). Lung primaries, which developed brain metastases had predominant acinar pattern. 25% of these patients had EGFR mutation and 28% patients harbored KRAS mutation. G12V in codon 12 was the most common KRAS mutation and E746 mutation in exon 19 was most common EGFR mutation in this subgroup. 2 patients had ALK gene rearrangements. Trend for increased survival was seen in patients with EGFR mutation (Log rank, p=0.067), but no difference in survival was seen in patients with KRAS mutation.

Conclusions: G12V is the most common KRAS mutation and E746 is the most common EGFR mutation in the patients with lung adenocarcinoma with brain metastasis. Patients with EGFR mutation had a trend for increased survival than those patients with EGFR wild type tumors.

1931 Lung Carcinoma Masquerading as Desquamative Interstitial Pneumonia (DIP): Report of 7 Cases and Review of Literature

K Raparia, J Ketterer, ML Dalurzo, Y-H Chang, TV Colby, KO Leslie. Northwestern University Feinberg School of Medicine, Chicago, IL; Italian Hospital of Buenos Aires, Buenos Aires, Argentina; Mayo Clinic, Scottsdale, AZ.

Background: Malignant tumors in the lung (both primary and metastatic) may rarely be associated with marked discohesion of tumor cells, with extension into the alveolar spaces in a pattern reminiscent of "desquamative interstitial pneumonia" (DIP). A peculiar aspect of this growth pattern is the relatively bland appearance of the tumor cells, in many cases simulating histiocytes, potentially a pitfall in the diagnosis.

Design: We searched the Charles Carrington Memorial consultation files in the Mayo Clinic Arizona Pathology Department for instances of malignant tumors in lung simulating DIP, from 1992 to 2011. We identified 7 cases involving the transbronchial biopsies, needle core samples and resected lung specimens. Clinical, histopathological and immunohistochemical analysis of these 7 patients was performed, including detailed morphometric analysis of the individual tumor cells using calibrated measurement tools on digital images. We compared the results to a control group of 4 patients with DIP-reactions in smoking-related disease.

Results: 5 males and 2 females, 48 to 86 years in age (mean: 67.8 years) comprised the study group. The radiologic findings included lobar consolidation, ground glass opacities, and rarely nodule formation. Microscopically, the lung parenchyma was dominated by prominent individual tumor cells within the alveolar spaces. 4 had primary lung carcinoma (adenocarcinoma), while 3 had metastasis from other sites. Immunostains were performed on 6 out of 7 cases to make the diagnosis. Nuclear diameter, cytoplasmic size and nuclear/cytoplasmic (N/C) ratios in patient and control groups were compared using the Wilcoxon Rank-sum test. No significant difference in the diameters of nuclear and cytoplasm between cases and control groups (p=0.3447 and p=0.7055, respectively) was seen, and only a marginal significant difference in N/C ratios (p=0.0890) was seen. A more complex analysis, Generalized Estimating Equation analysis, showed a significant difference in N/C ratio between the two groups (p=0.0278).

Conclusions: A "DIP-growth pattern" of malignant tumors in lung is presented. Although the N/C ratio difference approached statistical difference, the key to diagnosis is the individual cytology of the tumor cells. Immunohistochemical studies (keratin or other markers) are essential to make an accurate diagnosis in these tumors.

1932 Flow Cytometric Characterization of Peripheral Blood Fibrocytes in Lung Transplant Patients

AM Raza, Y Zu, PT Cagle, R Barrios, H Takei, Y Ge, A Ponce De Leon, A Ewton. Methodist Hospital, Houston, TX.

Background: Fibrocytes are bone marrow derived mesenchymal cells with properties of both macrophages and fibroblasts that participate in tissue repair and fibrosis. Increased circulating fibrocytes can be present in patients with pulmonary parenchymal diseases, nephrogenic fibrosis, pulmonary hypertension and in autoimmune disorders. The antigenic characterization of circulating fibrocytes in lung transplant patients may yield clues to disease progression, but have not been extensively studied.

Design: Pheripheral blood from 15 lung transplant patients (n=15) and 20 healthy controls (n=20) were examined by flow cytometry to quantify circulating fibrocytes among lung transplant patients. The panel of antibodies includes CD14, CD45, CD34 and collagen.

Results: The percentages of peripheral blood fibrocytes are significantly higher in lung transplant patients (9/15, 60%) (p=0.00027) compared to control patients.

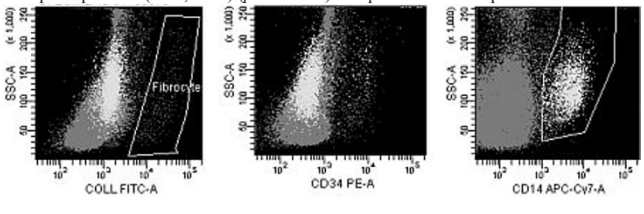

Population	#Events	%Parent	%Total
All Events	100,000	####	100.0
Monocytes	6,063	6.1	6.1
Fibrocytes	374	0.4	0.4

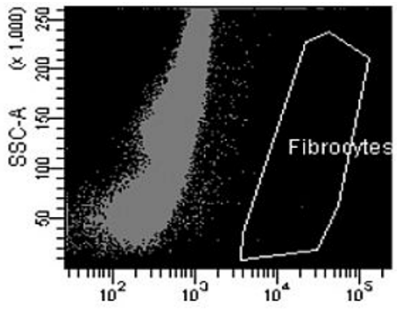

Population	#Events	%Parent	%Total
All Events	100,000	####	100.0
Fibrocytes	2	0.0	0.0

These fibrocytes are characterized by expression of CD34, CD14, CD45 and collagen.
Conclusions: Increased circulating fibrocytes are seen in majority of lung transplant patients. Our study showed significantly higher percentage of circulating fibrocytes in lung transplant patients compared to patients without transplant. Circulating fibrocytes could serve as a clinical biomarker and can provide a method of monitoring fibrosis of the transplanted lungs and may provide a therapeutic target for chronic graft rejection. However further studies are needed to determine the correlation between risk of fibrosis after lung transplantation and percentage of circulating fibrocytes.

1933 ALK Protein Expression Correlates with *ALK* Rearrangement, but Not Increased *ALK* Copy Number in Lung Adenocarcinomas

B Ren, LA McMahon, Q Yang, N Wang, P Rothberg, Z Zhou, F Li, H Xu. University of Rochester Medical Center, Rochester, NY.

Background: A small subset of non-small cell lung carcinomas (NSCLCs) harboring anaplastic lymphoma kinase (*ALK*) gene rearrangement are responsive to ALK inhibitor therapy. A novel, highly sensitive antibody against ALK has been developed for detecting *ALK*-rearranged lung adenocarcinoma. However, ALK expression in NSCLCs with increased *ALK* copy numbers is largely unknown. Our study aimed to evaluate the ALK expression in NSCLCs with *ALK* rearrangement and copy number change.
Design: *ALK* genetic status was determined by FISH using break apart probes in total 59 cases of NSCLC, including 20 confirmed extrapulmonary metastases, 20 lung biopsies, and 19 lung resection specimens. Fifty four cases were also analyzed for mutations in exons 19 and 21 of the *EGFR* gene using Sanger sequencing. ALK protein expression was detected by immunostain using a monoclonal antibody (Cell Signaling Technology) in 36 cases (5 *ALK*-rearranged adenocarcinomas, 19 NSCLCs with increased *ALK* copy numbers, and 12 normal *ALK* NSCLCs).
Results: Among 59 total cases, FISH analysis showed 7 adenocarcinomas with *ALK* gene rearrangement, 19 NSCLCs (16 adenocarcinoma, 2 squamous carcinoma and 1 adenosquamous carcinoma) with increased *ALK* copy numbers, and 33 NSCLCs (29 adenocarcinoma, 1 adenosquamous carcinoma, and 3 not otherwise specified NSCLCs) with normal *ALK*. One adenocarcinoma with increased *ALK* copy number and two adenocarcinomas with normal *ALK* harbored activating *EGFR* mutations. Positive ALK protein expression was observed in 80% (4/5) of *ALK*-rearranged adenocarcinomas, with 3 of them exhibiting moderate to strong staining in more than 90% of the tumor cells and one showing weak staining in 80% of the tumor cells. No ALK protein expression was detected in NSCLCs with increased *ALK* copy numbers or normal *ALK*. Immunostain failed to detect one *ALK*-rearranged adenocarcinoma which had only 6.5% cells with split signals. Five of 20 (25%) extrapulmonary specimens and 2 of 39 (5.1%) pulmonary cases had *ALK* rearrangement ($p<0.05$).
Conclusions: Our study indicates that immunohistochemical staining for ALK could be used as a surrogate assay to screen *ALK*-rearranged adenocarcinoma for targeted therapy. Also our results indicate a possible association of *ALK* rearrangement with metastatic lung adenocarcinoma. The clinical significance of increased *ALK* copy number in NSCLC merits further study.

1934 *MAML2* Rearrangements in Thymic Mucoepidermoid Carcinomas

AC Roden, M Erickson-Johnson, ES Yi, JJ Garcia. Mayo Clinic, Rochester, MN.

Background: Mucoepidermoid carcinoma (MEC) is a rare histologic subtype of thymic carcinoma and composed of epidermoid, intermediate and mucous cells. High grade MECs mainly consist of the epidermoid component and could be challenging to differentiate from squamous cell carcinoma. Substantial evidence from several anatomic sites including lung and head and neck has demonstrated a strong association between MEC and t(11;19)(q21;p13). The most common genes involved in this translocation are Mucoepidermoid Carcinoma Translocated 1 (*MECT1*) on chromosome 19p13 and a member of the MasterMind-Like gene family, *MAML2*, on chromosome 11q21. Although this translocation is often considered a disease-defining event for MEC, the incidence of this finding in the context of thymic MEC has not been explored. In this study we evaluate the diagnostic utility of detecting *MAML2* rearrangement by fluorescence in situ hybridization (FISH) in thymic MEC along with unequivocal examples of squamous cell carcinoma and adenosquamous cell carcinoma cases in order to evaluate its role in diagnosis and in understanding molecular pathogenesis.
Design: FISH was employed to detect *MAML2* rearrangements using a *MAML2* - 11q21 break apart probe (BAP) that consisted of bacterial artificial chromosomes (BAC) flanking the 5' and 3' sides of *MAML2*. 5' BACs were labeled in SpectrumOrange and consisted of RP11-1056O10, CTD-2325K3, and RP11-8N17. 3' BACs were labeled in SpectrumGreen and consisted of CTD-2252L1, RP11-123F20, RP11-7D4, and CTD-254417. At least 100 interphase tumor cell nuclei were evaluated per case. Identifying a split signal in more than 10% of tumor cells was considered positive.
Results: FISH for *MAML2* rearrangement was performed on low and intermediate-grade thymic MEC (n=1, each), poorly differentiated thymic squamous cell carcinoma (n=7) and thymic adenosquamous cell carcinoma (n=1). The two cases of low and intermediate-grade thymic MEC (38 yo male, 4.0 cm tumor; 68 yo female, 8.0 cm tumor, respectively) were positive for *MAML2* rearrangement. All other tested cases were negative.
Conclusions: FISH for *MAML2* rearrangement is likely a useful tool in the evaluation of thymic malignancies; specifically, distinguishing MEC from squamous cell carcinoma and adenosquamous cell carcinoma. These findings suggest that thymic MEC are not only histologically but also biologically related to MECs of the head & neck. Larger studies of thymic MEC are necessary to confirm our findings and to assess whether *MAML2* translocation status bears prognostic significance as well.

1935 Histopathologic Comparison of Biopsy with Subsequent Explant/Autopsy in Patients with Interstitial Lung Disease

AC Roden, RS Kuzo, DL Levin, T Moua, JH Ryu, ES Yi. Mayo Clinic, Rochester, MN.

Background: The temporal evolution of histologic features of interstitial lung disease (ILD) is not well characterized. Although literature suggests that for instance cellular non-specific interstitial pneumonia (NSIP) might evolve into fibrotic NSIP, the incidence of that process is unknown. Moreover, sampling might play a role in our ability to correctly diagnose ILD. We studied patients with clinically suspected ILD who underwent biopsy (bx) and subsequent lung transplant or autopsy.
Design: Patients with clinically suspected ILD, a lung bx and a subsequent explant or autopsy were included. Pathology was reviewed by two pulmonary pathologists and a consensus diagnosis was reached. CT scans at the time of bx were reviewed by two thoracic radiologists and a consensus was reached.
Results: 34 patients (19 men, 15 women) with a median age of 56.6 years (range, 25-76) underwent surgical (n=32) or transbronchial bx (n=2) and had a subsequent transplantation (n=21) or autopsy (n=13). Median time between bx and explant/autopsy was 3.8 years (range, 0-24). Tables 1&2 summarize the histologic diagnoses of patients with morphologic progression (n=10, 29.4%) and patients with stable ILD (n=19, 55.9%).

Table 1: Patients with morphologic progression (n=10)

Biopsy	Explant/Autopsy	# Patients	Comments
Hypersensitivity pneumonitis (HP)	Chronic HP	2	
Focal fibrosis	Usual interstitial pneumonia (UIP)	2	Increase in fibrosis, new honeycomb changes (HC)
Emphysema	UIP	1	Lower lobe not biopsied
Emphysema	Cystic bronchiectasis	1	
Organizing pneumonia (OP)	Fibrotic NSIP	1	
OP, fibroblast foci	HC &scarring	1	
Thickened pleura	Lymphangioleiomyomatosis (LAM)	1	
Chronic bronchiolitis &granuloma	Bronchiolocentric fibrosis &scarring	1	

Table 2: Patients with stable ILD (n=19)

Diagnosis Biopsy/Explant/Autopsy	# Patients
UIP	10
Emphysema	7
Chronic HP	1
LAM	1

In 5 patients (14.7%), the ILD could not be classified morphologically. In 23 patients, the bx results together with CT (n=31) and clinical workup (n=34) led to a diagnosis at time of bx that matched the diagnosis of the explant/autopsy. The median follow-up (n=34) time after bx was 6.6 years (range, 0.12-24.02). 26 patients died.
Conclusions: Histopathologic differences between bx and explant/autopsy were not uncommon and were due to disease progression and/or limited sampling in bx. However, in the majority of patients, the diagnosis at time of bx matched the diagnosis on explant/transplant when morphologic findings were combined with radiologic and clinical impression.

1936 Cytologic-Histologic Correlation of Lung Adenocarcinoma Subtyping

EF Rodriguez, S Monaco, S Dacic. University of Pittsburgh, Pittsburgh, PA.

Background: The significance of histological subtyping of surgically resected lung adenocarcinoma (ADC) was recently proposed by the IASLC/ATS/ERS classification. Approximately 70% of lung cancer patients present with advanced disease and small biopsies or cytology specimens are the only available diagnostic material. It is uncertain if proposed morphologic subtying of ADC can be applied to small specimens.The aim of this study was to assess the applicability of morphological subtyping of lung adenocarcinoma on cytologic specimens.
Design: 133 consecutive newly diagnosed primary lung ADC from patients who underwent surgical resection were selected for the study. 66 patients had 66 positive cytologies available for review. All surgical resection and cytology specimens were

reviewed and the dominant morphologic pattern was determined according to the IASLC/ATS/ERS classification. The number and percentage of malignant cells in cytology specimens were also evaluated.
Results: Cytology specimens included FNA (n=61), pleural fluid (n=3), and bronchial lavage (n=2) specimen. Twenty nine(44 %) cases had an estimated >300 neoplastic cells, 27 (41%) had 200-100 cells, and 10 (15%) had ≤50. Concordant subtyping of ADC between resection and cytology specimens was observed in 37 cases (56%) which were classified as acinar (n=26), solid (n=7), mucinous (n=2), and papillary (n=2). Discordant subtyping was seen in 21(32%) cases. The predominant pattern in resections with discordant cytologies was solid (n=6) followed by acinar (n=5). Eight cases were not possible to classify on cytology due to scant cellularity (n=3) or indefinite patterns (n=5). Cellularity did not seem to affect cytologic-histopathologic correlation. Of the 29 cases with >300 neoplastic cells, 19 (66%) showed correlation, and 6 of 10 cases (60%) with ≤50 cells.
Conclusions: Application of the 2011 IASLC/ATS/ERS ADC classification to cytologic specimens of pulmonary adenocarcinoma is feasible, although the concordance varies by histologic subtype. Future studies are needed to establish reproducible cytologic criteria for precise subtyping of lung ADC on small specimens.

1937 *EGFR* and *KRAS* Mutation Status in Patients with Non-Small Cell Lung Cancer and Additional Primary Colorectal or Gastric Cancer

MS Roh, PJ Choi, C Son. Dong-A University College of Medicine, Busan, Republic of Korea.

Background: The molecular analysis of multiple cancers occurring in a single patient may improve understanding of general molecular principles of carcinogenesis. Colorectal cancer (CRC) or gastric cancer (GC) frequently develops as the second primary cancer in Korean non-small cell lung cancer (NSCLC) patients, which might be due in part to a common molecular basis. To determine possible underlying molecular relationships, we analyzed *EGFR* and *KRAS* mutation status in patients with NSCLC and additional CRC or GC.
Design: Twenty-eight patients with NSCLC had an occurrence of primary CRC (15 patients) or GC (13 patients) in their history or in the follow-up period. After genomic DNA was extracted from paraffin-embedded tissues, mutation analysis of *EGFR* gene exons 19 and 21 and *KRAS* gene codons 12 and 13 were performed using peptide nucleic acid-clamp real-time PCR-based assay in both NSCLCs and their CRCs or GCs.
Results: In 15 NSCLC patients with CRC, the detection rate for *EGFR* mutation was 40.0% (6 cases: 3 each in exons 19 and 21) of NSCLCs and 13.3% (2 cases: 1 each in exons 19 and 21) of CRCs and that for *KRAS* mutation was 26.7% (4 cases: all in codon 12) of NSCLCs and 26.7% (4 cases: 3 in codon 12 and 1 in codon 13) of CRCs. Three (20.0%) showed an identical *EGFR* or *KRAS* mutation in both NSCLC and CRC: identical *EGFR* mutation in 2 patients and identical *KRAS* mutation in 1 patient. In contrast, the detection rate for *EGFR* mutation was 23.1% (3 cases: 1 in exon 19 and 2 in exon 21) of NSCLCs and 15.4% (2 cases: both in exon 21) of GC in 13 NSCLC patients with GCs. An identical *EGFR* mutation in both NSCLC and GC was found only 1 patient (7.7%). No *KRAS* mutation was found in the patients with both NSCLCs and GCs.

Comparison of the EGFR and KRAS mutation status between the non-small cell lung cancers and their additional primary colorectal or gastric cancers

Gene	Mutation status	Cancer	
		NSCLC/CRC (n=15,%)	NSCLC/GC (n=13,%)
EGFR	-/-	9 (60.0)	9 (69.2)
	-/+	0 (0)	1 (7.7)
	+/-	4 (26.7)	2 (15.4)
	+/+	2 (13.3)	1 (7.7)
KRAS	-/-	8 (53.3)	13 (100)
	-/+	3 (20.0)	0 (0)
	+/-	3 (20.0)	0 (0)
	+/+	1 (6.7)	0 (0)

NSCLC, Non-small cell lung cancer; CRC, Colorectal cancer; GC, Gastric cancer.

Conclusions: We found that *EGFR* or *KRAS* mutations may play a certain role in developing NSCLC and concomitant CRC, which may explain the association of the higher incidence of occurrence between the two cancers. Further studies with a large number of cases for other genetic changes leading to a higher susceptibility for cancer may determine why individuals with NSCLC have a higher risk of developing CRC or GC.

1938 An Intratumoral B-Cell Immune Response Determines Favorable Prognosis for Early Stage Lung Cancer and Can Be Assessed by Different Immunoscores

J Sanz, S Hernandez, F Hernando, JLG Larriba, J Puente, M Ferrer, B Perez Villamil, JL Subiza. Hospital Clinico San Carlos, Madrid, Spain.

Background: One third of patients with early stage NSCLC will relapse before 5 years after surgery. There is enough evidence that immune response against tumour is crucial and an efficient immuno-score is required to improve prognosis and therapy decisions. By unsupervised whole genome expression profiling we found and validate a 50-gene signature as the best predictor for disease free survival (DFS) in stage I/II NSCLC compared with TNM and other variables. The vast majority of the 50 genes were associated with a B cell humoral response. Our aim was to compare inmunoscores by morphology, immunophenotype or gene expression.
Design: 84 resected R0 stage I /II NSCLC without adjuvant therapy. Recurrence: 34.5%. TNM, clinicopathological variables, EGFR and Kras mutations, microarray expression and 50-gene signature, chronic inflammation on H-E, semiquantitatively by IHC for CD3, CD4, CD8, granzyme B, CD20, CD57, CD79 and CD19, Univariate and multivariate analysis for DFS were assessed.
Results: In our series, clinicopathological variables incluing TNM were not associated with DFS. K-ras mutations showed a tendency (p=0.07) and only immune scores showed significant association with DFS.

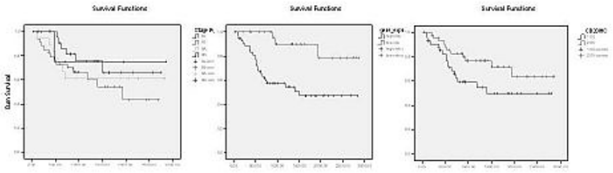

The best predictor/ immunoscore was the 50-gene signature (HR=3.44; p=0.001) that identified 1/3 of patients with good prognosis including both AC and SCC, stage I and II. Presence of CD20+ cells (>60 cells/mm3) in the center of the tumour was detected in 50% of cases associated with favorable prognosis (p=0.05). Morphologic evaluation of inflammation on H-E slides, T-cell and NK cells IHC markers, were not useful prognostic indicators. CD79 showed a tendency (p=0.08).
Conclusions: A B-cell immune response from B/plasma cells infiltrating the tumor is the best predictor of DFS for completely resected NSCLC. It can be more precisely assessed by expression profiling but also CD20 IHC could be a useful immunescore. Although immune mechanisms with cancer prognostic value have been related mainly to Tcells, some recent studies point to a key role for humoral adaptive immune response. Indeed, we can classify a subgroup of patients with very low risk of recurrence associated to a B-cell response, that may be candidates to avoid the toxicity of adjuvant therapy.

1939 Long Term Effects of EGFR Tyrosine Kinase Inhibitor Therapy on the Non-Neoplastic Lung

N Setia, PA Janne, LM Sholl. Brigham and Women's Hospital, Boston, MA; Dana Farber Cancer Institute, Boston, MA.

Background: Erlotinib, an EGFR tyrosine kinase inhibitor (TKI) was FDA-approved for treatment of advanced non small cell lung carcinoma (NSCLC) in 2004. Side effects of EGFR TKIs include interstitial pneumonitis, typically early in the course of therapy. Little is known, however, about the long term effects of EGFR TKI therapy. In this study, we examine the histology of non-neoplastic lung in patients receiving long-term EGFR TKI therapy for advanced NSCLC.
Design: Long term EGFR TKI therapy was defined as approximately 1 year or more. Cases were selected from the pathology department autopsy files based on a diagnosis of NSCLC, a history of treatment with erlotinib or other TKI therapy, and availability of lung tissue for histologic evaluation. Additional surgical specimens were identified from the authors' files. Demographic and clinical features, including history of lung disease, occupational exposures, smoking history, tumor *EGFR* mutation status, and treatment history was extracted from the medical record. Slides were reviewed for pathologic changes in the nonneoplastic lung in areas free of tumor and/or acute peri-mortem changes, for the autopsy cases.
Results: Seven cases (5 autopsies and 2 pulmonary wedge resections) were included. Patients received erlotinib for a mean of 38.3 (range 11-88) months. Mean age at diagnosis was 64.2 (range 47-79) years; 5 were male and 2 were female. None of the patients had a prior history of pulmonary fibrosis or significant occupational exposures. One patient was a smoker. All tumors contained an *EGFR* activating mutation. Prior to erlotinib therapy, all patients received ≥2 chemotherapeutic drugs, three patients received radiation therapy, and one had a lobectomy for tumor removal. The following histologic findings were noted: patchy mild-moderate interstitial fibrosis (3/7), fibroblastic foci (1/7), focal organizing pneumonia (2/7), obliterative bronchiolitis (2/7), hypersensitivity pneumonitis (1/7), pulmonary hypertensive changes (5/7) and organizing thrombi (2/7).
Conclusions: Relatively minor changes were seen in the non-neoplastic lungs of patients undergoing long term erlotinib therapy. However, obliterative bronchiolitis was noted in two cases, raising the possibility that EGFR TKIs may lead to small airways injury in a subset of patients receiving prolonged therapy. With advancements in targeted cancer therapies and associated improvements in patient survival time, the pulmonary effects of chronic EGFR TKI therapy may become clinically significant.

1940 Fatty Acid Hydrolase Is Preferentially Expressed in Pulmonary Carcinoid Tumors

K Shilo, J Ravi, M Nasser, D Cohen, W Zhao, M Villalona, J Fukuoka, J Jen, T Franks, W Travis, R Ganju. Ohio State University, Columbus, OH; Toyama University, Toyama, Japan; Mayo Clinic, Rochester, MN; JPC, Silver Spring, MD; Memorial Sloan-Kettering Cancer Center, New York, NY.

Background: Synthetic cannabinoids and the endocannabinoid system have been shown to play a role in inhibiting cancer cell proliferation and metastases in some solid tumor malignancies including non-small cell lung carcinoma. Endocannabinoids are degraded by various enzymes, including fatty acid amide hydrolase (FAAH) and thus enzymes catalyzing endocannabinoid hydrolysis represent potential new targets for cancer pharmacotherapies. The goals of this study were to investigate FAAH expression in a large cohort of pulmonary neuroendocrine tumors (NET) and to assess its possible association with clinicopathological variables.
Design: Clinicopathological features of 178 patients with NET including 48 typical carcinoids (TC), 31 atypical carcinoids (AC), 27 large cell neuroendocrine carcinomas (LCNEC), and 72 small cell lung carcinomas (SCLC) were analyzed with regard to FAAH expression utilizing tissue microarray based samples. Immunohistochemical staining (1:200, rabbit polyclonal antibody, Alpha Diagnostics, San Antonio, TX) was assessed in comparison to normal pulmonary parenchyma and recorded as: 0 (negative), 1+ (low) or, 2+ (higher than in normal bronchiolar epithelium or positive).

Correlation of FAAH expression with clinical-pathological variables was performed utilizing SYSTAT13.0 (SPSS Inc., Chicago, IL).
Results: FAAH expression was seen in tumor cells as diffuse cytoplasmic staining of variable intensity. Low levels of FAAH were present in normal bronchiolar epithelium but not in alveolar parenchyma. High levels of FAAH expression was identified in 48/126 (38.1%) of pulmonary NET, including 18/34 (53.0%) of TC, 14/27 (51.9%) of AC, 5/20 (25.0%) of LCNEC and 11/45 (24.4%) of SCLC. FAAH was more frequently detected in carcinoid tumors (52.5%) than in high grade NET (24.6%), p=0.001 and its expression correlated with tumor grade, p=0.02. No correlation between FAAH and patients' age, gender, tumor size, stage or outcome was identified.
Conclusions: FAAH expression is observed in a significant percentage of pulmonary NET and shows correlation with the tumor grade. FAAH is preferentially expressed in carcinoid tumors, suggesting that FAAH may lead to the degradation of endocannabinoids, thereby preventing the anti-tumorigenic effects of these compounds. Further investigation of FAAH and other endocannabinoid molecules as potential targets for therapy of NET is warranted.

1941 Protein Arginine Methyltransferase-5 Overexpression Is Frequently Observed in Non-Small Cell Lung Carcinomas

K Shilo, X Wu, S Sharma, M Welliver, W Duan, M Villalona, J Fukuoka, C Li, S Sif, R Baiocchi, G Otterson. Ohio State University, Columbus, OH; Toyama University, Toyama, Japan.
Background: Protein arginine methyltransferase-5 (PRMT5) is a chromatin remodeling enzyme capable of methylation of histone and non-histone proteins and is involved in a wide range of cellular processes. As such its overexpression has been linked to the tumor suppressor genes silencing, enhanced tumor cells growth and survival in lymphomas, gliomas and melanomas. The enzyme's active site is an attractive target for anti-cancer therapies and has prompted *in silico* development of a novel PRMT5 specific inhibitor (OSU BLL1). Since only limited data is available regarding PRMT5 role in lung cancer, the goals of this study were to evaluate PRMT5 expression in a large cohort of patients with non-small cell lung carcinomas (NSCLC) and its potential suitability for targeted therapy.
Design: Clinicopathological features of tissue microarray based samples of 300 patients with NSCLC were analyzed with regard to PRMT5 expression (1:70, rabbit polyclonal, Abcam, Cambridge, MA). The results were evaluated in comparison to normal lung parenchyma and recorded as negative, cytoplasmic, and cytoplasmic plus nuclear. The patterns of PRMT5 expression were also evaluated in NSCLC cell lines (NCI-H1299, A549, NCI-H520) as well as in 6 surgically resected NSCLC. Possible correlations were assessed utilizing SYSTAT13.0 (SPSS Inc., Chicago, IL).
Results: PRMT5 was identified in the majority of NSCLC with cytoplasmic expression seen in 188 (83.2%) and nuclear expression in 125 (55.3%) of 226 cases but not in normal alveolar parenchyma (44/44). Nuclear PRMT5 was more frequently observed in squamous cell carcinomas (64.9%, 74/114) than in adenocarcinomas (45.5%, 51/112), p=0.006. The patterns of expression (cytoplasmic vs. nuclear) correlated with tumor type but not with patients' age, gender, tumor grade, stage or outcome. Both cytoplasmic and nuclear PRMT5 was present in NSCLC cell lines (3/3) and surgically resected NSCLC (6/6). Additionally, nuclear PRMT5 was also identified in the areas adjacent to tumors in reactive type 2 pneumocytes, respiratory epithelium, and alveolar macrophages but not in normal alveolar parenchyma away from tumors (6/6).
Conclusions: PRMT5 overexpression is observed in a high percentage of pulmonary NSCLC, suggesting its role in pulmonary carcinogenesis. While PRMT5 is present in the cytoplasm of a majority of NSCLC, its nuclear localization is more variable and is more frequently detected in squamous cell carcinoma. Further study of the role of PRMT5 in lung carcinogenesis and as a potential target for chemotherapy is warranted.

1942 *MET* Copy Number by Dual Color Brightfield *In Situ* Hybridization and Fluorescence *In Situ* Hybridization Correlates with Met Protein Expression in Lung Adenocarcinomas

L Sholl, H Sun, A Ligon, M Butaney, PA Janne, S Rodig. Brigham and Women's Hospital, Boston, MA; Dana Farber Cancer Institute, Boston, MA.
Background: Met pathway activation drives resistance to EGFR tyrosine kinase inhibitors in some patients with *EGFR*-mutated lung adenocarcinoma (ACA). Mechanisms of Met pathway activation include *MET* amplification, HGF-mediated signaling, and EGFR crosstalk. *MET* amplification and/or Met protein overexpression may predict response to combination EGFR and Met inhibitor therapy. This study correlates *MET* copy number (CN) by fluorescence and dual color *in situ* hybridization (FISH and ISH) with protein expression by immunohistochemistry (IHC) in a cohort of lung ACA enriched for *EGFR* mutations.
Design: Studies were performed on 4um formalin-fixed paraffin embedded tissue sections from 32 patients with advanced lung ACA and known *EGFR* mutation status (66% *EGFR*-mutated). *MET* CN was assessed by FISH using probes to the *MET* locus and CEN7 and by dual color ISH using probes to the *MET* locus and CEN7 with dual color open probe software (Ventana Medical Systems, Tucson, AZ). Met IHC was performed using Met antibody clone SP44 on the Benchmark XT with ultraView DAB detection per manufacturer's instructions (Ventana). *MET* CN was categorized by signals/cell as disomic (1-2), low (3-5) or high polysomy (6-9), or amplified (≥10 and/or *MET* signal clusters). IHC was scored from 0 as absent to 4 as strong membranous and cytoplasmic staining; populations of differing intensity were multiplied by % of cells staining and summed for an H score ranging from 0 to 400.
Results: FISH and ISH for *MET* CN were highly correlated (Spearman's ρ=0.72, p<0.0001). By ISH, 12 cases were disomic, 5 had low and 8 had high polysomy, and 7 were *MET* amplified with gene clusters. Gene amplification consistently occurred on a background of polysomy and was associated with significantly higher protein expression compared to tumors with disomy or low or high polysomy (mean H scores 354 vs. 165, 165, and 221, respectively; ANOVA p=0.0002). However, one *EGFR* WT tumor was *MET* disomic and had an IHC H score of 380.
Conclusions: FISH and dual-color brightfield ISH are comparable for assessing *MET* CN on FFPE tissue slides. *MET* CN gain is common in a cohort of lung ACA enriched for *EGFR* mutations, and *MET* amplification is highly correlated with strong cytoplasmic and membranous Met protein expression. Of note, strong Met expression can occur in the absence of *MET* amplification, an observation that suggests other mechanisms of upregulation, and may have implications for identification of patients for targeted Met therapy.

1943 ROS Immunohistochemistry Is a Sensitive and Specific Tool for Detection of ROS Rearrangements in Lung Adenocarcinoma

L Sholl, H Sun, M Butaney, C Lee, PA Janne, S Rodig. Brigham and Women's Hospital, Boston, MA; Dana Farber Cancer Institute, Boston, MA.
Background: *ROS1* gene rearrangements occur in 1-2% of lung adenocarcinomas (ACA) and are associated with response to the multitargeted tyrosine kinase inhibitor, crizotinib. *ROS1* gene rearrangements can be detected using fluorescence in situ hybridization (FISH), however a novel immunohistochemistry (IHC) antibody for ROS protein has shown promise as an alternate screening tool. In this study we examine the sensitivity and specificity of IHC for the presence of *ROS1* rearrangements by FISH, and use ROS IHC to screen genetically characterized lung ACA for *ROS1* rearrangements.
Design: ROS IHC was carried out using clone D4D6 (Cell Signaling Technology; 1:1000, 1 hour incubation) on 4 micron whole tissue sections; expression that was weak/multifocal or greater was considered positive. IHC was compared to breakapart FISH using probes (RP11-59K17 and RP1-92C8) flanking the *ROS1* gene in 50 cases of lung ACA with known FISH translocation status. We then used ROS IHC to screen 167 cases of lung ACA with known *EGFR* and *KRAS* mutation and *ALK* rearrangement status. *ROS1* FISH was performed on all IHC positive cases.
Results: In the IHC validation cohort, 6 cases were FISH positive. All 6 were IHC positive, 5 strongly. One additional FISH-negative case was strongly ROS IHC positive. 42 cases were negative by FISH and IHC. Two ROS-negative cases failed FISH. One case failed both FISH and IHC. In the screening study, 105 wild type cases were tested, and 2 had strong, diffuse ROS IHC; a rearrangement was confirmed by FISH in both. 18 *EGFR* mutated cases were tested and all were negative for ROS IHC. 39 *KRAS* mutated cases were tested, and one had weak, multifocal ROS staining; FISH was negative. 7 *ALK* rearranged cases were tested, one had weak, multifocal ROS expression; FISH was negative. ROS was expressed in reactive type II pneumocytes, occasionally strongly, in a subset of FISH-negative cases.
Conclusions: In this study, diffuse ROS protein expression in tumor cells was 100% sensitive and 98% specific for *ROS1* rearrangements by FISH. The significance of strong ROS protein expression in FISH-negative tumor cells is unknown, but may be functionally significant and requires further study. In a screen of genetically characterized lung ACA, ROS protein expression was detected in 4 of 167 (2.4%) cases overall and FISH confirmed in 2 cases, for a detection rate of 1.2% overall and 1.9% in the pan-WT cohort. ROS IHC is an effective screening tool for this rare but clinically important subset of lung ACA.

1944 NKX2.8 Expression in TTF-1 Negative and KRAS-Mutant Pulmonary Mucinous Adenocarcinoma Supports the Concept of a Biologically Distinct Category of Lung Adenocarcinoma

J Suh, S Krauter, L Chiriboga, H Pass. NYU Langone Medical Center, New York, NY.
Background: The 2011 IASLC/ATS/ERS multidisciplinary classification of lung adenocarcinoma defined the entity of invasive mucinous adenocarcinoma (formerly mucinous bronchioloalveolar carcinoma; IMA), which has approximately 76% 5-year disease-free survival in Stage I patients. IMA has been correlated with TTF-1/NKX2.1 negativity and KRAS mutation, suggesting that it is biologically distinct from non-mucinous lung adenocarcinoma (NMA). Our aim is to investigate whether immunohistochemical expression of NKX2.8, a lung developmental transcription factor and potential tumor suppressor, can be detected in IMA.
Design: 10 consecutive cases of surgically resected IMA and 10 non-consecutive cases of surgically resected NMA at one institution (2011-12) were reviewed. NMA cases were selected to include 2 adenocarcinoma in situ, 2 minimally invasive adenocarcinoma, 2 lepidic predominant adenocarcinoma and 1 each of acinar, papillary, micropapillary and solid predominant adenocarcinoma while blinded to tumor mutation status. Immunohistochemistry was performed on formalin-fixed paraffin-embedded tissue to evaluate expression of CK7, CK20, TTF-1, Napsin-A, CDX-2 and NKX2.8. Molecular mutation status was recorded for each case.
Results: IMA was positive for CK7 in 10/10 cases, CK20 in 4/10 cases, TTF-1 in 2/10 cases, Napsin-A in 3/10 cases, CDX-2 in 4/10 cases and NKX2.8 in 8/10 cases whereas NMA was positive for CK7 in 10/10 cases, CK20 in 0/10 cases, TTF-1 in 10/10 cases, Napsin-A in 10/10 cases, CDX-2 in 0/10 cases and NKX2.8 in 4/10 cases. The difference in the numbers of NKX2.8 positive cases between the two groups was not statistically significant (p-value = 0.1698), but NKX2.8 was positive in 7/8 cases of TTF-1 negative IMA. Five KRAS and zero EGFR mutations were identified in IMA whereas three KRAS and two EGFR mutations were identified in NMA. The difference in the numbers of KRAS-mutant cases between the two groups was not statistically significant (p-value = 0.6499), but NKX2.8 was positive in 4/5 cases of KRAS-mutant IMA. EML4-ALK translocation was not detected.
Conclusions: NKX2.8 expression is present in up to 88% of TTF-1 negative and 80% of KRAS-mutant pulmonary mucinous adenocarcinomas, providing further evidence that IMA is biologically distinct from NMA. Additional studies are needed to determine whether NKX2.8 can be used to distinguish IMA from metastatic adenocarcinomas of upper gastrointestinal tract and pancreatobiliary origin.

1945 The Role of Immunohistochemical Analysis in the Evaluation of EML4-ALK Rearrangement Status in Lung Cancer

HC Sullivan, MT Siddiqui, J Wang, C Cohen. Emory University, Atlanta, GA.

Background: A number of mutations have been described in association with Non-small cell lung carcinoma (NSCLC). One such mutation is a rearrangement resulting from a small inversion within chromosome 2p that leads to the formation of a fusion gene, echinoderm microtubule-associated protein-like 4-anaplastic lymphoma kinase (EML4-ALK). Studies demonstrate lung cancers harboring EML4-ALK rearrangements to be sensitive to EML4-ALK inhibitors, like Xalkori (crizotinib), and possibly responsive to other medications such as Alimta (Pemetrexed), a folate antimetabolite. Currently, fluorescence in situ hybridization (FISH) is the gold standard for the detection of the EML4-ALK rearrangement. This method is time consuming, labor intensive, and technically difficult at times. The recent development of an antibody directed against a protein product of the EML4-ALK rearrangement, offers an immunohistochemistry (IHC) method for detection. The purpose of this study is to evaluate the IHC stain to determine whether it is a comparable, less expensive, and less cumbersome alternative to FISH analysis in the detection of the EML4-ALK rearrangement.

Design: 117 NSCLC cases included 64 primary lung cancers, 48 cytology specimens, and 5 metastases. All specimens had been tested for the EML4-ALK rearrangement by FISH; 8 (6.8%) tested positive for the rearrangement. Paraffin-embedded tissue sections were immunostained for ALK using monoclonal EML4-ALK, clone 5A4 (Leica Microsystems, Bannockburn, IL). ALK expression was cytoplasmic. An immunostain intensity of 1 (scale: 0-3) and a percentage of positive-staining cells of >5% were considered positive.

Results: The sensitivity and specificity of the EML4-ALK IHC stain compared to the ALK FISH analysis as the gold standard were 100% and 96.3%, respectively. All eight FISH positive cases stained positive by IHC while four FISH negatives also stained positive. Thus, IHC identified all FISH positive cases with 4 false positives. Kappa agreement between the two methods is 0.78, which, depending on the source, is characterized as substantial or excellent.

Conclusions: Although the specificity of the EML4-ALK IHC stain is high (96.3%), it is not sufficiently specific to supplant FISH analysis in the detection of the EML4-ALK rearrangement and would overestimate the presence of the translocation. However, with its extremely high sensitivity, the IHC stain shows promise as a screening tool that would prevent superfluous and unnecessary FISH analysis.

1946 Diffuse Alveolar Damage Is Not a Prominent Feature of Non-Lung-Transplant-Related Pleuroparenchymal Fibroelastosis

JJ Tanguay, E Ofek, S Keshavjee, TK Waddell, MM Gomes, DM Hwang. University Health Network, Toronto, ON, Canada; Ottawa Hospital, University of Ottawa, Ottawa, ON, Canada.

Background: Pleuroparenchymal fibroelastosis (PPFE) is a clinicopathological entity characterized by pleural and subpleural upper lobe predominate fibrosis and fibroelastosis in patients presenting with a chronic interstitial pneumonia. The etiology and pathogenesis of PPFE remain poorly understood. PPFE was recently described as a major histologic correlate of post-lung transplant restrictive allograft syndrome, and has been described following bone marrow transplantation (BMT). We reviewed our files to identify cases of non-lung-transplant-related PPFE and assess histopathologic features and clinical associations.

Design: Lung biopsy and resection cases from 2002 to 2012 containing areas of fibroelastosis, infarct-like fibrosis, or apical cap-like fibrosis were identified and reviewed. Histopathological findings were assessed by three pathologists with pulmonary expertise. Cases of restrictive allograft syndrome were excluded.

Results: In total, 37 cases were identified, of which 12 demonstrated typical features of PPFE. Of these, 5 were idiopathic and 7 were in post-BMT patients. Most cases showed subpleural, paraseptal, and peribronchovascular distribution of fibroelastosis. Diffuse alveolar damage (DAD) was identified in only 1 case. All idiopathic cases occurred in females aged 20 to 64. The post-BMT group included 6 females and 1 male, aged 17 to 52, with BMT occurring 3 to 13 years prior to the pathology specimen. Four of 7 post-BMT patients developed clinical graft versus host disease (GVHD), while two additional patients showed histologic features suggestive of GVHD.

Conclusions: While some cases are idiopathic, PPFE may also develop as a late complication of BMT. In contrast to PPFE in post-lung transplant restrictive allograft syndrome, diffuse alveolar damage is not a prominent feature in either idiopathic or post-BMT cases of PPFE.

1947 Pulmonary Sarcomatoid Carcinoma – Immunohistochemical Study of 35 Cases with Emphasis on the Utility of Napsin

SBSP Terra, MC Aubry, ES Yi, JM Boland. Mayo Clinic, Rochester, MN.

Background: Lung sarcomatoid carcinomas (SC) present a challenging differential diagnosis. Immunohistochemical (IHC) markers are often used in the distinction between SC and tumors with overlapping morphologic features, including sarcomatoid mesothelioma and sarcomas. Napsin has recently emerged as a marker of lung adenocarcinoma, and some studies have shown it to have superior sensitivity and specificity than the alternative marker TTF-1. However, literature on napsin expression in SC is very limited. The goal of this study is to evaluate the usefulness of napsin in addition to the standard IHC panel often applied to pulmonary sarcomatoid malignancies.

Design: Cases of SC surgically treated at Mayo Clinic were evaluated morphologically, and with IHC for napsin, TTF-1, Oscar keratin, CAM5.2, AE1/3, desmin, SMA, S-100, CK5/6, calretinin, D2-40, and WT-1. Cases were excluded if they were keratin negative or were suspected mesothelioma.

Results: The 35 patients were 24 men and 11 women, with a mean age of 70 years (range 46-93). Cases consisted of 26 pleomorphic carcinomas, 5 spindle cell carcinomas, 3 carcinosarcomas and 1 giant cell carcinoma. 20 cases had an identifiable non-small cell component: 14 adenocarcinoma, 3 squamous, 2 large cell, and 1 adenosquamous carcinoma. All cases were positive for at least one keratin, although staining was often focal: AE1/3 was positive in all 35 cases, Oscar in 33 cases (94%), and CAM5.2 in 31 cases (89%, weaker and more focal staining). Napsin was positive in 14 cases (40%): 8 diffuse, 3 focal and 3 rare positive cells. TTF-1 was positive in 21 cases (60%): 14 diffuse, 3 focal and 4 rare positive cells. No cases were napsin positive and negative for TTF-1. While no tumors showed diffuse positivity of multiple mesothelial markers, some cases showed some staining for calretinin (12 cases, 34%), WT-1 (6 cases, 17%, 1 diffuse), D2-40 (5 cases, 14%, 2 diffuse), and CK 5/6 (9 cases, 26%, 2 with squamous morphology). Mesenchymal markers were also sometimes positive, although the staining was usually very focal, including S-100 (4 cases, 11%, including 2 carcinosarcomas with cartilage), desmin (4 cases, 11%, including one carcinosarcoma with rhabdomyoblasts), and SMA (6 cases, 17%, 1 diffuse).

Conclusions: TTF-1 is more sensitive than napsin in the detection of SC, and no cases were positive for napsin but negative for TTF-1. CAM5.2 is less sensitive than AE1/3 and Oscar, and often shows more focal staining. Use of an IHC panel is important in evaluation of sarcomatoid lesions of the lung and pleura, since isolated mesothelial and mesenchymal markers can be expressed in SC.

1948 Clinicopathologic, Immunohistochemical, and Molecular Characteristics of Pleomorphic Malignant Mesothelioma

M Vivero, LR Chirieac, F Galateau-Salle. Brigham and Women's Hospital, Boston, MA; CHU Caen Cote De Nacre, Caen, France.

Background: Pleomorphic malignant mesothelioma (PMM) is a variant of epithelioid malignant mesothelioma (EMM) that has recently been shown to have a worse prognosis than other variants. Short survival in PMM has prompted the suggestion that it be reclassified as a variant of sarcomatoid malignant mesothelioma (SMM), but a recent published analysis has demonstrated immunophenotypic and ultrastructural similarities to EMM. The aim of this study was to further define the histologic, immunophenotypic, and molecular characteristics of PMM.

Design: We studied 27 pleural PMMs, 24 EMMs and 11 SMMs collected between 1998 and 2011 by the French mesothelioma study panel. Tumor necrosis, mitotic index, and nuclear grade were assessed on hematoxylin and eosin-stained slides. AE1/AE3, WT-1, calretinin, CK5/6, EMA, and KL1 expression were evaluated by immunohistochemistry in all mesotheliomas, and deletion of p16 by fluorescence in-situ hybridization in PMMs and EMMs. Clinicopathologic characteristics were assessed and compared with overall survival.

Results: The PMM group included 20 males and 7 females, with a median age of 67. No major differences in demographic characteristics were present between the three groups. Necrosis was present in 74% of PMMs, 29% of EMMs, and 27% of SMMs ($p=0.002$). The median mitotic index per 10 high power fields was 10 in PMM, 1 in EMM and 9 in SMM ($p<0.0001$). High nuclear grade was present in 74% of PMMs. The overall immunophenotype of PMM reflected a pattern that more closely resembles EMM than SMM. p16 was deleted in 61% of PMMs and 74% of EMMs ($p=0.5146$). Overall survival in PMM was similar to SMM and worse than EMM (median OS of 7, 7, and 15 months, respectively, $p=0.044$).

Conclusions: Our results indicate an immunophenotypic profile in PMM more similar to EMM than SMM, despite a poor prognosis closer to that of SMM. p16 deletion rate was also similar to EMM, and different than the reported rate in SMM. This suggests that PMM should remain classified as a variant of EMM, and highlights the biologic complexity and heterogeneity of malignant mesothelioma.

1949 Wedge Resection and Staging Lymphadenectomy Can Downstage Primary Pulmonary Adenocarcinomas

AE Walts, AM Marchevsky. Cedars-Sinai Medical Center, Los Angeles, CA.

Background: There is increasing interest in treating clinical Stage I primary pulmonary adenocarcinoma (AC) with wedge resection and staging lymphadenectomy (SLN). Studies have evaluated survival and recurrence rates following these procedures but there is no information about the possible effect of this approach on pathologic staging of AC patients.

Design: 241 consecutive AC wedge resections followed by immediate lobectomy or trisegmentectomy and SLN between 2008 and 2012 were retrieved from our pathology database. Demographics, tumor location, size, pT (AJCC 7th ed.) and distance from tumor to closest margin (D) were recorded in the wedge specimens and compared with the presence of residual and/or additional tumor in the lung parenchyma of the 2nd specimens and with pN in the peribronchial lymph nodes (PBLN) and in the SLN.

Results: The 241 wedges (99 RUL, 13 RML, 41 RLL, 57 LUL, 31 LLL) were from 130 females and 111 males (median age 71 yrs). Tumors in the wedges were 0.6 to 7.2 cm (median 1.8 cm) in diameter and included 116 pT1a, 38 pT1b, 78 pT2a, and 9 pT3 lesions. D ranged from 0.1 to 5.0 cm (median 0.5 cm). The 2nd specimens consisted of 225 lobectomies, 13 trisegmentectomies, and 3 bilobectomies with 0 to 13 PBLN per case (median 2 per case). SLN consisted of 0 to 30 nodes per case (median 7 per case). Residual AC (n=14), additional AC nodules (n=9), and both (n=1) were found in the 2nd specimen lung parenchyma in 24 (10.0%) cases. Problems orienting residual tumor to tumor in the wedge made it difficult to accurately determine total tumor size and final pT in these cases. D was <1 cm in 13 of the 15 cases with residual tumor in the 2nd specimen. The 10 cases with additional AC nodules would have been downstaged as pT1 rather than pT3 by wedge resection. Metastatic AC was found in the nodes in 44 (18.3%) cases including PBLN (n=10), SLN (n=20), both (n=14). The 10 (4.1%) cases with positive PBLN would have been downstaged as pN0 rather than pN1 by wedge resection with SLN.

Conclusions: Wedge resections with SLN would have downstaged 7.9% of our cases (9 as pT1 rather than pT3, 9 as pN0 rather than pN1, and 1 as both). Wedge resection

margins >1 cm were associated with residual tumor in <1% of our cases. Future studies are needed to determine whether correlation with imaging would improve pathologic staging accuracy in AC patients undergoing lung-sparing procedures.

1950 Current American Joint Commission on Cancer (AJCC) Guidelines Upstage Patients with Synchronous Bilateral pM1a Pulmonary Adenocarcinomas

AE Walts, TK Leong, AM Marchevsky. Cedars-Sinai Medical Center, Los Angeles, CA.

Background: The American Joint Commission on Cancer Staging Manual (AJCC 7th ed) recommends that separate tumor nodules in the contralateral lung without distant metastases be staged pM1a (anatomic stage/prognostic group IV; pStage IV). Criteria to distinguish synchronous primaries from intrapulmonary metastases are not provided by AJCC. We sought to test the clinical validity of this recommendation in patients who underwent resection of synchronous bilateral pulmonary adenocarcinomas (PAC).

Design: Data from our hospital Cancer Registry were used to evaluate 5-year overall survival (OS), 5-year disease free survival (DFS) and median disease free survival (MDFS) in 18 consecutive pM1a patients who underwent resection of synchronous (defined as within 6 mos) bilateral PAC at our hospital. Patients with malignant pleural or pericardial effusions and/or distant metastases were excluded. Results were compared with those in a cohort of 573 consecutive patients (201 pStage I, 64 pStage II, 17 pStage III, 291 pStage IV) who underwent resection of PAC at our hospital during the same time period.

Results: The 18 pM1a patients (10 females, 8 males) ranged from 57 to 83 years in age (median 69.5 yrs) at operation. Their PACs ranged from 0.2 to 5.0 cm in diameter (median 1.3 cm). 17 (94.4%) of these 18 patients had invasive PAC; 1 had minimally invasive PAC. Only 5 (27.8%) patients received chemo- and/or radiation therapy; the remaining 13 received neither. The 5-year OS, 5-year DFS, and MDFS for the 18 pM1a patients were 64.5%, 94.4%, and 646 days, respectively. The 5-year OS, 5-year DFS, and MDFS for the 291 pStage IV patients in the registry cohort were 13.0%, 2.7%, and 0 days, respectively. When compared to results in pStages I-IV of the registry cohort, results in the pM1a study group best approximated those in the pStage I group (5-year OS, 5-year DFS, and MDFS were 69.0%, 27.5%, and 488 days, respectively).

Conclusions: In our patient population, synchronous bilateral pM1a PAC should not be staged as pStage IV in the absence of malignant effusion. Survival statistics for these pM1a patients were far superior to those for pStage IV and appear similar to those for patients with pStage I PAC. Our findings suggest that these pM1a lesions represent synchronous primary lung cancers. There is a need for future AJCC guidelines to include criteria that enable reliable distinction between multiple synchronous primary PACs and intrapulmonary metastases.

1951 Complex Acinar Pattern: A Distinct Morphologic Subtype and a Poor Prognostic Indicator in Primary Lung Adenocarcinoma

C Wang, HY Durra, Y Huang, V Manucha. Temple University Hospital, Philadelphia, PA.

Background: The newly proposed IASLC/ATS/ERS classification of lung adenocarcinoma has emphasized the prognostic significance of histologic subtyping. In this study two surgical pathologists evaluated the histological patterns of primary lung adenocarcinoma in different stages. The predominant patterns were correlated with established histological prognostic markers and tumor stage.

Design: 49 cases of lung adenocarcinoma diagnosed between 1998 to 2012 were retrieved from our archives. The H&E stained slides were evaluated by two surgical pathologists (VM and HD), 17 cases together and 32 cases independently. Histologic subtyping was performed according to the IASLC/ATS/ERS classification, each histologic component was recorded in 5% increments and the predominant pattern was defined as the one with the highest percentage. Tumors were staged based on the AJCC 7th edition. Cohen's kappa, k was calculated to evaluate the agreement between reviewers. The potential association of various patterns with established prognostic histologic parameters was assessed by chi-square.

Results: The two raters agreed on the predominant pattern in 23 out of 32 independently reviewed cases (k=0.634), and had different opinions on 9 cases including 2 cases of acinar vs papillary and 2 cases of acinar vs lepidic. In the remaining 5 cases, the disagreement was between acinar and a more complex pattern consisting of irregular, jagged, fused, closely packed glands with cribriform architecture, designated as complex acinar pattern in this study. Accordingly 4 cases were reclassified into this pattern. On correlation, 24 solid and micropapillary predominant tumors were associated with high mitotic count (> 5/10HPF; p=0.0003; ranging 6-54/10HPF) and severe cytologic atypia (p=0.0034), but not with higher stage (beyond IA; p=0.0599) and vascular invasion (p=0.2124). The association became more significant (higher stage: p= 0.0067; high mitotic count: p<0.0001; severe cytologic atypia: p= 0.0020; vascular invasion: p=0.0017) after combining tumors with predominant complex acinar pattern.

Conclusions: Agreement on the predominant histologic pattern was good between two pathologists despite minor disagreements in quantitative assessment of patterns. Tumors with complex acinar pattern may behave completely different form those with classic acinar pattern and should be recognized as a distinct subtype. A more detailed description of this pattern in the classification system and a large-scale study to evaluate its prognostic significance are indicated.

1952 WHO Histologic Classification Is an Independent Predictor of Prognosis in Lung Neuroendocrine (NE) Tumors but Ki-67 Proliferation Rate Is Not

H Wang, A Iyoda, MS Roh, G Sica, N Rekhtman, MC Pietanza, I Sarkaria, WD Travis. Memorial Sloan-Kettering Cancer Center, New York, NY; Kitasato University, Kanagawa, Japan; Dong-A University College of Medicine, Busan, Korea; Emory University, Atlanta, GA.

Background: Proliferation rate (PR) by Ki-67 immunohistochemistry has been shown to be useful in predicting prognosis of extrapulmonary NE tumors and has been incorporated into some classification schemes. A small number of studies have shown PR to be of prognostic significance in lung NE tumors, but it has not been rigorously compared with other prognostic factors.

Design: We studied 190 NE lung tumors including 87 typical carcinoids (TC), 22 atypical carcinoids (AC), 41 large cell NE carcinomas (LCNEC) and 40 small cell lung carcinomas (SCLC) diagnosed according to 2004 WHO criteria (WHO-C). Immunohistochemistry for Ki-67 (Ventana clone 30-9, Rabbit monoclonal antibody) was performed on whole tissue sections from 190 resection specimens. Nuclear positive cells were counted in hot spots per 100 cells.

Results: The mean (range) of mitoses per 2mm^2 vs PR was for TC: 0.6 (0-1) vs 4.15 (1-15); AC: 4.55 (1-9) vs 17.8 (8-35); LCNEC: 49 (18-121) vs 63.9 (40-90); and SCLC: 56.3 (25-137) vs 77.5 (50-100). In all NE tumors (NET), necrosis (p<0.001), mitoses (p<0.001), PR (p<0.001), tumor size (p<0.001), stage (p<0.001), WHO-C (p<0.001) and age (p=0.002) were significant for overall survival (OS). For all NET in multivariate analysis stratified for stage, including WHO-C, PR, size, and age, WHO-C was the only independent predictor of survival (p=0.026). For TC/AC alone, necrosis (p<0.001), WHO-C (p<0.001) Stage (p=0.024), PR (p=0.001), and mitoses (p=0.007) were significant for OS. However in TC/AC, multivariate analysis stratified for stage including PR and WHO-C, showed only WHO-C was an independent predictor of survival. Within TC/AC, a PR cutoff of 10% (p=0.014), but not 5% (p=0.079) was predictive of OS.

Conclusions: Classification of pulmonary NET according to WHO criteria by routine light microscopy based on mitosis counting and assessing necrosis is an independent predictor of prognosis in pulmonary NET but PR assessment by Ki-67 is not. This finding applies to classification of NET overall as well as for TC/AC alone. Ki-67 staining is particularly useful as an aid in determining histologic grade in NET where mitoses are difficult to appreciate due to poor fixation, sectioning, staining, necrosis or crush artifact. However, these data do not support incorporation of Ki-67 as a primary criteria in the classification scheme of pulmonary NET.

1953 Comparative Immunohistochemical Analysis of Pulmonary and Thymic Neuroendocrine Carcinomas Using Pax8 and TTF-1

A Weissferdt, N Kalhor, CA Moran. University of Texas Health Science Center at Houston, Houston, TX; MD Anderson Cancer Center, Houston, TX.

Background: Pax8 has recently been described to be expressed in thymic epithelial neoplasms and a subset of neuroendocrine carcinomas (NEC) of gastrointestinal origin but not pulmonary NEC. Thyroid transcription factor 1 (TTF-1) is known to be positive in NEC of pulmonary origin but studies investigating the expression of this marker in thymic NEC are lacking. To date, there are no comprehensive studies focusing on the comparative expression of Pax8 or TTF-1 in pulmonary and thymic NEC.

Design: Twenty-five cases of low and intermediate grade NEC of pulmonary and thymic origin, respectively were reviewed and representative sections were selected for immunohistochemical studies using antibodies directed against Pax8 and TTF-1. The percentage of positive tumor cells as well as the intensity of staining were evaluated and scored.

Results: Among the 25 pulmonary NEC were 21 low grade (typical carcinoid) and 4 intermediate grade (atypical carcinoid) tumors; the thymic tumors consisted of 8 low grade and 17 intermediate grade NEC. Only 2 (8%) of the pulmonary tumors showed nuclear expression of Pax8 whereas 19 (76%) expressed TTF-1. Of the thymic tumors, 8 (32%) were positive for Pax8 and only 2 (8%) showed TTF-1 positivity.

Conclusions: Primary NEC of the thymus are rare neoplasms that display a more aggressive clinical course than their pulmonary counterparts. Due to their rarity, metastasis from a pulmonary tumor always needs to be excluded by clinicoradiological means before a diagnosis of primary thymic tumor can be rendered. To date there are no specific immunomarkers to distinguish between neuroendocrine tumors of pulmonary and thymic origin. The differential expression of Pax8 and TTF-1 may prove useful in this context as a Pax8+/TTF-1- immunophenotype appears to be more common in thymic NEC while the reverse (Pax8-/TTF-1+) is true for pulmonary NEC.

1954 Application of the New Proposed Adenocarcinoma Classification – A Reproducibility Study

JM Wells, S Mukhopadhyay, H Mani. Penn State Milton S. Hershey Medical Center, Hershey, PA; SUNY Upstate Medical University, Syracuse, NY.

Background: The proposed IASLD/ATS/ERS adenocarcinoma classification document has stressed the need for further validation. The aim of this study was to assess whether the determination of tumor pattern is reproducible among pulmonary pathologists in routine daily practice.

Design: All slides (median 4, range 1-9) from 75 consecutive resected T1 adenocarcinomas were assigned a primary and secondary pattern by 3 pathologists with pulmonary subspecialty training and at least 5 years' experience, practicing at different institutions. A pre-study training set was not used. Results were analyzed for reproducibility.

Results: The most common predominant patterns were acinar (31%) and solid (27%), as were the most common secondary patterns (acinar 40%, solid 13%). The most

common combination of predominant and secondary patterns was acinar/solid (25%). The kappa value for interobserver agreement was 0.32 for predominant pattern, 0.26 for secondary pattern and 0.26 for the combination of primary/secondary patterns. All 3 readers agreed on a predominant pattern in only 26/75 (33%) cases; there was complete disagreement in 19/75 (25%) cases. The most common area of discordance was in assigning acinar vs. lepidic predominant pattern (15 cases). Reproducibility was best for solid pattern (k=0.65), followed by micropapillary (k=0.35), lepidic (k=0.28), papillary (k=0.2) and acinar (k=0.08) patterns. The number of slides per case did not significantly impact reproducibility (k=0.33 for cases with up to 4 slides and 0.28 for cases with more than 4 slides). Kappa values were similar (k=0.3 to 0.39) when comparing each pair of reviewers.

Conclusions: Inter-observer reproducibility in the determination of predominant and secondary patterns in resected pulmonary adenocarcinomas is poor, even among pulmonary pathologists, when applied to evaluating actual slides of resected tumors. Previously reported high kappa correlations based on representative images may not apply to routine everyday practice. The inability to reproducibly distinguish lepidic vs. acinar patterns, in particular, adversely impacts the reliable diagnosis of adenocarcinoma in situ.

1955 Immunohistochemical Profile of Resected Large Cell Carcinoma of the Lung

J Xie, Y Liu, JF Silverman. Allegheny General Hospital, Pittsburgh, PA.

Background: By definition, large cell carcinoma (LCC) is an undifferentiated non-small cell carcinoma that lacks architectural and cytologic features of adenocarcinoma (ACA) or squamous carcinoma (SCA) based on histologic examination. Although it should not change the diagnosis, LCC can express immunohistochemical (IHC) markers for ACA or SCA. In addition, the immunophenotypic profile of a LCC may potentially be helpful in directing additional molecular analysis that can influence therapeutic options. Accordingly, we performed an immunophenotypic analysis of previously diagnosed LCC.

Design: 34 cases of LCC diagnosed from 2000 to 2008 were selected. None of these cases had morphologic features of specific subtypes of LCC or large cell neuroendocrine carcinoma (LCNEC). All diagnosis was based on the absence of either glandular or squamous differentiation in the H&E examination and none showed a small cell carcinoma component. Eight cases previously underwent limited IHC studies for neuroendocrine markers and six cases had IHC work-up to either separate a primary lung carcinoma from a metastatic carcinoma or to further classify the primary LCC. Five cases were stained with mucicarmine. A contemporary IHC panel for classification of non-small cell carcinoma consisting of p63, p40, CK5/6, Napsin-A, TTF-1, chromogranin, and synaptophysin was performed on all cases. The results of the IHC stains were independently graded semi-quantitatively on a scale of 0-2+ positivity and 1-4+ for range of percentage of positive cells (1-25%, 26-50%, 51-75% and 75-80%) by two pathologists. The staining results of LCC were subject to cluster analysis. The control group consisted of 3 cases each of ACA, SCA and LCNEC.

Results: Immunohistochemical staining for p63, p40, CK5/6, chromogranin, synaptophysin, Napsin-A and TTF-1 showed 12%, 24%, 6%, 9%, 15%, 53% and 68% positively, respectively. Based on cluster analysis, we were able to place LCC into three immunophenotypical groups demonstrating IHC profiles of ACA, SCA or LCNEC in 56% (9/34), 12% (4/34) and 6% (2/34), respectively. There were 9/34 (26%) LCC which did not express any of the IHC markers. We found that p40 staining intensity was weaker with fewer cells positive compared to p63 in the same case.

Conclusions: Using a contemporary IHC panel, 74% of LCC expressed immunophenotypic profiles of ACA, SCA, or LCNEC. 56% of LCC demonstrated immunophenotype expression for ACA, 12% for SCA and 6% for LCNEC. IHC profiles of LCC may potentially be helpful in directing further molecular analysis for targeted therapy.

1956 Application of the IASLC/ATS/ERS Classification of Lung Adenocarcinomas and Implications for Tumor Grading

L Xu, T Huebner, F Tavora, A Burke. University of Maryland Medical Center, Baltimore, MD; Messejana Heart and Lung Hospital, Fortaleza, CE, Brazil.

Background: The International Association for the Study of Lung Cancer (IASLC) in association with the American Thoracic Society and European Respiratory Society has recently re-classified adenocarcinomas of the lung based on histological patterns. However, there is lack of consensus about a grading system for these tumors. We studied a series of invasive lung adenocarcinomas and correlated the revised classification system with histologic features and metastatic potential to identify features relevant to grading.

Design: A series of invasive lung carcinomas resected over a 5-year period were retrospectively reviewed and classified by the new IASLC system. Proportion of each histologic subtype was estimated at 5% increments. Tumors with clinical and pathologic staging were included. 15 histologic parameters were blindly recorded and subsequently correlated with lymph node and distant metastasis.

Results: There were 125 patients 61 men (66 ± 8 years) and 64 women (65 ± 11 years). Tumors were reclassified by predominant pattern as lepidic predominant (LPA) (n=9), acinar (n=71), solid (n=21), papillary (n=11), and mucinous (n=13). Rate of lymph node metastasis was greatest in the solid type (p=.02). Rate of distant metastasis was greatest in the mucinous and solid groups (p<.02). Features associated with metastasis in the acinar group included predominant cribriform pattern (P=.03), prominent nucleoli (p=.05), solid or micropapillary areas <20% (p=.01), mitotic activity > 5/10 high power field (hpf) (p=.005) and lymphovascular invasion (p=.005); the latter 3 were independently significant when adjusted for tumor size. A 3 tiered grading system was devised with LPA, papillary, and acinar tumors as well differentiated, mucinous tumors moderately differentiated, and solid tumors poorly differentiated. Furthermore, solid growth <20%, lymphovascular invasion, or mitotic activity >5/10 hpf increased LPA, papillary, acinar, and mucinous tumors up one grade. Using this system, there was a stepwise increase in rate of lymph node metastasis (p<.0001) and distant metastasis (p=.0004) from well, moderately, to poorly differentiated tumors, which numbered 38, 45, and 42, respectively.

Conclusions: Application of the IASLC classification in this series resulted in a predominance of acinar adenocarcinomas. In order to stratify tumors into clinically relevant grades, additional histologic features of increased mitotic rate, lymphovascular invasion, and non-predominant areas of solid growth are useful.

1957 Honeycombing in Idiopathic Pulmonary Fibrosis: Pathology and Imaging Correlations

L Xu, S Kligerman, A Burke. University of Maryland Medical Center, Baltimore, MD.

Background: The pathologic features of honeycombing in idiopathic pulmnonary fibrosis (IPF) have not been well correlated with CT imaging findings.

Design: We compared histologic features with CT scans from 48 patients with usual interstitial pneumonia (UIP). CT scans were evaluated for multiple parameters, including honeycombing and ground glass opacities. The explanted lungs were inflated with formalin, and representative peripheral and central sections were taken with areas of cystic change. Areas of remodeling were classified histologically as dilated single cysts lined in part by respiratory epithelium and by fibroblast foci (respiratory cysts), fibrotic clusters of compressed cysts lined in part by respiratory epithelium (lobular remodeling), cysts lined by fibrous tissue and macrophage giant cells (septal emphysema), and bronchiectasis (bronchioles extending to within 1 cm of the peripheral pleura). In addition, areas of uniform small cysts, <1 mm, lined by reactive pneumoyctes with minimal interstitial fibrosis were semiquantated as NSIP-like areas. Subpleural cystic spaces > 2mm and areas of lobular remodeling were measured morphometrically.

Results: There were 63 lungs from 48 patients (33 men, 65 ± 11 years, 14 women, 65 ± 10 years). Histologically, respiratory cysts were observed in 30 explants (63%), septal emphysema in 10 (21%), and bronchiectasis in 25 (52%). Lobular remodeling was extensive in 22 (46%). NSIP-like areas were present in 24 (50%), and extensive in 22 (46%). CT determined honeycombing showed a positive correlation with respiratory cysts (p=.03), bronchiectatic cysts (p=.02), and all cysts combined (p=.004). Ground glass opacity was positively associated with NSIP-like areas (p=.0002), and not other parameters. Morphometrically, bronchiectatic cysts measured 3.7 ± 1.6 mm; respiratory-lined cysts 3.8 ± 1.8 mm; giant cell-lined cysts 6.3 ± 2.8 mm; and lobular remodeling nodules 3.8 ± 1.2 mm.

Conclusions: Honeycombing by CT is associated with heterogeneous pathological findings. In patients with IPF, ground glass opacity is correlated with NSIP-like areas histologically.

1958 Idiopathic Pleuropulmonary Fibroelastosis: Fact or Fancy?

X Yang, P Ahmadi Moghaddam, A Akalin, A Fraire. UMass Memorial Medical Center, Worcester, MA; Contribute Equally, UMASS Medical Center, Worcester, MA.

Background: Criteria for the diagnosis of Idiopathic Pleuropulmonary Fibroelastosis (IPPFE) have been recently formulated. Proposed basic criteria for diagnosis include upper lobe predominance, dense interstitial intraalveolar fibrosis, prominent elastosis, dense fibrotic thickening of the overlying pleura and by definition no known cause. These features however are all non-specific and may be seen in other conditions such as advanced sarcoidosis, drug or radiation induced fibrosis, connective tissue disorders and asbestosis.

Design: We recently studied one case of possible IPPFE. The patient, an 85 year old woman, had thick white fibrotic patches in both the RUL and the LUL of the lung. Microscopically, the pleura had extensive fibrosis with elastotic changes of the subjacent pulmonary parenchyma. A search of our files was conducted and identified 20 additional cases with localized areas of pleuropulmonary fibroelastosis. Eleven of the 21 cases were men and 10 were women. Their ages ranged from 32 to 85 with a median of 67 years. Radiologically (CXR and CT), 7 had pneumothorax, 3 had emphysema, 3 had both pneumothorax and emphysema, and 6 had nodular lung lesions including 3 carcinomas, 1 hamartoma, and 1 old infarct. Some patients had more than 1 lesion identified and three patients had no imaging studies available.

Results: Grossly identifiable pathologic changes were identified in all 21 cases. These changes included emphysema, focal areas of lung consolidation, white pleural patches, subpleural nodularities, bullae, blebs and in one case a cavitary lesion. Nine cases were distinctly apical in location and 3 were both apical and lower lobe. A precise location was not determined in the remaining nine cases. Elastosis and /or fibroelastosis of varying degree were microscopically observed in all 21 cases. Our index case, the 85 year old woman, had resolving pneumonia at autopsy.

Conclusions: IPPFE has been described as a distinct clinicopathological entity with a striking upper lobe predilection and no known cause. Our study disclosed a wide variety of associated conditions, most frequently underlying pneumothorax and emphysema, with or without bullous change. These findings suggest that at least in our case material, IPPFE is commonly a localized phenomenon, likely secondary to a wide variety of associated post pneumonic or post pleuritic injuries. None of our cases appeared to be truly idiopathic.

1959 Clinicopathological Significance of Early-Stage Lung Adenocarcinoma with Micropapillary Component: Associations with Prognosis, *EGFR* and *KRAS* Gene Mutations

A Yoshizawa, S Sumiyoshi. Shinshu University Hospital, Matsumoto, Nagano, Japan; Kyoto University Hospital, Kyoto, Japan.

Background: Lung adenocarcinoma with micropapillary component (LA-MPC) is known to have biologically aggressive behavior and its predominant tumor was listed up as a new entity of invasive adenocarcinoma by the International Association for the Study of Lung Cancer, American Thoracic Society, and European Respiratory Society. The aim of this study was to evaluate the clinicopathological characteristics of early-stage LA-MPC and to investigate correlations between LA-MPC and the *EGFR* or, *KRAS* mutation status.

Design: We retrospectively reviewed 440 LA patients who underwent resection. We defined LA-MPC as adenocarcinoma with MPC occupying at least 5% of the entire tumor. *EGFR* and *KRAS* mutations were detected using the established methods.

Results: Of 440 cases, 256 cases were classified as Stage IA cases. Of which, 53 cases (20.7%) had MPC. The disease-free 5-year survival rates of the MPC-negative and MPC-positive groups in stage IA tumors were 92.1% and 77.6%, respectively, and there was statistically significant difference between the groups ($p = 0.003$). On the other hand, the overall 5-year survival rates of the MPC-negative and MPC-positive groups in stage IA tumors were 91.8% and 92.3%, respectively, showing no statistically significant difference ($p = 0.973$). Recurrent rates of LA-MPC were significantly higher ($n = 10$, 17.8%) than cases without MPC (4.4%) ($p < 0.001$). No *KRAS* mutation was detected in all the ten cases. Of the six alive cases with disease, *EGFR* mutations were detected in 5 cases (83.3 %) and the four of them were treated with a tyrosine kinase inhibitor (TKI) with long survival (median: 64.6 months). Additionally, one case with *EGFR* mutation was detected in four dead cases, who died 100.6 months later after initial resection with using TKI.

Conclusions: LA-MPC, defined as occupying 5% or more of the entire tumor, was associated with a strongly invasive nature and was a prognostic factor in early-stage patients. Moreover LA-MPCs were biologically aggressive but could be controlled by EGFR-TKIs.

1960 The Histopathology of End Stage Pulmonary Sarcoidosis: Comparison of 11 Explanted Lungs with Usual Interstitial Pneumonia

C Zhang, K Chan, H Ames, J Myers, L Schmidt. University of Michigan, Ann Arbor, MI.

Background: Sarcoidosis is an idiopathic multi-system disease that commonly affects the respiratory tract and is characterized by nonnecrotizing epithelioid granulomas. In 10 to 30% of cases the lungs undergo progressive fibrosis resulting in respiratory failure. Pathologic features of end stage pulmonary sarcoidosis (ESPS) have not been well described; anecdotal reports have suggested that it may mimic usual interstitial pneumonia (UIP). We hypothesized that ESPS has distinct histologic features.

Design: We identified 11 patients with a clinical diagnosis of ESPS who underwent lung transplantation between 1995 and 2012. Controls were 10 age and sex matched lung transplant patients with UIP (IPF=8; systemic lupus erythematosis=2). H&E-stained sections of each case were examined for the following features: extent/pattern of fibrosis; presence/quantity (per 10 high power fields) of fibroblastic foci and granulomas; distribution and morphology of granulomas; presence of granulomas in hilar lymph nodes; presence/extent of honeycomb change; bronchiectasis; hypertensive vascular change. Extent of fibrosis and honeycomb change were scored as follows: 1=1-25%; 2=26-50%; 3=51-75%; 4=76-100% of lung parenchyma.

Results: Well-formed granulomas with a lymphangitic distribution (visceral pleura, bronchovascular bundles, and interlobular septa) were seen in all ESPS cases, but none of the control cases. Granulomas were present in hilar lymph nodes from 9 of 9 ESPS cases, and none of 8 control cases. Ten of 11 ESPS cases showed patchy fibrosis with a lymphangitic distribution; 7 of 10 control cases showed patchy fibrosis but in a random distribution. One of the 11 ESPS cases showed diffuse fibrosis, while diffuse fibrosis was seen in 3 of 10 control cases (9% vs 30%, $p<0.05$). The average extent of fibrosis was significantly lower in ESPS cases, as compared with that in control cases (2.5 ± 0.5 vs 3.5 ± 0.5, $p<0.05$). There was no significant difference in honeycomb changes, fibroblastic foci, bronchiectasis and hypertensive vascular changes between the ESPS group and control group.

Conclusions: ESPS and UIP have distinct histopathologic features in explanted lungs. ESPS is characterized by a combination of well-formed granulomas and a lymphangitic pattern of fibrosis that differs from the patchwork pattern of fibrosis seen in UIP. Granulomas in hilar lymph nodes are limited to patients with ESPS.

Quality Assurance

1961 Evaluation of ER, PR and Her2 in Breast Carcinoma Metastatic to Bone: A Comparison of Results between FNA Cell Blocks and Surgical Biopsies

G Aggarwal, J Magda, ME Arcila, O Lin, M Edelweiss. Memorial Sloan-Kettering Cancer Center, New York, NY.

Background: Immunohistochemical profile (IHC) is critical in the management of patients with metastatic breast carcinoma. Accurate detection of ER, PR and Her2 require strict adherence to ASCO/CAP guidelines. The decalcification process (decal) performed in surgical biopsies (SB) of bone metastasis (bmets) has the potential to cause IHC alterations and delayed reporting. Cell blocks (CB) obtained from FNA of bmets represent a viable alternative. In the present study we aimed to compare ER, PR and Her2 IHC results on formalin-fixed CB to those on concurrent formalin-fixed decalcified SB.

Design: Thirty nine archival FNA samples with concurrent SB from patients with bmets were identified over a period of 12 months. Tumor cells were present in 31/39 CB (80%) of which 22/31 (71%) had more than 20 tumor cells. Archival blocks or IHC stains were available in 27 CB/SB pairs. IHC for ER, PR, and Her2 were performed/evaluated on these 27 CB and compared to those of the paired SB. Interpretation of ER and PR IHC included intensity of nuclear staining (weak, moderate, strong), and % of stained tumor cells. Her2 IHC scoring, was evaluated for complete membranous staining, uniformity (present or absent) and intensity of staining pattern. This semiquantitative scoring system was used for both CB and SB.

Results: Discrepant IHC was found in 4/27 cases in which the CB showed cells positive for ER (ranging from 5-98% of the cells) while no ER staining was seen in the matching SB ($p=0.29$). Interestingly, crush artifact was noted in 3 of these 4 SB cases. ER was originally positive in the primary breast carcinoma in 3 of such cases, while negative in 1. Seven (35%) of the remaining 20 ER positive SB cases showed a lower % of ER positive tumor cells (> 30% difference), as well as, decreased intensity of staining when compared to CB. Overall, comparison of ER staining (including number of discordant cases, decrease in intensity and % of stained tumor cells in SB) showed significant difference of results between CB and SB ($p =0.0002$). PR and Her2 comparison between CB and SB did not yield significant results.

Summary of IHC results on 27 paired CB and SB

	CB	SB	Discordant IHC	p value
ER+	24	20	4	0.29
ER-	3	7	4	0.29
PR+	15	13	2	0.78
PR-	12	14	2	0.78
Her2 (3+)	2	2	0	>0.5
Her2 (2+)	5	2	3	>0.5
Her2 (0/1+)	20	23	3	>0.5

Conclusions: Formalin-fixed CB that are adequately cellular represent a better platform for IHC studies in patients with metastatic breast cancer to bone when compared to SB. The decal and crush artifact in SB can lead to delayed reporting and less accurate IHC results.

1962 Studying Amended Reports: Testing Effects of Time of Sign Out, Resident Involvement, and Specimen Type on Amendments

O Alassi, R Varney, F Meier, R Zarbo. Henry Ford Health System, Detroit, MI.

Background: Amended reports may provide insights into conditions of practice that contribute to errors that lead to amendment.

Design: Among amended reports over 18 months. Amendments that revised primary diagnoses, revised secondary diagnostic information (tumor stage, grade, and margin), corrected patient mis identification (mis-ID) were examined. We also noted whether amendments were due to omitted diagnoses. We excluded amendments due to Mis-IDs undiscoverable at the time of sign-out. The reports were studied for date and time of original case signout, resident involvement and their level of training (junior,1st and 2nd year) and senior (3rd and 4th year) and type of specimens whether it is biopsy or large specimen.

Results: The amendments on 9/64 (14%) of examined reports had been initially misclassified: 8 designated 'diagnosis omitted' proved to be revised primary diagnoses, 1 'revised secondary diagnostic information' proved to be a revised primary diagnosis. After these corrections, among 64 amendments we found 16 primary revised diagnoses, 12 revisions of secondary diagnostic information (6 staging, 3 locations, and 3 laterality). 15 omitted diagnoses, and 15 corrected discoverable Mis-IDs. Almost three quarters [47/64 (73%)] of amendments were signed out in the afternoon, more than a third [23/64 (36%)] after 3:00 PM. Residents were involved in only 9/64 (14%) of amendments; senior residents were involved in 6 of these 9 cases. 13/16 (81%) of primary revised diagnoses were biopsies. More than 9/10 of omitted diagnoses were also biopsy specimens. The 15 discoverable misIDs were all biopsies. 7/12 (58%) of revised secondary information, however, regarded large specimens.

Conclusions: First, [14%] of amendments had been initially misclassified: better education of staff about amendment classification is necessary. Second, although we are working towards a continuous specimen flow, cases for sign-out accumulating in the afternoon; we hypothesize, increases staff fatigue and pressure to finalize biopsies within the expected two-day turnaround time: in the afternoon haste makes waste measured by amendments. Third, resident involvement did not appear to figure in amendments. Fourth, biopsies, in greater volume, nature of biopsy to reach an initial diagnosis, and great similarity from case to case, accounted for most primary diagnoses requiring revision, most of the omitted diagnoses, and most preventable misIDs. large specimens, on the other hand, with more secondary features, required more amendments for secondary diagnostic attributes.

1963 A Temporal Analysis of Trends in Intraoperative Consultation in a Large Academic Center

JA Bennett, M Walls, HS Crist, H Mani. Penn State Hershey Medical Center, Hershey, PA.

Background: Evaluation of trends in utilization of laboratory services is important for quality assurance, planning and education. We undertook a temporal analysis of the utilization of pathology intraoperative consultation (IOC) services in a large academic center, to look for changing trends, if any.

Design: The pathology database was searched to identify all cases that had IOC over two different periods (2002-2003 and 2010-2011). Results were tabulated by specialty, reason for consultation (diagnosis, margins, or both), deferral rates, and discordance, and trends were evaluated.

Results: Overall, IOC utilization remained comparable between the two periods analyzed (4.2% of all surgical cases for 2002-2003 and 3.6% for 2010-2011, p